# Structure and Function in Early Glaucoma

by

Yuan-Hao Ho

A thesis
presented to the University of Waterloo
in fulfillment of the
thesis requirement for the degree of
Doctor of Philosophy
in
Vision Science

Waterloo, Ontario, Canada, 2016

## AUTHOR'S DECLARATION

I hereby declare that I am the sole author of this thesis. This is a true copy of the thesis, including any required final revisions, as accepted by my examiners.

I understand that my thesis may be made electronically available to the public.

# Abstract

Glaucoma is a group of diseases, which exhibit a characteristic optic neuropathy and may result in progressive visual field loss. The most important risk factor is raised intraocular pressure (IOP) usually secondary to reduced aqueous outflow through the anterior chamber angle. It is the second leading cause of blindness globally. The diagnosis of glaucoma is difficult, as there is currently no widely-accepted "clinical standard" for diagnosis, although "progressive structural optic nerve and/or nerve fiber layer damage" is currently the most commonly accepted diagnostic criterion. Current treatments are to reduce the level of IOP, either by topical medication or surgery. Unfortunately, medical intervention frequently takes place after visual field loss has occurred. Consequently, much effort has been placed into the early diagnosis of glaucoma, in order to prevent damage.

Visual field tests have been a popular clinical method to determine functional defects, and they are essential for managing and diagnosing glaucoma. Various methods and test strategies have been developed. Computerized threshold static perimetry involves determining the dimmest stimulus that can be seen at a number of pre-determined test point locations. An examiner can interpret the resulting pattern of defect; also, disease progress can be followed over time. Visual fields should not be interpreted in isolation but in conjunction with other clinical findings[1]. Standard automated perimetry (SAP) is our oldest and best documented, computerized, subjective visual function test. Threshold tests are commonly used for both detection and follow-up of glaucoma patients. Different testing strategies and different stimuli have been developed with expectations of raising the sensitivity for early detection of glaucoma-related functional change, such as short wavelength automated

perimetry (SWAP), high-pass resolution perimetry (HRP), frequency doubling technology (FDT) and Flicker Defined Form (FDF). FDF is a temporally driven illusion in which background elements and stimulus elements are flickered in counterphase at a high temporal frequency, creating an illusory contour at the boundary between the background and the stimulus. It has been described to be a predominantly magnocellular-based stimulus due to its dependence on high temporal frequencies and its perceived low spatial frequency. The random flickering dots throughout the field of view and the complex nature of the stimulus, a phase-difference percept requiring higher order processing.

Clinically, besides testing for deficits in function, measuring of retinal structure plays an important role in the diagnosis of early glaucoma. Damage results in characteristic signs in the retinal nerve fiber layer, the parapapillary retina and the optic nerve head, due to the oriented distribution of the nerve fiber in the retina. Scanning laser tomography (SLT; Heidelberg Retina Tomograph, Heidelberg, Germany) is a confocal scanning laser device that provides accurate and reproducible topographical information of the optic disc and peripapillary retina. Other methods such as optic disc photography, retinal nerve fiber layer photography, scanning laser polarimetry, and optical cohererence tomography are also designed to detect structural changes. By analyzing the neuroretinal rim within the optic disc, the SLT provides evidence of glaucoma related structural change, such as changes in the cup to disc ratio and notching and narrowing of the neuroretinal rim. Measurements were affected by age, but it is fairly robust to astigmatism and working distance.

Studies have shown correlation between visual field test results and optic nerve head structural measurements. The correlation analysis of structure and function was performed to

evaluate the spatial relationship. It has been proposed that both structural and functional diagnostic methods have unique value, but the combination of methods might provide early evidence for glaucoma diagnosis and management.

The objectives of this thesis are:

1. To determine the normal sensitivity and confidence limits for FDF perimetry as a function of age;

2. To determine the test-retest repeatability of FDF perimetry for stable glaucoma; and

3. To investigate the structure function relationship in glaucoma using FDF perimetry and the HRT.

Normative data for different perimeters are well established. It is critical to establish normal sensitivity for the FDF perimetry. Age related sensitivity loss throughout the visual field has been previously reported. Confidence limits for normality will be established in this thesis, as only then can we examine the ability of the new clinical test to detect early glaucoma. Measures of function and structure are both relevant and required for the early diagnosis of glaucoma. The relationship between the points tested in the visual field and corresponding positions at the optic nerve head have been previously described. Comparing the FDF perimetry results with the HRT optic nerve head results has the potential to be of significant value in the diagnosis of glaucoma.

# Acknowledgements

The thesis cannot be completed without the support of my supervisor- Dr. John G. Flanagan. Thank you Dr. John G. Flanagan for your continued guidance and friendship.

I would like to also thank Dr. Natalie Hutchings for her determined encouragement in the last years of my program, very much appreciated.

Thanks Dr. Trefford Simpson for the weekends spent inspiring me with ideas.

Thanks Dr. McCulloch for her pep talks and prompt feedbacks on this thesis.

Special thanks to Jim Cassidy, Dr. Deborah Goren and Mark Lisetto-Smith.

Thanks for all the funding provided throughout my PhD program:

CNIB Ross C. Purse Fellowship,

Ontario Graduate Scholarship,

Glaucoma Research Society of Canada,

Heidelberg Engineering GMbH

UW President Graduate Scholarship.

Various opportunities working at/for the School of Optometry and Vision Science.

# Dedication

This thesis is dedicated to the participants that made the research possible, John and my wife Jiachang Shen.

# Table of Contents

# List of Figures

# List of Tables

# Chapter 1

# Introduction

## 1.1 Glaucoma

### 1.1.1 Overview

Glaucoma is a group of diseases that exhibit irreversible characteristic optic neuropathy, which can eventually lead to blindness.

Dating back to ancient Greece in 400BC, the term "glaucosis" was used to refer to the greenish-blue appearance of the pupil associated with vision loss[1]. The term included a wide group of blinding diseases including cataract and keratitis[2]. The definition varied from the term "glaucoma" in current medicine. Von Graefe first described glaucoma related central and peripheral vision loss in 1856. In 1958, Heinrich Muller described optic cupping as a characteristic optic nerve head damage associated with glaucoma.

Glaucoma is currently one of the leading causes of irreversible blindness throughout the world. According to documents published by the World Health Organization (WHO), glaucoma is the second leading cause of blindness globally[3–5], and the fourth leading cause of vision loss in Canada[6]. The estimate of worldwide people affected by glaucoma in 2010 is 60.5 million, and is predicted to reach 79.6 million by 2020[7]. It has also been estimated that the number of people to be effected by glaucoma worldwide will increase to 111.8 million by 2040[8].

Glaucoma has been classified as being primary, secondary or developmental. "Primary" glaucoma is defined when the initial outflow obstruction of aqueous humor or intraocular

pressure elevation is not secondary to another ocular or systemic disorder. Based on the mechanism of onset primary glaucoma can be divided in to “closed angle” or “open angle”, dependent on whether the anterior chamber angle is obstructed or not. The speed of onset is also used to classify glaucoma as “acute” or “chronic”. “Secondary” glaucoma, in contrast, is generally developed by the result of another ocular or systemic disorder.

Although glaucoma commonly occurs in the older population, it nevertheless boosts significant health and economic consequences[6]. Several studies investigated the quality of life in glaucoma patients, with the quality of life decreasing with visual function loss through the different phases of the disease[9–13]. Thus, the ability to detect and treat such disease prior to progression in vision loss is important.

### 1.1.2 Anatomy of the Optic Nerve and Pathogenesis of Glaucoma

Elevated intraocular pressure slowly causes damage to the ganglion cells and their axons, most notably at the level of the laminar cribrosa, and blockage of axonal transport may occur. Various theories have been proposed to describe the cause of the damage, including mechanical, vascular and/or biochemical theories.

The optic nerve head is approximately 4 mm medial and 1mm superior to the center of the macula at the medial-posterior region of the eye. The optic nerve begins from the retina and ends at the lateral geniculate body in the thalamus, it consists of ganglion cell axons and accompanying glial cells. By the passage of the optic nerve, it can be subdivided into intraocular, intraorbital, intracanalicular and intracranial portions. There are both transverse and longitudinal

blood vessel systems in all portions. The short posterior ciliary arteries contribute to some extent to the blood supply of all portions, whereas the branches of the central retinal arteries supply the nerve fiber layer and the axial portion of the postlaminar region. The longitudinal system supplies regions from the nerve fiber layer to the postlaminar region[14,15].

Between the inner limiting membrane of the retina (anteriorly) and the back surface of the scleral lamina cribrosa (posteriorly) is the intraocular portion of the optic nerve. The intraocular portion is subdivided into the surface nerve fiber layer, the prelaminar and laminar regions. The width of this portion of the optic nerve often increases from anterior to posterior, giving it a conical shape.

The nerve fiber layer of the retina is composed of unmyelinated axons of retinal ganglion cells, and the number of nerve fibers is often estimated at approximately 1 million per eye[16–19]. Blood vessels and glial tissue occupy about 5% of the volume of the layer[20]. There is an overproduction of nerve fibres during the first half of gestation. Between weeks 16 and 30 the nerve fibres are pruned by apoptosis (programmed cell death) and can result in significant differences in the ultimate number of axons remaining in the developed eye[21]. With aging, some studies have proposed no loss of axons[18,22], whereas others have shown a loss of 500 to 5500 axons per year[17,19,23].

The nerve fiber layer is supplied by branches of the central retinal artery, with venous drainage into the central retinal vein. There is a continuous capillary network from the level of the surface nerve fiber layer back through the postlaminar region of the optic nerve[14,15]. Capillaries on the surface of the optic nerve are also continuous with those in the peripapillary

retina[14,15,24]. Some choroidal vessels may contribute to the blood supply of the nerve fiber layer, especially on the temporal side of the optic nerve head[14,15].

Ganglion cells axons from the macula pass to the temporal portion of the optic nerve head, forming the papillomacular bundle. Axons from the nasal, superior and inferior retina enter the nasal, superior and inferior portion of optic nerve respectively. The axons from the temporal retina that arc above the macular region (the superior arcuate nerve fiber bundle) enter the superior temporal portion of the optic nerve; the axons below the macular region (inferior arcurate nerve fiber bundle) enter the inferior temporal portion of the optic nerve. This superior and inferior arcuate nerve fiber bundle creates the horizontal raphe, which is located temporal to the macular region. The greatest number of axons enter the superior and inferior poles of the optic nerve. The neuroretinal rim is slightly thicker inferiorly than superiorly, this is due to the slightly inferior position of the fovea.

The axons make a 90 degrees turn to exit the eye. Based on the location of the ganglion cell nuclei, axons from the peripheral retina are deeper in the nerve fiber layer and enter the outer edge of the neuroretinal rim of the optic nerve. Axons from ganglion cells closer to the optic nerve head are more superficial in the nerve fiber layer and enter the optic nerve toward the inner edge of the neuroretinal rim. When axons pass through the posterior scleral foramen, they become segregated into bundles or fasciculi by glial cells. Astrocyte glial cells comprise 50% of the prelaminar portion of the optic nerve[25]. In a cross-section view of the prelaminar region, the astrocytes surround the bundles of axons and are parallel to the direction of the optic nerve throughout the laminar and postlaminar, with blood vessels supplying the nerve fiber[25].

Between the inner limiting membrane of the retina and the anterior border of the scleral lamina cribrosa, axons of ganglion cells (along with astrocytes and blood vessels) form the prelaminar region of the optic nerve. The outer edge of the prelaminar portion of the optic nerve is covered by a mantle of glial cells. The prelaminar portion of the optic nerve receives its blood supply from centripetal branches of the peripapillary choroid[14,15]. These branches arise from short posterior ciliary arteries and have a segmental (sectorial) distribution. Capillaries from the prelaminar region drain into the central retinal vein or through the choroid into the vortex veins.

The outer portion of the prelaminar region of the optic nerve, which clinically is called the "neuroretinal rim", consists of bundles of ganglion cell axons, whereas the center of the prelaminar region is occupied by additional fibrous astrocytes.

Across the posterior scleral foramen, the inner two-thirds of the sclera continue to form the (scleral) lamina cribrosa. It is made up of approximately 10 lamellae (sheets, trabeculae) of fenestrated connective tissue to allow for the passage of nerve fiber bundles[26]. The lamellae contain approximately 200 to 600 pores[26], and the pores are greater in number and larger in size in the lamellae located more anteriorly. Pores in the superior and inferior poles of each lamella are larger and less supported by surrounding connective tissue than in the nasal or temporal regions[26,27]. Also, there is increased complexity of axonal channels superiorly and inferiorly. These areas are more likely to be damaged with elevated intraocular pressure[26,28]. Each lamella is composed of a core of elastin fiber, a network of filamentous basement membranes, and sparse, patchy areas of type III collagen, which is different from rest of the sclera[29]. Capillaries supplying the lamina cribrosa are found within these sheets of connective tissue. The lamellae are anchored firmly at the periphery to the surrounding sclera, centrally to the connective tissue

envelope of the central retinal vessels, and posteriorly to the septa of the retrolaminar optic nerve[14,15]. The medial and temporal regions of the lamina cribrosa anterior surface are more anterior than the superior and inferior region[26]. The outer surface of the lamina cribrosa is separated from the sclera by a thin envelope of glial tissue.

The laminar region contains both a transverse system of vessels located within the lamellae and a longitudinal system of capillaries interconnecting the various regions of the optic nerve[14,15]. Although some centripetal vessels arise from pia mater arterioles, the major centripetal supply is from the circle of Zinn-Haller. The venous capillaries of lamina cribrosa primarily drains into the central retinal vein.

Due to the myelination of the ganglion cell axons and the meningeal sheaths covering the surface of the optic nerve, the diameter of the nerve doubles compared to the intraocular portion when the optic nerve passes the posterior scleral lamina cribrosa and enters the orbit. Oligodendroglia (a type of glial cell) participates in the formation of myelin in the intraorbital portion of the optic nerve. The central retinal artery and vein run along the inferior lateral region of the nerve and penetrates the meningeal sheaths to enter/exit the nerve 12 mm behind the posterior surface of the sclera.

Blood supply to the postlaminar region is more complex than in other portions of the optic nerve. It consists of branches from muscular arteries, the ophthalmic artery, recurrent branches from the peripapillary choroid and the central retinal artery. Venous drainage from the postlaminar region is into the central retinal vein.

In glaucomatous eyes, elevated intraocular pressure will gradually damage the optic nerve head. This is, in part explained by blockage of axonal transport which leads to apoptosis of

the ganglion cells[30,31]. Genetically driven responses after blockage of axonal transport breaks down the DNA of ganglion cells by endonuclease enzymes[32,33], which is different from necrosis[33]. Thus, thinning of the nerve fiber layer/neuroretinal rim, and cupping of the optic nerve head can be seen[34–36].

Abnormal intraocular pressure, insufficient blood supply and apoptosis of ganglion cell axons result in the remodeling of the optic nerve head[37]. Lamina cribrosa extracellular matrix remodelling and reactivation of type 1β astrocytes is present in the early stage of glaucoma at the optic nerve. These changes result in the blockage of axonal transport. Swelling of the axons and cystic degeneration of the ganglion cells cause tissue loss of the optic nerve, which later is filled in by hyperplasia of the glial cells[36,38]. The largest of the ganglion cell axons (M cells, large P cells) located in the superior and inferior regions of the optic nerve are affected first[32,39,40]. Nerve fiber bundles located in the middle are less affected than those located peripherally[41].

In advanced stages of glaucoma, with more compression of the scleral laminar sheets, the surface area of the scleral lamina cribrosa expands, along with outward displacement of the lamina[42] and extension of the lamina out and under the choroid. At later stages, backward bowing of the entire scleral lamina cribrosa can be seen[43]. Capillaries in the optic nerve are lost at a rate that maintains the usual ratio of capillaries to axons to glial cells[43].

There can be diffuse or focal damage to the optic nerve in glaucoma[44]. Focal damage can be seen in the superior and inferior regions of the optic nerve, due to less support of laminar pores, showing an hourglass-shaped damage[45], presenting vertical elongation of the optic cup and notching of the neuroretinal rim. Diffuse damage is distributed uniformly over the surface of

the optic nerve and scleral laminar sheets[36,46], such as in symmetrical enlargement of the optic cup and symmetrical thinning of the neuroretinal rim.

Mechanical and vascular factors can both occur in glaucomatous damage, there remains significant debate regarding the cause of axonal transport blockage in glaucoma. In summary, abnormal levels of intraocular pressure can eventually cause remodelling of the optic nerve, causing degenerative changes in the extracellular matrix and reactivation of astrocytes. Excavation of the surface of the optic nerve is a result of backward displacement of the laminar sheets. Compressed laminar sheets and distorted laminar pores can mechanically compress axons of the ganglion cells and their blood supply as they pass through this region. When blockage of axonal transport occurs, this genetically triggers the process of ganglion cell apoptosis, presenting a loss of nerve fiber layer, cupping of the optic nerve, and thinning of the neuroretinal rim tissue.

### 1.1.3 Important Studies

There is a large number of studies investigating topics related to glaucoma. In the following paragraph, I will concentrate on studies that yield higher level of quality and evidence using population based data.

Studies have investigated the risk factors of glaucoma. The Blue Mountain eye study was conducted in Australia; 3654 subjects between age of 49-96 were examined. They suggested that there was a relationship between diabetes and open angle glaucoma, with prevalence of glaucoma being found to be higher in people with diabetes[47]. Participants with myopia were

reported to have a two to threefold increased risk of developing glaucoma[48]. Participants with pseudoexfoliation were also reported to have an increased risk of glaucoma[49]. Hypertension was significantly associated with open angle glaucoma[50]. Other risk factors reported included larger optic disc size[51], use of inhaled corticosteroids and a family history of glaucoma[52].

The Canadian Glaucoma Study[53–55] looked at systemic risk factors for glaucoma progression. The multicenter prospective longitudinal study examined a total of 258 patients. Baseline systemic measures included assessment of peripheral vasospasm and markers for hematopathology, coagulopathy and immunopathology. Participants were followed at 4-month intervals with perimetry and optic disc imaging. If visual field progression was found, a standardized interventional protocol for intraocular pressure control was initiated. Median follow up was 5.3 years. Abnormal anticardiolipin antibody level, higher mean follow-up IOP, higher baseline age, and female sex were significant independent risk factors for visual field progression in glaucoma.

The SAFE (structure and function evaluation) study[56,57] developed criteria for detecting glaucoma visual field loss for standard automated perimetry (SAP) and short-wavelength automated perimetry (SWAP). They concluded that the following six criteria demonstrated high specificity for correctly identifying eyes with normal visual fields for both SAP and SWAP: 1. Pattern standard deviation (PSD) worse than the normal 1% level; 2. Glaucoma hemifield test (GHT) outside normal limits; 3. One hemifield cluster worse than the normal 1% level; 4. Two hemifield clusters worse than the normal 5 % level; 5. Four abnormal locations ($p<0.05$); and 6. Five abnormal locations on the PD plot. All criteria were reported to need a second visual field test for high specificity. The study concluded that the glaucomatous optic disc is predictive of the

subsequent development of glaucomatous visual field loss, although this may have been influenced by the study inclusion criteria.

Studies have investigated treatment in glaucoma. The Early Manifest Glaucoma Trial (EMGT) examined 255 patients aged between 50 and 80 years. After a median of 6 years follow-up, they described that reduction of IOP by 25% or 5.1mmHg can significantly delay glaucoma progression in newly diagnosed patients. In the study, progression was 45% in the treatment group compared to 62% in the control group. The beneficial effect of treatment was more pronounced with less visual field loss[58].

The Ocular Hypertension Treatment Study (OHTS) looked at 1636 subjects with elevated IOP with no apparent glaucomatous damage and concluded that treatment lowering IOP can prevent or delay the onset of POAG[59]. After 5 years of follow up, 4.4% of treated and 9.5% of untreated participants developed glaucoma. Thirty-five percent of patients reached study endpoint only showed visual field defect and no optic disc abnormality. Corneal thickness, baseline age, vertical cup disc ratio, visual field defects and intraocular pressure were all predictors of progression[59].

The Collaborative Normal Tension study (CNTGS) tested 140 patients with normal tension glaucoma. Intraocular pressure was lowered by 30% from baseline. 12% of the treated eyes and 35% of the control group progressed to the study end point[60].

The Advanced Glaucoma Intervention Study (AGIS)[61–64] investigated 591 subjects with two sequences of surgical treatment in advanced glaucoma; either argon laser trabeculoplasty followed by trabeculectomy or vice versa. The study showed beneficial effect of lowering IOP,

they reported 25% of patient who had all IOP recordings less than 18mmHg during the 6 year follow-up showed no progressive mean visual field loss.

The Collaborative Initial Glaucoma Treatment Study (CIGTS)[10,65] looked at the initial treatment method for 607 open angle glaucoma patients and showed no statistical difference in visual field progression over 5 years. However, surgical methods lowered the IOP slightly more than the medical treatment.

These studies provided evidence for risk factors of glaucoma, visual field detection criteria and the effect of early treatment. There is currently no cure for glaucoma, but the earlier diagnosis of glaucoma and the earlier treatment can be initiated, the better chance of delaying further damage.

## 1.2 Function Testing:

### 1.2.1 Perimetry in Glaucoma

The normal boundaries of the field of vision is approximately 60 degrees superior and nasal, 75 degrees inferior and 100 degrees temporal to fixation[66]. Within the boundaries of vision, the central fixation has the highest sensitivity, and sensitivity decreases from central fixation to the boundary, this could be described by Traquair's analogy of the "island of vision". A blind spot is found in the island of vison approximately 15 degrees nasally from fixation. This "island of vision" would change its appearance in glaucoma.

Perimetry is used to assess visual function. Two types of perimetry, whether static or kinetic, could be classified based on the testing method. Kinetic perimetry uses a moving target

with fixed target size and fixed luminance to plot out the contours or isopters of the "island of vision"; static perimetry uses psychophysics to test for sensitivity of fixed locations using fixed target size and variable luminance. On the Humphrey visual field analyzer, flashing targets presented at 200ms duration are randomly projected on a bowl in front of the subject with variable luminance. The patient reacts to the stimuli in the bowl, by pressing a button when they see the stimuli. Test pattern selected chooses where the stimuli are presented, and test strategy determines the luminance steps to achieve final sensitivity. When glaucoma is present, the sensitivity within the defect area decreases. Perimetry is performed to measure sensitivity. By comparing fields throughout the progress of disease, we can quantify the sensitivity change through a given time period. Described by Bjerrum, an arcuate shaped scotoma extending from the blind spot on the superior or inferior visual field to the horizontal median raphe, could be a strong indication of a glaucomatous visual field defect. Sensitivity between superior and inferior locations in the nasal tested points could appear to differ significantly in glaucoma, this is called a nasal step. Retinal nerve fibers seldom cross the horizontal raphe, nasal peripheral scotomas result in the appearance of the nasal step.

In early stages of glaucoma, visual field defects are not apparent. Typical arcuate defects or scotomas, often start as single localized loss or small clusters of visual field loss. Gradually, through the progression of the disease, the defects appear to be deeper and larger, creating a more extensive arcuate loss, that may eventually lead to double arcuate scotomas and blindness.

Standard automated perimetry has been used for many years and is well documented for the diagnosis of glaucoma. Standard automated perimetry serves as an objective tool to detect glaucoma or monitor glaucoma progression. Detection of clustered sensitivity loss or sup/inferior

hemifield differences can be signs for glaucomatous visual field change. However, identifying early glaucoma and its progression can be difficult on the standard automated perimeter.

The initial detection of defect is related to how "normal" is defined. The criteria for a normal database and collection methods used to carry out the study or the analysis influences the classification of tested subjects. Test strategy used to determine the sensitivity would also influence the outcome of testing. The Hodapp-Parrish-Anderson criteria[67], provides a classification for the 30-2 test to identify glaucoma defects and stages the disease (table 1-1). It is reported at least 25% to 35% of ganglion cell loss relates to the significant field changes by the visual field[68].

| Glaucoma Stage Classification | MD | PD at 5% level | PD at 1% level | Points in the central 5 degree. |
|---|---|---|---|---|
| Early | No worse than -6dB | Fewer than 18 of 76 points | Fewer than 10 points | None less than 15dB |
| Moderate | Exceeds one or more criteria of "early" classification | | | |
| Severe | Worse than -12dB | More than 37 of 76 points | More than 20 points | One with 0dB or under 15dB in both the upper and lower central 5 degrees |

Table 1-1 Hodapp-Parrish-Anderson criteria for glaucoma stage classification

Detecting progression is another aspect in perimetry testing. Test variability of the visual field affects the ability to detect true field change[69]. Variability was found more in the periphery than the central field, results are also more variable at locations with defects. This increased variation when testing the disease makes separating true progression from variability of the test difficult.

Additional analysis was introduced to aid the diagnosis of glaucoma. The glaucoma hemifield test compares five sectors in the superior hemifield and mirrored sectors in the inferior hemifield. If the difference is significant between either sector in the superior and inferior, there is possible glaucoma loss. The visual field index (VFI) was also developed to aid in progression analysis. This index uses the pattern deviation plot, weighted toward central points, to calculate "the normal percentage of visual field" remaining[70].

Other pre-retinal factors also influence visual field testing in glaucoma. Such as media opacity, pupil size, refraction, patient instruction and testing environment. Cataract is another disease that affect the elderly population, it decreases the general visual field sensitivity. Pupil size can influence the visual field sensitivity, comparing patients that had dilated pupils and normal conditions, the difference is reported to be 1.95 dB at the fovea and MD difference of 1.15dB[71]. Without proper refraction to correct for field testing, optical blur would reduce visual sensitivity significantly by 1.26~1.45dB per diopter[72–74]. These factors would affect the visual field sensitivity, and should be investigated in new visual field testing.

### 1.2.2 Perimetry Parameters

Units: The units used in the flicker defined form perimeter (Heidelberg Edge Perimeter, HEP) are displayed in Decibels (dB). Decibels are a relative unit on a logarithmic scale, the reference 0 dB is when the instrument is at its maximum stimulus luminance. FDF ranges from 0 to 28dB, HEP-SAP size III ranges from 0 to 40 dB. SAP increase in stimuli size when reaching sensitivity lower than 15 dB, to give perceptual equivalence to the traditional SAP stimuli.

Test pattern: The test pattern defines the grid at which the stimuli are presented. The test patterns seen on the HEP are 30-2, 24-2, 10-2, 10-3 and S-30. 30-2 measures 76 locations within 30 degrees to fixation. 24-2 measures 54 locations. The 10-2 measures 68 locations within the 10 degrees to fixation. Both 30-2 and 24-2 patterns are on a 6 degree grid, whereas 10-2 is a on a finer grid of 2 degree.

Test strategy: The test strategy allows different algorithm used to determine the sensitivity of the tested retina. The HEP tests can be examined with full threshold strategy (FT) or Adaptive Staircase Thresholding Algorithm (ASTA) or with a screening strategy. The full threshold strategy (FT) was used in the original central 30-2 visual field testing on the Humphrey system in 1984. Sensitivity is first determined at four primary locations in the field using a 4-2-2 algorithm, which double crosses threshold, starting at 25dB. After the primary locations are tested, the test continues to nearby points to determine sensitivity throughout the visual field. The Standard Adaptive Staircase Thresholding Algorithm (ASTA-std) also uses a 4-2-2 algorithm to measuring the primary seed points in each quadrant. After the primary points are determined, estimated sensitivity of neighboring points are tested using a 2-2 algorithm, with the test terminating when crossing age-match limits. Retest of locations within session are performed

when sensitivity was significantly different from neighboring points or those of the age-matched normals. Screening strategies can be used for screening purposes, testing whether a subject can observe a stimuli 5dB brighter than the age match normal sensitivities. Locations tested that respond to the suprathreshold stimuli are terminated and marked “within normal limits” if suprathreshold stimuli were not seen, the location would be tested a second time with the same luminance. A 2dB brighter stimuli would be presented if the second presentation was not seen to determine if the location is a “relative defect” or “absolute defect”. Screening strategies are generally less time consuming when compared to a thresholding strategy.

Total deviation plot (TD): The total deviation plot shows the difference of measured sensitivity to age-matched normal subjects. This allows the examiner to find general height reduction of the visual field.

Pattern deviation probability plot (PD): The pattern deviation plot displays localized defect. It takes the 85% percentile ranked value of the TD plot to weight the baseline height of the visual field. This removes general loss of sensitivity, normalizing the general height of the visual field, that is, the locations that are away from the 85% percentile of the field would be detected.

Glaucoma hemifield test: The glaucoma hemifield test compares the sensitivity of five sectors in the superior and inferior hemifield. A significant difference of sectoral asymmetry may indicate early glaucomatous damage.

Mean deviation (MD): The mean deviation is the average of the total deviation.

Pattern Standard Deviation (PSD): The pattern standard deviation is the standard deviation of the MD index. PSD calculation is also weighted by location. It represents the roughness of the visual field.

False positive errors: When patient responds to a stimulus when the stimuli is not present or at the initial 200 msec of stimulus presentation, a false positive is recorded. Trigger happy patients tend to show more FP.

False negative errors: False negative catch trials are presented during the testing. Testing a suprathreshold stimuli (6dB for FDF and 9dB for SAP) on an already terminated location provides information when patients fail to respond to a visible stimulus. It tends to identify patient fatigue.

Fixation loss: Fixation losses are monitored by a real-time eye tracker. A 5 degree or more fixation loss, at the time of stimulus presentation, would be recorded as a fixation loss.

Pupil size monitor: Pupil size is measured throughout the duration of the visual field test after the initial 45 seconds of testing. Measurements are made in millimeters.

### 1.2.3 The Heidelberg Edge Perimeter

The Heidelberg Edge Perimeter is a modern automated perimetry designed to measure the visual field. It allows the examiner to understand the sum total of visual perception for the eye fixed on a target when the head and body are fixed in position. A CRT screen was used to present the stimuli within a 30 degree field of view. A lens in front of the CRT monitor

determines the field of view and adjusts for optical infinity, therefore requiring distance correction when testing. Stimuli of various contrast levels were presented across the tested area of field on a rectilinear grid, while the computer controls the thresholding algorithm. The participant was guided to use a trigger to notify the computer whether the stimuli can be seen. This allows determination of visual sensitivity at any pre-determined location in the visual field. Two types of targets could be displayed in the perimeter: Flicker defined form (FDF) stimuli and standard automated perimetry (SAP) stimuli.

Flicker Defined Form (FDF) is perceived when a 5 degree diameter patch of high temporal frequency (15Hz) flickering dots flicker in counterphase to the background flickering dots superimposed on a fixed luminance background (50cd/$m^2$). The border of the counterphase flickering dots generates perception of an illusionary edge, while the observer cannot discriminate the phase of the flickering dots. This temporally driven stimuli is thought to be magnocellular pathway dominant, and can potentially show advantage in early glaucomatous visual field loss detection.

The standard automated perimetry (SAP) targets presented on the HEP are designed to be equivalent to the dynamic range of Goldmann size III targets presented by most projection standard automated perimeters, for example the Humphrey Field Analyzer (HFA; background luminance of 31.5asb, and maximum luminance of 10000 asb). From 40dB to 16dB, stimuli size remains a constant 0.43 degree diameter, with luminance increasing as sensitivity decreases. From 15dB to 0dB, the size of the stimuli on the HEP-SAP enlarges to provide perceptual equivalence to the range of the HFA projection perimeter.

A prototype Heidelberg Edge Perimeter was used in all our examinations, and it is comparable to the commercial production unit. It incorporates a real-time fixation monitor that tracks gaze information during visual field testing. False positive and false negative catch trials were implemented in the testing algorithm. Chin/head rest adjustments and a flipping translucent eye cover allowed selection of tested eye.

## 1.3 Structure Measurement: Scanning Laser Tomography (SLT)

### 1.3.1 Principles of Scanning Laser Tomography

The scanning laser tomographer is a tool that complements other techniques that examine the optic nerve head. It allows the observer to acquire topography map of optic nerve head region to detect if damage or change is present.

The SLT is a confocal scanning laser ophthalmoscope, ie, multiple images are acquired along the longitudinal axis of the optic nerve head (z-axis), then the peak signals that coincide with the focal plane within each image were combined together to establish a three dimensional topographic image of the optic nerve head.

A 670 nm diode laser was used to perform the acquisition, the theoretical resolution of the scanning laser tomography images of the eye is 10 μm transverse resolution and 300 μm in axial resolution, with 50-60 μm of resolution within the axial plane. A resolution of 384X384 pixel is achieved at the 15 degree X 15 degree scans, giving a transverse resolution of 10 μm/pixel.

The ability of the SLT to detect glaucoma is similar to stereo-photographs of the optic nerve head assessed by experts. Operation of the HRT-SLT is not complicated. After aligning the optic nerve head with the camera, the operator would adjust the focus to acquire clear images.

The HRT-SLT will automatically determine the scan depth using a pre-scan of the optic nerve head, followed by three scans, which are aligned and averaged to create the mean topography image. This scan process usually takes 5-10 seconds.

### 1.3.2 Scanning Laser Tomography Parameters

After the acquisition of SLT images, a contour line of the optic nerve head is drawn by the operator, defining the internal margin of Elschnig's ring of the optic nerve head. Based on the contour line, the SLT subtracts 50 microns from the height of the papillomacular bundle (350-356 degree on the optic nerve head) to define the reference plane from which various parameters are calculated and statistical analysis performed[77,78]. There are several parameters that were proposed to be capable of detecting early glaucomatous loss[79]. Age, refraction and disc area were believed to effect parameters obtained by the HRT-SLT[80].

The followed is a list of common HRT-SLT parameters and an explanation of each parameter:

Rim Area: The rim area is the measured area of the neuroretinal rim enclosed by the contour line that is above the determined reference plane.

Rim Volume: The rim volume is the volume of the neuroretinal rim within the contour line and above the reference plane

Cup Shape Measure: A measurement of the distribution frequency of cup depth within the contour line. This could be a useful indicator of the degree of ONH damage[81] and visual field loss[82].

Height Variation Contour: The maximum difference between the highest and lowest measurement of the height along the contour line.

Mean RNFL Thickness: The mean thickness of retinal fiber layer measured above reference plane along the contour line.

Topography Standard Deviation: This is the average standard deviation of all pixels in the topography image, and represents the quality of acquired image. Quality of images can be effected by pupil size, and density of cataracts in patients.

### 1.3.3 Scanning Laser Tomography in Glaucoma

The structural measurements by the HRT-SLT have been shown to be reliable and repeatable[83,84], and can be performed without dilation[85–87]. However, pupil size could affect the variability and quality of the image[88], and dilation is preferred with small pupils and in patients with cataracts[89]. Rim area was reported to be the least variable parameter[90]. When investigating regional variability of the HRT, the highest variation was found at steeper areas, at the edge of optic disk cup and along blood vessels[91].

In order to discriminate between “normal” and “glaucoma”, Moorfields regression analysis was introduced. Taking aging effect into account, the Moorfields regression analysis

(MRA) compares the measured logarithms of the rim area and optic disc area of the optic nerve head to values for the normal database. The optic nerve head is divided into six sectors: Nasal, Temporal, Inferior-temporal, Inferior-nasal, Superior-temporal and Superior-nasal. The normative database of the MRA is race specific. Results should be interpreted carefully for subjects with different ethnic background, high refractive error and tilted discs.

HRT allowed comparison of the symmetry of the rim area in both eyes. When observing normal subjects, little asymmetry between the optic nerve head was found. Significant difference of the optic nerve head could be an indication of glaucoma. However, asymmetry for both eyes could be normal. In the studied population, 6% of cup/disc asymmetry over 0.2 was reported[92].

Disagreement between observers' contour placement is something that needed to be taken into account, this can effect parameters measured by the HRT; rim/disc area is reported to be least affected[93].

Using HRT as a tool for glaucoma detection. Studies have reported adequate sensitivity and specificity, range from sensitivities of 74-92% and specificity of 81-93%. The ability to detect glaucoma was reported to be comparable to expert's evaluation of stereo photographs.

Glaucoma progression has also been studied using the HRT. The alignment of the optic nerve head image in baseline visits and subsequent visits allows comparison of change in optic nerve head parameters. Change in glaucoma could show localized loss in the optic nerve head, with some bundles of axons prone to earlier damage than the others. The parameters measured were divided into six sector, this better isolated earlier changes in the damaged sector from the

sectors that show no change, and avoided change being averaged out of the signal when looking at global indices.

Trend analysis of the stereometric parameters are also provided by the HRT as a tool to present progression. Trend analysis normalizes several parameters by setting the initial baseline visit as 0. The normalization is based on the difference of measured value and baseline measurements to the difference of normal eye measurements and advanced glaucoma measurements. The parameters include rim area, rim volume, cup volume, cup shape measure, mean RNFL thickness, mean height countour variation, mean contour elevation, mean cup depth and mean height inside contour line. As time progresses it could show a range of change from 0 (baseline) to +1(maximum improvement) or -1 (maximum damage). This allows us to see the "trend" of progression. A continuous down trend indicates damage.

Topographic change analysis (TCA) is another tool used to track progression. The HRT uses the first two acquired images as baseline topographic information, and compares the consecutive topographic maps with the baseline. The topographic change analysis does not use the parameter measured after drawing the contour line. Instead, direct comparison of the topographic superpixels are performed. Areas of 4X4 pixels, i.e. "super pixels" are used to compare the height change of the topographic map. When the height of super pixels measured are significantly different, the possibility of change is high. When three consecutive changes were shown, colored pixels are used to illustrate the change. Red pixels on the map show depression or green pixels on the map show elevation of the area. The magnitude of change and the area of change should be taken into account when looking at glaucoma progression.

However, to date, there is no accepted clinical standard of what defines "progression" using the TCA.

## 1.4 Structure & Function relationship in Glaucoma

### 1.4.1 Relationship

Glaucoma is a disease that affects the number of retinal ganglion cells. Visual fields are used in glaucoma to test the function of ganglion cells, some tests are type specific, and some are non-specific. Structure tests allows the measurement of retinal tissue or optic nerve head structure that is related to ganglion cell loss. When relationships of structure and function are compared, it is better to judge correlation between parameters that related to ganglion cell numbers[94]. Structure or function measurements can be linear or non-linear, the dynamic range of structure or function measurements and statistical methods used affects the relationship[95,96].

Kerrigan-Baumrind et al. investigated the relationship between ganglion cell loss and visual field sensitivity in post-mortem humans[68]. Ganglion cell density was found to be nearly 10 times higher near fixation than in the peripheral locations in normal eyes, and 7205 axons were lost per year. They also reported that a 0.05dB loss in MD of the visual field was associated with each 1% of ganglion cell loss. Larger ganglion cell axons had a higher likelihood of ganglion cell death in glaucoma, in agreement with several other studies[40,41,46].

Harwerth et al.[97] investigated the relation of sensitivity and ganglion cell loss in glaucoma using a monkey model. They reported an approximately 6 dB loss in sensitivity before measurable ganglion cell loss. Sensitivity loss did not correlate well with ganglion cell loss,

when the ganglion cell loss was less than 50%; a 0.42 dB/percent of cell loss was found with cell loss greater than 50%.

Structure and function relationships have been reported to be significant with different clinical techniques and measurements. Airaksinen et al.[98] compared measurements of planimetry and Octopus visual field results on 29 normal subjects, 52 glaucoma suspects and 51glaucoma patients. A significant correlation was found between the structure of the retina and visual function. They reported a quadratic function to better describe the structure and function relationship and concluded that the non-linear relationship suggests a greater amount of structure change can occur before measurable visual function change.

In a recent review paper Malik et al summarized the linear relationship between structure and function measurements when comparing sensitivity and log ganglion cell number[99]. They described the linear relationship as a Hockey Stick model, due to the different slope of relationship within the central 15 degrees and outside the central 15 degree region. However, with current measurement techniques, there is clearly a larger confidence interval generated by the measurement of function when compared to the measurement of structure[100]. This increased variability decreases the ability to detect early functional change in glaucoma when compared to early structural change.

Another aspect of the measurement of the structure and function relationship is their spatial relationship. Structural tests often measure the optic nerve head. Functional measurements such as standard automated perimetry measures the visual field on a fix grid. The spatial distribution of ganglion cell of the retina or nerve fiber layer measured from the optic

nerve head doesn't correspond with the visual field sampling grid. This results in the over or under sampling of different structural measurements compared to functional measurements. Mapping of the optic nerve head against the visual field test grids showed that the nasal sector of the optic nerve head is under-sampled by the visual field compared to superior or inferior sectors of the optic nerve head. Ganglion cell density varies across the retina, with 50% of ganglion cells within the central 20 degrees of the retina[101]. However, our current functional measurements, i.e. standard automated perimetry, provides only12 test points in the central 20 degree retina. This difference in sampling ratio could possibly affect how we look at the structure and function relationship in different regions/sectors measured.

### 1.4.2 Detection & Progression

When investigating glaucoma detection, structural damage is often reported to detect damage prior to standard automated perimetry field loss[102,103]. The Ocular Hypertension Treatment Study (OHTS) examined subjects without initial optic disc or visual field damage. Thirty-five percent of patients who reached study endpoint only showed visual field defects and no optic disc abnormality[59]. Function or structure alone has its irreplaceable value in disease detection. Whether structural damage precedes functional defect in glaucoma detection is relative to the relation between the measured structure parameter and function parameter.

Progression can be monitored by the change or rate of change of measured parameters. However, the results of glaucoma progression measurement depend heavily on the instrument used to perform the measure. Seventy-seven patients with early glaucomatous visual field

damage were followed for a median of 5.5 years. Scanning laser tomography and conventional perimetry were performed every 6 months. They found that 27% showed no progression with either test. 40% progressed with only HRT, and 4% progressed on visual field measures only. In the patients that had both structure and function progression, 14% progressed at the same time, 45% showed HRT progression first, and 41% with perimetry progression first[104]. Another study looked at patients from the OHTS; out of 21 patients that converted from ocular hypertension to early glaucoma, 13 patients showed glaucomatous change measured by the HRT. 47 out of 164 eyes from participants with ocular hypertension and normal visual fields showed change measured by the HRT[105]. These studies provide evidence that both structure and function tests are important in monitoring glaucoma progression.

No single examination alone could diagnose or measure glaucoma progression. Utilizing the results of both structural and function tests showed better sensitivity and specificity in disease diagnosis than one test alone[106,107]. The ability to detect the disease and follow up using our current clinical tools is dependent on the tool itself and how well it can measure the structure or function of retinal ganglion cells or ganglion cell loss related parameters. The included test population also influences the structure-function relationship found in various studies.

Retinal structure and visual function are examined to provide diagnosis of glaucoma, and to measure the disease progression. Different tests or test parameters allow different dynamic ranges to be measured over the course of the disease. This results in variables that are difficult to define when investigating the structure and function relationship, such as the dynamic range of the test, the stage of the disease, and the relationship between test parameters and RGC cell loss.

There are factors that can affect the measurement of structure, such as blood vessels and optic nerve head tilt. There are other factors that increase variability of structure and function, such as media opacity, pupil size and optical blur, all of which can influence the structure function relationship.

## 1.5 Summary

Glaucoma is a group of diseases that exhibit characteristic optic nerve head neuropathy and may result in progressive visual field loss. It is the second leading cause of blindness globally, and the estimated number of people affected by glaucoma is growing.

Irreversible optic nerve damage and visual field loss can significantly affect quality of life. Early diagnosis and early treatment of glaucoma can help prevent or slow down the rate of disease progression, therefore maintaining quality of life.

The early diagnosis of glaucoma is difficult. A 25-40% RGC loss is needed to be detected by current functional tests. Standard automated perimetry is widely used in glaucoma function testing, but is not ideal for early detection of glaucoma.

Flicker defined form is a stimulus generated when a patch of high temporal frequency random dots flicker in counterphase to the background random dots, creating an illusory border between the out of phase flickering dots of the stimulus and the background. This high temporal frequency stimulus is reported to be magnocellular pathway dominant while maintaining input from the parvocellular pathway. This stimulus was developed for the early detection of glaucoma.

In this thesis, I will test flicker defined form as a visual field stimulus, and establish the normative database for the flicker defined form. The effect of dioptric blur on FDF perimetry will be examined. A study will be carried out to measure the test-retest characteristics of flicker defined form in stable glaucoma. Structure and function relationships in early glaucoma will also be investigated.

Rationale:

Studies have shown correlation between visual field test results and optic nerve head structural measurements. The correlation analysis of structure and function was performed to evaluate the spatial relationship. It has been proposed that both structural and functional diagnostic methods have unique value, but the combination of methods might provide early evidence for glaucoma diagnosis and management.

The objectives of this thesis are:

1. To determine the normal sensitivity and confidence limits for FDF perimetry as a function of age;

2. To determine the test-retest repeatability of FDF perimetry for stable glaucoma; and

3. To investigate the structure function relationship in glaucoma using FDF perimetry and the HRT.

Normative data for different perimeters are well established. It is critical to establish normal sensitivity for the FDF perimetry. Age related sensitivity loss throughout the visual field has been previously reported. Confidence limits for normality will be established in this thesis, as only then can we examine the ability of the new clinical test to detect early glaucoma. Measures of function and structure are both relevant and required for the early diagnosis of

glaucoma. The relationship between the points tested in the visual field and corresponding positions at the optic nerve head have been previously described. Comparing the FDF perimetry results with the HRT optic nerve head results has the potential to be of significant value in the diagnosis of glaucoma.

Null Hypothesis:

1. Age has no effect on Flicker Defined Form stimuli detection.
2. Dioptric blur has no effect on Flicker Defined Form sensitivity.
3. There are no differences in test-retest repeatability of Flicker Defined Form sensitivity between patients with glaucoma.
4. The results of Flicker Defined Form perimetry showed no difference to standard automated perimetry in the detection of early glaucoma.
5. There was no correlation between Flicker Defined Form perimetry and SLT indices using optic nerve head topographic maps.

# Chapter 2

# Normal Aging Characteristics of the Heidelberg Edge Perimeter

## 2.1 Overview

**Purpose:** To establish the range of normative data for flicker defined form perimetry and report the characteristics of the reference database used on the Heidelberg Edge Perimeter (HEP; Heidelberg Engineering, Heidelberg, Germany).

**Methods:** Six study sites recruited 308 normal volunteer subjects between the ages of 20 and 80 years. Gender ratio was approximately 50:50 within each decade. All subjects went through standard baseline measurements and ocular health screening to ensure they met the normal criteria. For each subject, testing was performed over 3 study visits within 6 months. Tests included HEP-FDF ASTA 24-2 ($5^o$), HFA SITAstd 24-2 (size III), HRT and digital fundus photography on each eye, and HEP-FDF Full threshold 24-2 ($5^o$), SAP 24-2 (on HEP, size III) and HEP-FDF 10-3 ($3^o$) on one, randomly selected eye. HEP measurements were conducted using a prototype production device.

**Results:** The effect of age on sensitivity was best described using a second order polynomial, it showed a relatively linear and shallow decrease between 20 and 60 years and a slightly steeper decrease between 60 and 80 years. Confidence intervals were established for each stimulus location, and increased slightly with eccentricity. Sensitivity was significantly greater in the inferior hemifield compared to the superior hemifield. An average of 0.747dB difference was found between the first and second tested eye. Test time averages 290.2 ±46.5 sec.

**Conclusions:** The distribution of normal data, and the effect of age, eccentricity and location are presented for FDF perimetry. Characteristics were similar to that reported for other visual field devices. The normative database will permit the development of analytical tools for the HEP perimeter and the establishment of normal structure/function relationships with imaging devices.

## 2.2 Introduction

Flicker defined form (FDF) is an illusionary visual stimulus. Random dots on an achromatic background flicker at high temporal frequency (15Hz) and a 5 degree patch of random dots within the random flickering background dots flicker out of phase with the background dots. The border/edge between of the out-of-phase dots allows perception of an illusionary border, creating the 5 degree FDF stimulus. Illusory border perception of a high frequency counter phase edge was first described by Livingstone and Hubel[1]. Later Ramachandran et. al perceived an illusionary borderline between two groups of counterphase flickering random dots, and called it the phantom contour illusion[2]. Flanagan et.al used this contour illusion to create a letter test, and found the letter test demonstrated the ability to detect early glaucoma[3]. When perceptual limits of flicker defined form (FDF) was further researched, they concluded that larger stimuli increased sensitivity, and a higher background dot density increased sensitivity [4]. A 3.5 dots/degree with a random dot background of 0.34 degree diameter was used in the flicker defined form perimetry to avoid a ceiling or a floor effect. The advantage of the larger target size used for FDF perimetry testing compared to the SAP should allow

improvements in test-retest characteristics and greater resistance to optical blur. As such, it is also hypothesized that it will be a sensitive test for the detection of early glaucomatous damage.

Studies have reported that with increased age, visual field sensitivity decreases.[5–10] While testing the central 30º field, one study using a standard automated perimetry (SAP) Goldmann size three stimulus showed a -0.5dB to -0.9 dB decrease per decade at different tested locations[5]. Variability of sensitivity also increased with increased eccentricity using SAP[5,9]. Studies reported a -0.7 dB per decade decrease in sensitivity using the frequency doubling technology (FDT), they also reported a 0.7dB sensitivity difference between first and second tested eye[6,7].

The Heidelberg Edge Perimeter (HEP), an automated static perimeter, was designed to present FDF stumuli. Flicker defined form, a temporally driven task, has the potential to detect early glaucoma[4,11]. In order to discriminate between "normal" and "abnormal", a reference normal database is needed. The normal aging effect on FDF, which defines the normative database needs to be established.

The aim of this study is to describe the normal aging effect on the perception of flicker defined form (FDF) stimulus and to establish a reference database for the Heidelberg Edge Perimeter. (HEP; Heidelberg Engineering, Heidelberg, Germany)

## 2.3 Methods

308 normal subjects between the age of 20 to 80 were recruited at six study sites: the School of Optometry and Vision Science, University of Waterloo; Ophthalmology and Visual Sciences, Dalhousie University; Illinois College of Optometry, Chicago; Southern California College of Optometry; Department of Veterans Affairs, NY Harbor Health Care System,

Hewlett; University of Houston College of Optometry; Department of Ophthalmology & Vision Sciences, University of Toronto, Toronto Western Hospital. The study protocol adheres to the declaration of Helsinki. Research ethical approval was granted at each test site. Informed consent was given by all participants prior to testing.

General ocular history was collected with all subjects going through baseline measurements, including best corrected visual acuity (BCVA), Goldmann applanation tonometry (IOP), anterior segment biomicroscopy, Volk funduscopy, digital fundus photography, keratometry and refractive error. Participants were excluded from the study if they met the following exclusion criteria: BCVA worse than 6/9, any ocular disease or condition that is likely to affect the visual field outcome, refractive error greater than ±5 diopters sphere or ±2.50 diopters cylinder. A visual field false positive catch trial rate of 15% or greater, or a false negative rate of 20% or greater also resulted in exclusion.

A series of visual fields were performed over three visits on three different test days. At the first visit, participants were encouraged to practice through a certain period of demonstration testing to familiarize themselves with the FDF stimulus. One eye was randomly chosen to be the study eye. Tests included on visit 1 were HEP FDF ASTA 24-2 for the study eye, Humphrey visual field 24-2 SITA-std for both eyes, and HRT ONH imaging on both eyes. On visit 2, HEP FDF 24-2 ASTA was peformed on both eyes, HFA 24-2 SITA-std was performed on the non-study eye, HEP SAP 24-2 on the non-study eye, and HRT imaging on both eyes. On visit 3, HEP FDF 24-2 ASTA was performed on both eyes, and HFA 24-2 SITA-std/HEP SAP 24-2 was performed on the non-study eye (Table 2-1). Test order was randomized. A minimum 5 minutes

of rest time was given to the participants between each visual field test to minimize the effect of fatigue.

A prototype of the HEP perimeter was used for data collection. Mean luminance of the HEP screen was 50 cd/$m^2$, the random dots remained stationary and flickered at a frequency 15 Hz. Dot size was displayed at 0.34º diameter with a density of 3.5 dots/degree. The instrument was calibrated each time before the study started. FDF stimulus presentation had a ramp time of 150ms to reach desired contrast, followed by a 400ms presentation time and 150ms off transition time. 500ms inter-stimulus time was provided. A real time video eye tracker allowed tracking of patients' fixation during testing.

| **Test Algorithm** | **Visit 1** | | **Visit 2** | | **Visit 3** | |
|---|---|---|---|---|---|---|
| | **OD** | **OS** | **OD** | **OS** | **OD** | **OS** |
| HEP 24-2 ASTA | $\alpha^{\surd}$ | | $\surd$ | $\surd$ | $\surd$ | $\surd$ |
| HFA 24-2 SITA STD | $\surd$ | $\surd$ | | $\beta^{\surd}$ | | $\beta^{\surd}$ |
| HEP 24-2 SAP | | | | $\beta^{\surd}$ | | $\beta^{\surd}$ |
| HRT 3 ONH imaging | $\surd$ | $\surd$ | $\surd$ | $\surd$ | | |

Table 2-1 Test sequence. In three visits α represents the one eye chosen randomly for each volunteer, β represents the other eye. Test order is randomized, always testing OD (right eye) then OS (left eye) if testing OU (both eyes).

Statistical analysis: Scatterplots of visual field sensitivity were plotted for each tested location and eye as a function of age. The mean average was fitted by a second order

polynomial. The 95% confidence limits were also determined at each location. The effect of age was also demonstrated by plotting surface quadratic functions of the hill of vision. Sensitivity of first and second tested eye were compared using a Student's dependent t-test. Test time was also compared between age groups using analysis of variance (ANOVA).

## 2.4 Results

308 subject were included in our analysis. The frequency was plotted to each age group (figure 2-1), and the average age was 47.8±15.6 years. The Male/Female ratio was 0.86 (142/166). Visual field sensitivity decreased with age by an average of 0.6 dB per decade using a linear fit. However, a second order polynomial better fit the distribution, see figure 2-2 and figure 2-3. A relatively linear and shallow decrease between 20 and 60 years, with a slightly steeper decrease between 60 and 80 years, was found. The second order polynomial fit along with one-tailed 95% confidence intervals were plotted for each location, see figure 2-4 and figure 2-5. Confidence intervals were established for each stimulus location, and increased slightly with eccentricity. A topographic quadratic function was used to plot sensitivity values for the hill of vision using FDF, see figure 2-6 and figure 2-7. Sensitivity was significantly higher in the inferior hemifield ($p<0.001$). Average test time for completing a HEP-FDF 24-2 ASTA standard test was 290.2 ±46.5 seconds in our group of normal participants, and plotted by age group in figure 2-8. We found a significant difference between age groups 20-29, and 40-49 ($p=0.03$) and 50-59 ($p=0.04$) using a Bonferroni post-hoc analysis; other groups showed no statistical difference.

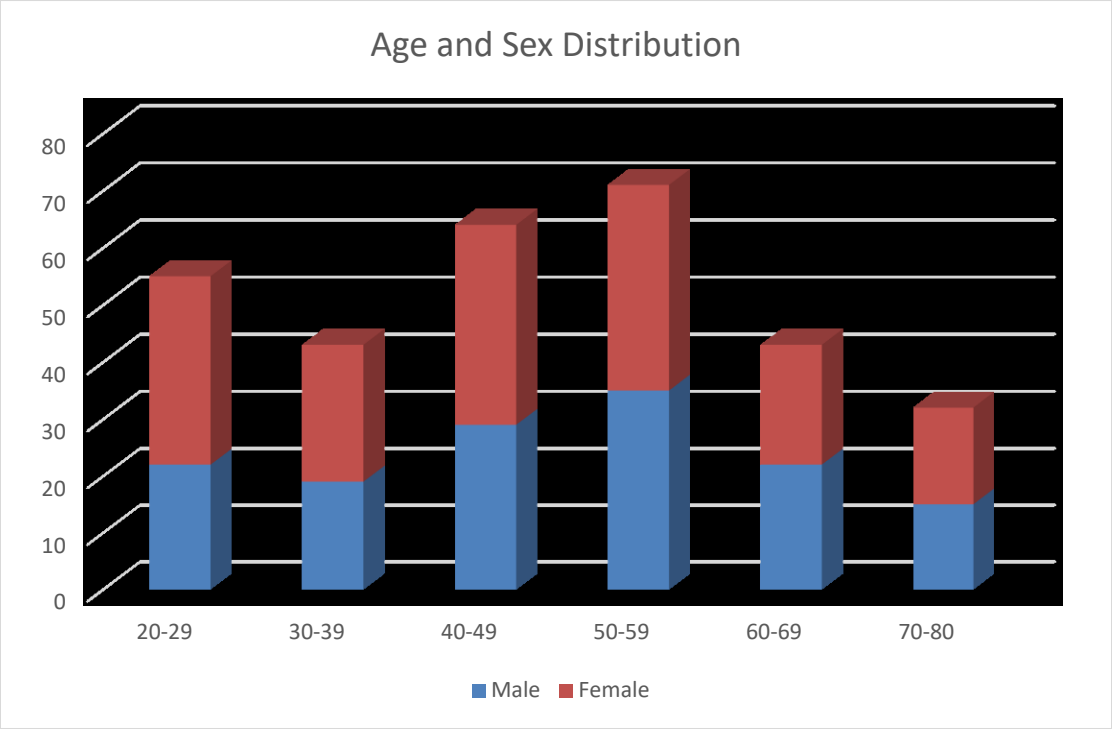


Figure 2-1 The distribution of participants' age and sex.

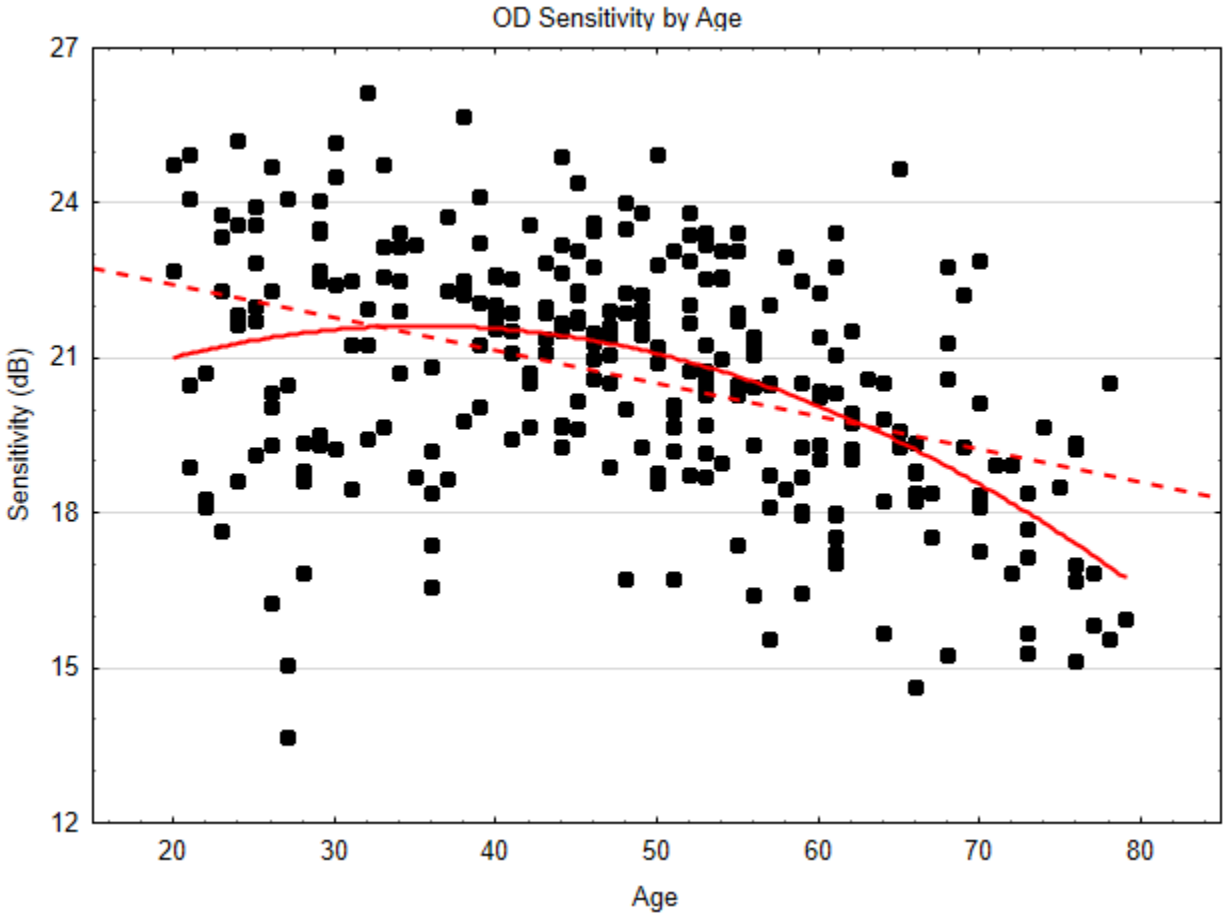


Figure 2-2 Flicker Defined Form OD sensitivity by age. OD average sensitivity of all stimulus locations by age (n=308). Linear fit: $y=23.683-0.063x$, $r^2=0.163$. 2nd order polynomial fit: $y=18.384+0.183x-0.003x^2$, $r^2=0.231$

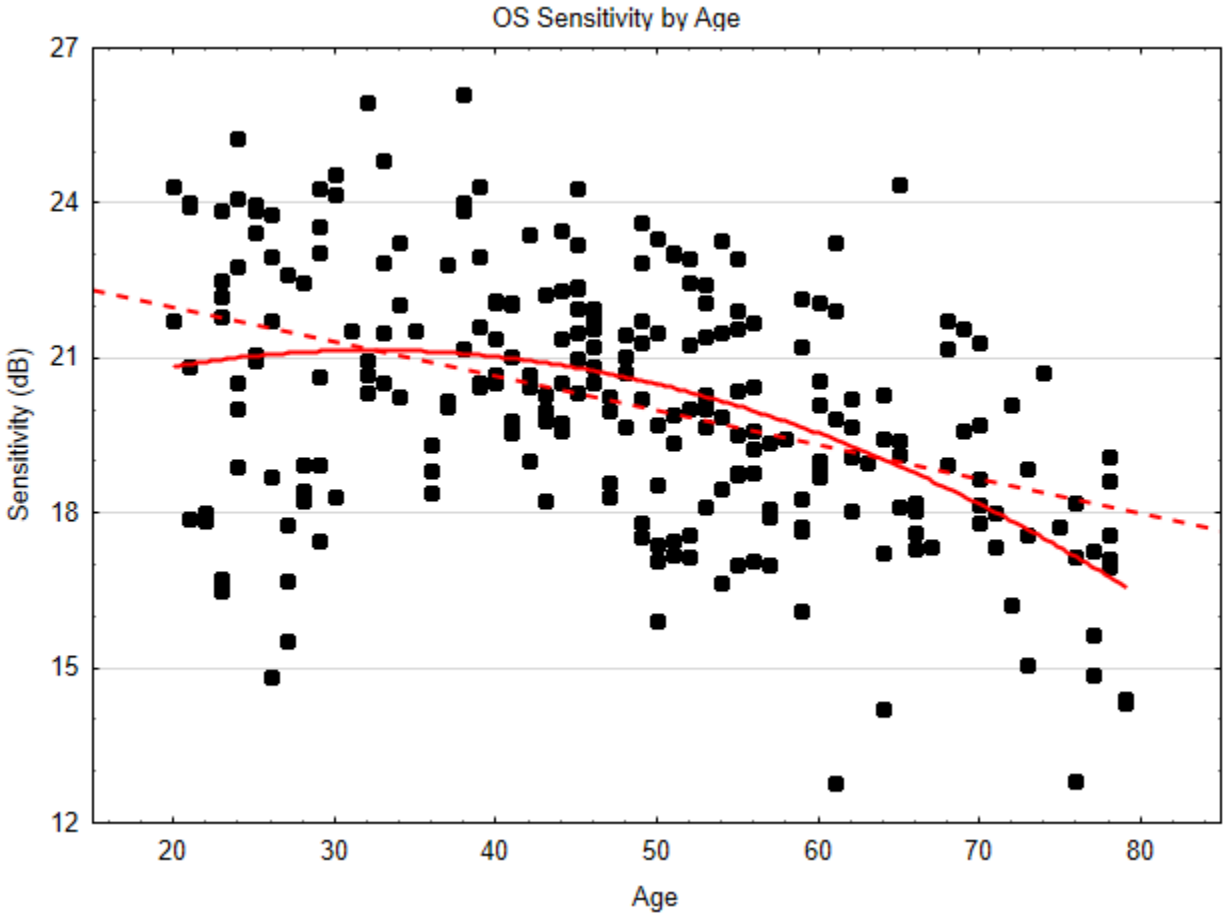


Figure 2-3 Flicker Defined Form OS sensitivity by age. OS average sensitivity by age. Linear fit: $y=23.313-0.067x$, $R^2=0.185$. 2nd order polynomial fit: $y=18.971+0.135x-0.002x^2$, $R^2=0.235$

Figure 2-4 Sensitivity for each location as a function of age (right eye).

Figure 2-5 Sensitivity for each location as a function of age (left eye).

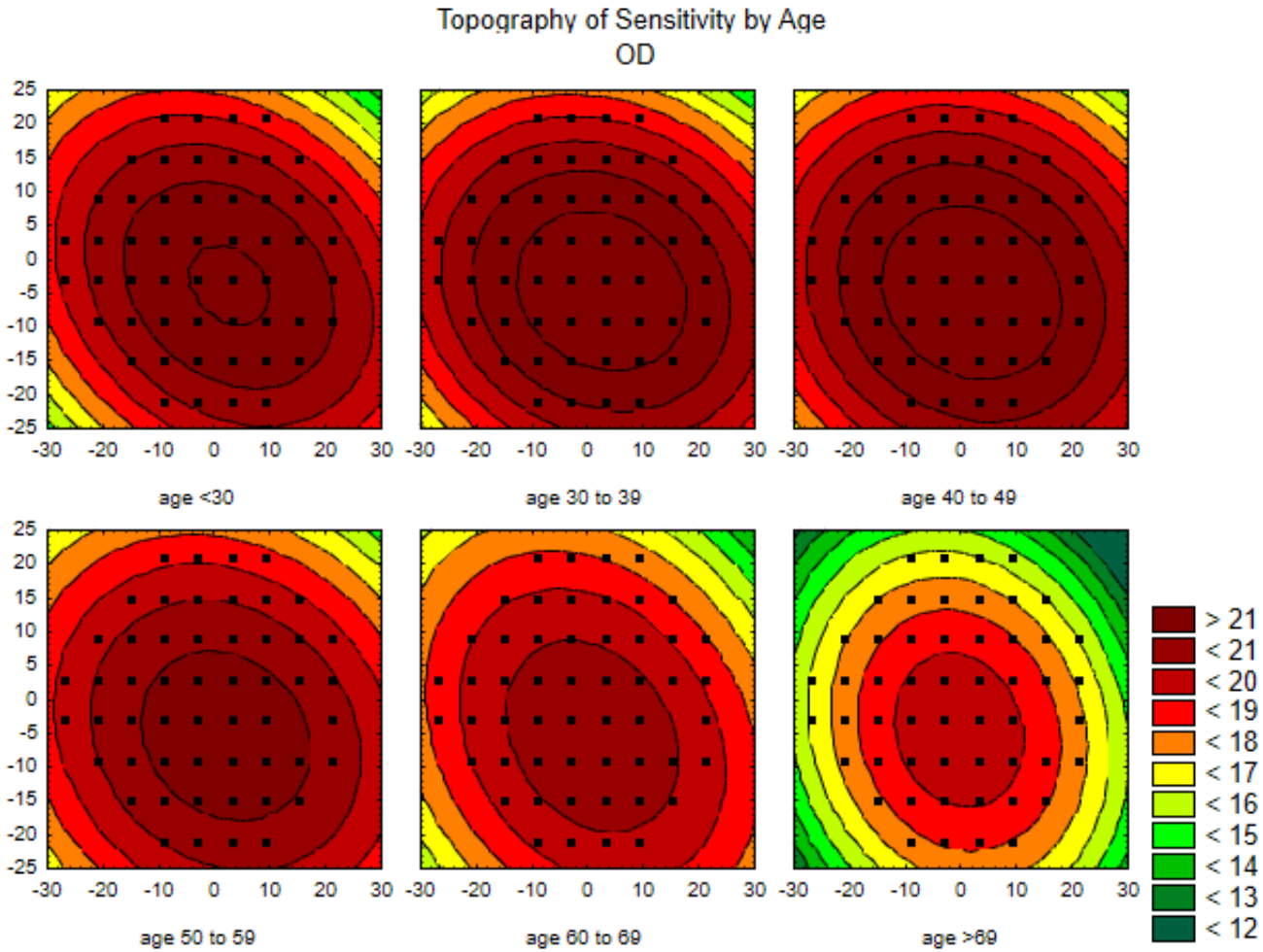


Figure 2-6 Topographic quadratic functions of sensitivity as a function of age (right eye). Test locations were superimposed onto the topography maps.

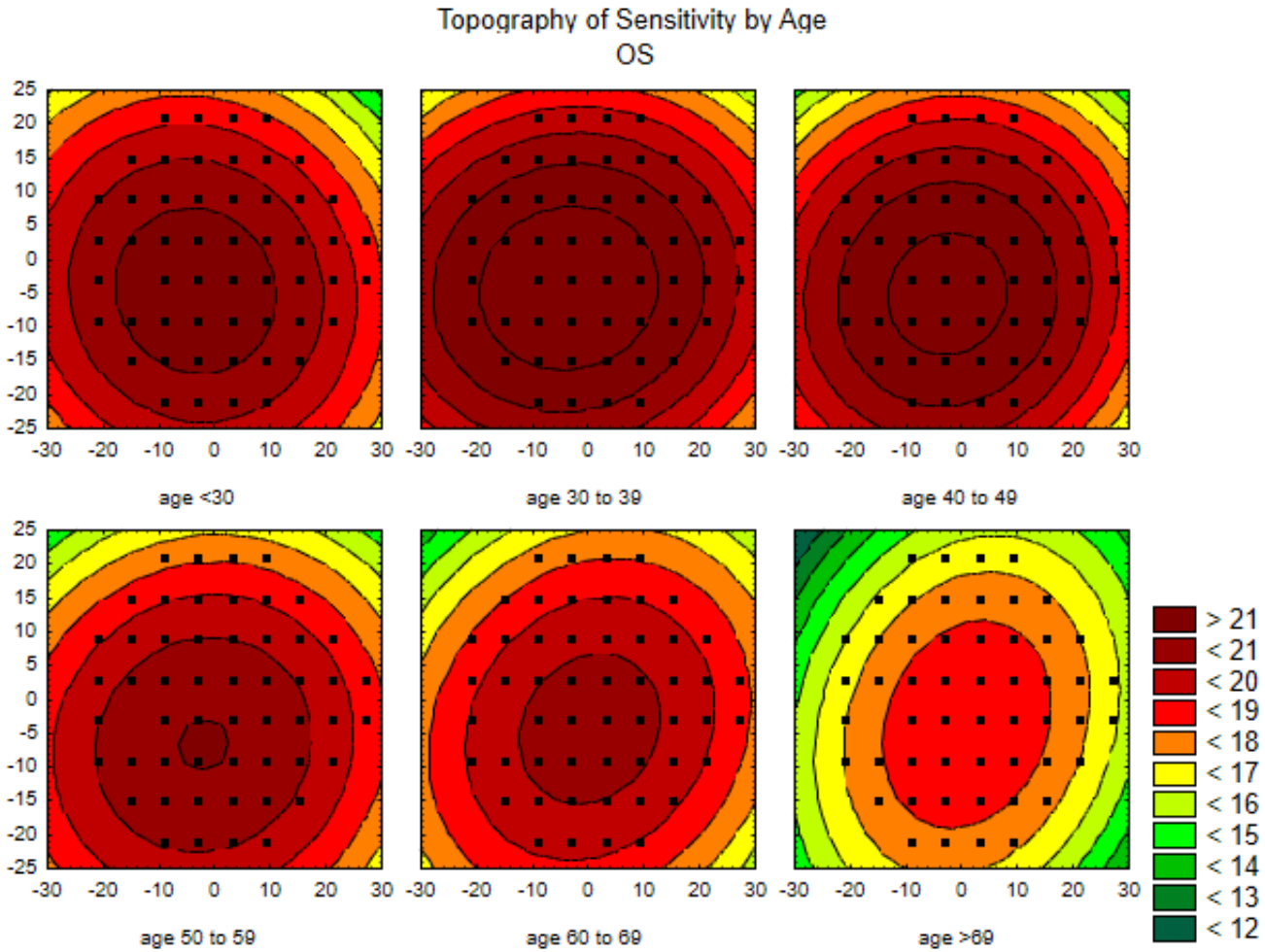


Figure 2-7 Topographic quadratic functions of sensitivity as a function of age (left eye). Test locations were superimposed onto the topography maps.

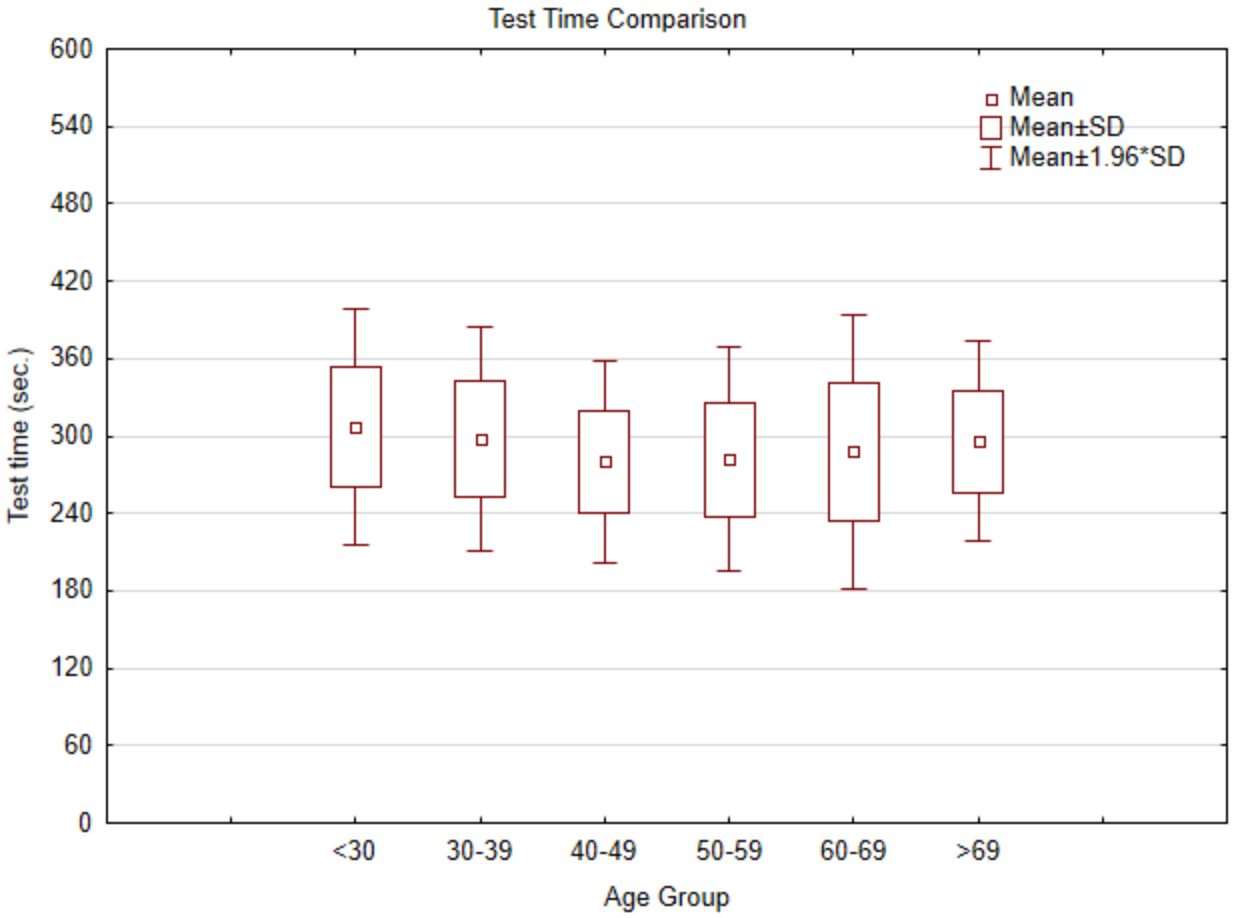


Figure 2-8 Test time in different age groups. Test time was similar across different age groups. An average of 290.2 ±46.5 seconds was recorded.

## 2.5 Discussion

The Flicker Defined Form (FDF) sensitivity decreased with age. Using a linear fit, the decrease was -0.6dB per decade, however, a better fit was described using polynomial regression. A steeper decrease was found in our elder age groups (60-80). Contrast sensitivity decreases with age, by approximately 0.6 dB per decade in the central visual field using both SAP and FDT[5–10]. However, it is important to note that all the perimeters have a different dynamic range, and the detection of nonlinear loss of ganglion cell loss might be influenced by preferred perception pathways, the similar magnitude of sensitivity loss may not be strictly equivalent[8,12,13].

The better fit using the second order polynomial (OD: $r^2$=0.231; OS: 0.235) was found for our data. Previous studies have discussed the effect of aging on SAP mean visual sensitivity using different fitting functions and found that a single term nonlinear function best represented the relationship between sensitivity and aging[14]. In our study (figure 2-2 & 2-3), the linear function overestimated the aging changes from 30 to 60 years and underestimated aging changes for subjects older than 60 years, when compared to the 2$^{nd}$ order polynomial function. A similar 2$^{nd}$ order polynomial function has been previously reported as the best fit for SAP.

The hill of vision represented by the topographic maps in figure 2-6 and figure 2-7 supports previous findings that the inferior hemifield has a higher sensitivity than the superior hemifield, and that the superior temporal quadrant demonstrates slightly lower sensitivity then the rest of the field[5,9]. The topographic isopters further illustrate the steeper drop in sensitivity for participants >60 years.

Previous studies using the FDT[6,7] stimulus reported a significant reduction of 0.7dB between first and second tested eye. A study conducted to investigate the difference sensitivity between the first and second tested eye stated that the reduction with the second tested eye is caused by the difference of light adaptation between the tested and occluded eye[15]. Other possible explanations were the fatigue effect and/or contrast adaptation[16–18]. The flicker defined form perimetry target presentation time is 400ms with a 150ms ramp time, we suspect the contribution of contrast adaptation is minimal. There was a minimum of 5 minutes of rest time between tests, so the possibility of fatigue was also unlikely. The FDF perimeter uses a white translucent occluder that can be placed in front of the non-tested eye. However, We investigated the difference of test sequence using a subset of our data (site 1, n=66), we found a 0.156±2.900dB reduction (p=0.001) among first and second tested eye, see figure 2-9.

Test time between the flicker defined form periemtry 24-2 ASTA-standard test and 24-2 SITA standard were quite similar, ranging around 4-6 minutes on a normal field[19,20]. The similar test time was expected. Due to similar numbers of presentation occurred during the threshold testing, test time to reach completion should not differ.

The normative database will permit the development of analytical tools for the HEP perimeter and the establishment of normal structure/function relationships with imaging devices.

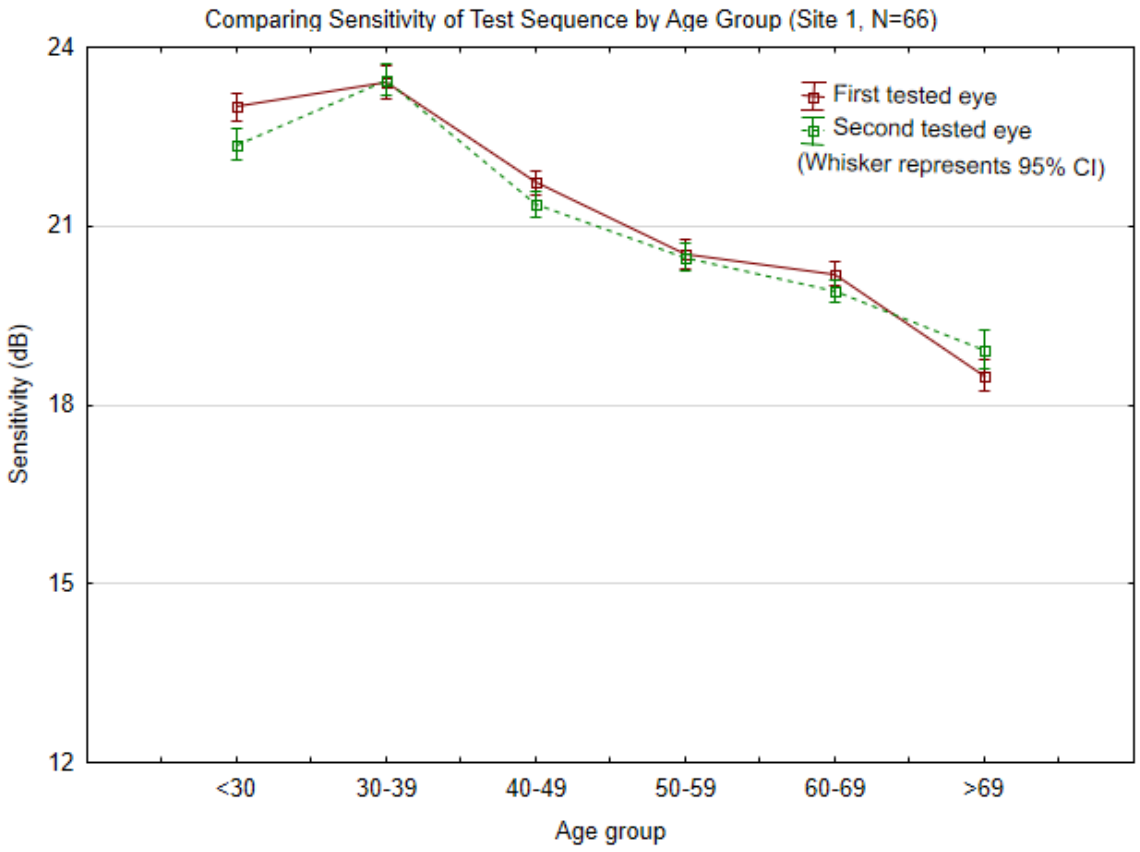


Figure 2-9 Comparison of Site 1's first tested eye & second tested eye by age group. 0.16 dB of difference was found (p=0.001).

# Chapter 3

# The Effect of Dioptric Blur on Flicker Defined Form Perimetry

## 3.1 Overview

**Purpose:** To investigate the effect of dioptric blur on retinal sensitivity for the Flicker Defined Form (FDF) stimulus used in the Heidelberg Edge Perimeter.

**Methods:** The sample consisted of 10 normal subjects (mean age ±SD: 24.3 ± 3.3; M:F 1:1). Visual function was tested over two visits using emmetropic conditions (0 Dioptres of Sphere (DS)) and with 1, 2, 3, 4, 5, 6, 8, 10, and 12 DS of positive blur, tested in random order. The FDF stimuli (5° diameter) were generated using the Heidelberg Edge Perimeter (HEP) and presented at 0°, 4.2°, 12.7°, and 21.2° along the minor meridians of each quadrant of the visual field. The retinal sensitivity was determined using a Bayesian, adaptive staircase threshold estimation method.

**Results:** A linear relationship was found between decreased sensitivity and increased optical blur. FDF sensitivity at fixation was significantly reduced by +10 DS; +6 DS at 4.2° and 12.7°; and +4 DS at 21.2°. There was a significant interaction between Dioptric blur and eccentricity ($p<0.001$); 21.2° gave a steeper slope (-0.79) than that found at fixation (-0.49), 4.2° (-0.42) and 12.7° (-0.47). There was a significant difference between the superior and inferior hemifield ($p<0.001$), with the superior hemifield being more affected by blur, with a steeper slope (-0.68) than the inferior hemifield (-0.44).

**Conclusions:** The FDF stimulus was relatively resistant to positive dioptric blur when compared to previous studies using the contrast pedestal stimuli of standard automated perimetry. There was a significant effect of both eccentricity and hemifield.

## 3.2 Introduction

Dioptric blur reduces contrast sensitivity and visual acuity[1-13]. It has also been shown to influence differential light sensitivity, as typically measured in standard automated perimetry (SAP)[4-7]. In addition, the effect of dioptric blur has been shown to co-vary by eccentricity and target size[1, 2, 5, 13, 14]. Heuer et al. (1987), using a Goldmann size III (0.43 degrees) white on white, contrast pedestal stimulus documented an average 1.27dB decrease in sensitivity per dioptre of sphere (DS). They tested up to 6 DS of blur projecting the stimulus along the horizontal meridian out to 25° eccentricity nasally and found a similar magnitude of sensitivity decrease across eccentricities[15]. This agreed with Weinreb and Perlman[4] who showed an average 1.26dB per dioptre decline in sensitivity within the central 6° also using a Goldmann size III stimulus. They reported that the average decrease in retinal sensitivity was independent of refractive error. Goldstick et al.[6] examined the effect of blur using the standard Goldmann size III stimulus across the entire 30° central field and found an average sensitivity decrease of 1.45 db/DS. The effect of eccentricity was not analyzed.

Stimuli that test temporal vision have been found to be more robust to refractive defocus. Tyler[16] showed resistance up to +10 DS of blur in the fovea using flicker sensitivity with a 5 degree, long wavelength (660 nm) target over a range of frequencies. Similar results were reported by Lachenmayr and Gleissner[17] testing critical fusion frequency (CFF) across the

central 25 degree of visual field. They reported a 5 cycle mean CFF decrease under the effect of +9 DS, suggesting the effect of blur was minimal.

Frequency Doubling Technology (FDT; Carl Zeiss Meditec, Dublin, CA, USA) uses flicker detection sensitivity to a low spatial frequency, high temporal frequency counterphase flicker stimulus to measure visual function across the visual field[18-21]. The sensitivity of FDT was shown to reduce with dioptric blur, but to a lesser extent than differential light sensitivity[22, 23]. It was also shown that the effect of blur was slightly stronger in the center than peripheral locations[22]. Anderson and colleagues[23] reported that 6 diopters of defocus decreased the sensitivity by 0.4 log units for a 5 degree stimulus and 0.1 log units for a 10 degree stimulus, presented at the fovea.

Flicker defined form (FDF) was recently introduced as a stimulus for perimetry (Heidelberg Edge Perimeter, Heidelberg Engineering)[21, 24-27]. FDF is a phase difference stimulus, generated within a field of flickering random dots. Given the temporal flicker characteristics of the FDF stimulus, we hypothesize that it would demonstrate better tolerance to optical blur than differential light sensitivity, as used in standard automated perimetry. The purpose of this study was to investigate the effect of induced dioptric blur and eccentricity on the FDF stimulus.

## 3.3 Methods

Ten participants between the age of 20 and 31 years (gender ratio: 1:1, mean age ± SD: 24.3 ± 3.3) were recruited for the study. All subjects underwent a preliminary examination to ensure they met the inclusion criteria: best-corrected visual acuity of 6/6

(20/20) or better, refractive error less than ±3.50 DS and ± 1.75 dioptres of cylinder (DC), no history of ocular or neurologic disease, or previous ocular surgery. The research adhered to the tenets of the Declaration of Helsinki and informed consent was obtained from all participants. The research was approved by the Human Research Ethics Committee of the University of Waterloo.

Flicker defined form stimuli were presented using a prototype of the Heidelberg Edge Perimeter (HEP; Heidelberg Engineering, Heidelberg, Germany). The stimuli were generated within a field of random dots flickering at 15Hz against a mean luminance background of 50cdm$^{-2}$. The dots within the 5º diameter circular stimulus area were flickered in counterphase to generate a phase contrast stimulus (Dot diameter: 0.32 degrees, dot density: 2.28dots/degree$^2$).

Testing was performed over two visits on two separate days within one week. Participants were given the opportunity to familiarize themselves with the test prior to data collection in order to reduce the effect of learning. This was achieved using the demonstration test mode of the HEP, which illustrates the test procedure. The right eye of each subject was examined using the best-corrected ocular refraction (0D of blur) and with the addition of +1, +2, +3, +4, +5, +6, +8, +10, +12 dioptres of spherical optical blur (DS), in a random order. Full-aperture trial lenses were used and positioned in the HEP trial lens holder. FDF stimuli were presented randomly at 0, 3*3°, 9*9° and 15*15° eccentricity (actual eccentricity of each point 0°, 4.2°, 12.7°, 21.2°) along the 4 minor meridians of the visual field (Figure 3-1), one sensitivity estimate was made per session for each data point. Sensitivity values were determined by a Bayesian staircase threshold estimation algorithm, a

4-2-2 staircase strategy was used at four seed points at 9*9°. Neighboring locations were seeded and a 2-2 staircase was used with a fast termination paradigm incorporated for crossings that happened within the 95$^{th}$ percentile of normality for the age of the subject at the given eccentricity.

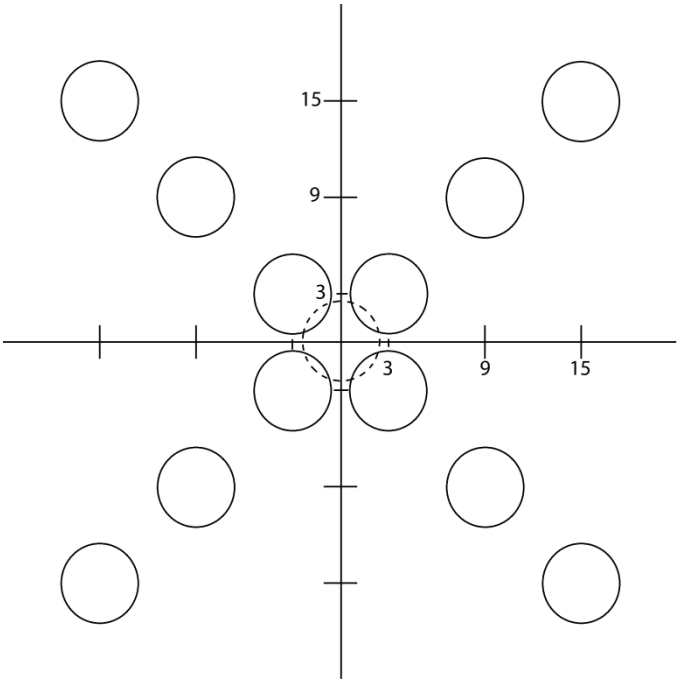


Figure 3-1 Flicker Defined Form stimuli locations. FDF stimuli were presented randomly at 0, 3*3°, 9*9°, 15*15° (actual eccentricity of each point 0, 4.2°, 12.7°, 21.2°) along the minor meridian of each quadrant.

In addition, if the staircase proceeds in a single direction for 3 * 2 dB steps it reverts to 4 dB steps. There are also several endpoint retest strategies[28]. Fixation was monitored using a real-time eye-tracker, which also monitored pupil size throughout each test. Subjects were requested to respond by pressing a button whenever they perceived a stimulus. A

minimum of one minute of resting time was given between each test to reduce the effect of fatigue. Each test condition took approximately 1.5~2 minutes. False positive (FP) and false negative (FN) responses were monitored, any data sets exceeding 20% FPs and FNs were excluded.

Linear regression analysis was performed to show the relationship between the level of Dioptric blur and sensitivity, with particular reference to slope. Repeated measures ANOVA was performed to determine the significance between variables, with eccentricity, hemifield and level of blur as within subject variables. Tukey's HSD post hoc analysis was used to compare pairwise differences.

## 3.4 Results

The effect of dioptric blur was significant ($F_{(9,81)} = 31.860$, $p<0.001$) at all eccentricities in all quadrants. The mean sensitivity decreased by an average of 0.56 dB per diopter (Figure 3-2), with a group mean linear regression of $y=24.49-0.56x$ ($r^2=0.984$). There was a significant difference ($p<0.001$) in mean sensitivity following +5 DS blur compared to the no blur condition. No test results were excluded due to poor reliability.

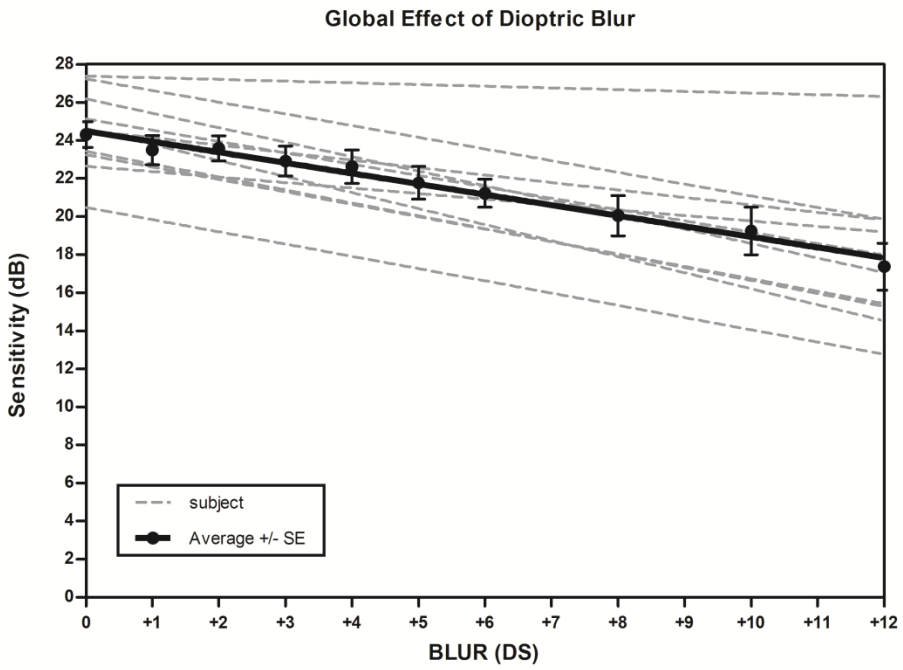


Figure 3-2 Illustration of the global effect of dioptric blur. Showing the linear regression for each subject. Sensitivity decreased with increasing Dioptric blur ($p<0.001$, at +5DS).

Blur had a statistically significant effect on FDF stimuli presented at the foveal point ($F_{(9,81)} = 4.90$, $p<0.001$). The fovea showed a mean sensitivity of 24.40 ± 1.03 dB (Mean±SE) between subjects at Best Corrected Visual Acuity (BCVA) and the sensitivity decreased with increased blur, with a linear regression of $y=25.00-0.49x$ ($r^2=0.877$) (Figure 3-3). The average decrease per dioptre was 0.49 dB. A significant effect of positive dioptric blur on sensitivity change was found with +10 DS and greater (compared to 0 DS, $p=0.007$).

The mean sensitivity without blur at 3*3° eccentricity was 25.63 ± 0.55 dB (mean ± SE) and decreased by 0.42 dB per DS (linear regression: $y=25.72-0.42x$, $r^2=0.968$). The mean sensitivity at 9*9° eccentricity was 25.00 ± 0.80 dB (mean ± SE) and decreased by

0.47 dB per DS (linear regression: y=25.11-0.47x, $r^2$=0.986). The mean sensitivity at 15*15° eccentricity was 22.28 ± 1.00 dB (mean ± SE) and decreased by 0.79 dB per DS (linear regression: y=22.52-0.79x, $r^2$=0.968) (Figure 3). There was a significant interaction between eccentricity and the level of dioptric blur ($F_{(27, 243)}$=1.812, p=0.010), with a steeper decrease of sensitivity at 15*15° compared to fixation, 3*3° and 9*9° eccentricity (p<0.001). Tukey HSD test showed a significant decrease in sensitivity at 3*3° (p=0.035) and 9*9° (p=0.017) using +6 DS of blur or greater, compared to the no blur condition. At 15*15° there was a significant sensitivity decrease using +4 DS or greater (p=0.019).

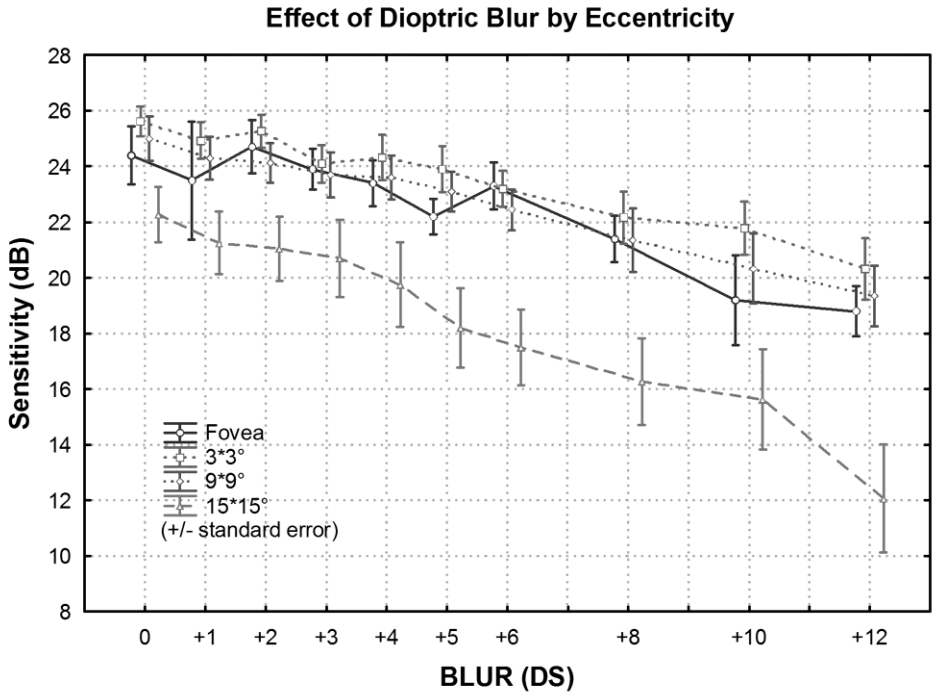


Figure 3-3 Illustration of the effect of blur by eccentricity. Significant differences were found at 21.2° (15*15; p<0.001).

**Effect of Blur Within Hemifield**

The mean sensitivity of the superior hemifield (mean ± SE: 20.16 ± 1.04 dB) was significantly lower ($F_{(1,9)}$= 36.093, p<0.001) than the mean sensitivity of the inferior hemifield (mean ± SE: 23.02 ± 0.72 dB). Linear regression for the superior hemifield was y=23.64-0.68x ($r^2$=0.990), and the inferior hemifield was y=25.26-0.44x ($r^2$=0.946). An average decrease in sensitivity of 0.68 dB per DS was found in the superior hemifield, and 0.44 dB per DS was found in the inferior hemifield. The Tukey HSD test showed a significant sensitivity difference between no blur and +4 DS in the superior hemifield (p=0.003), and between no blur and +8DS in the inferior hemifield (p<0.001) (Figure 3-4). There was a significant interaction between dioptric blur and hemifield ($F_{(9,81)}$= 3.331, p=0.002), with blur being better tolerated in the inferior hemifield.

There was no significant difference ($F_{(1,9)}$= 3.779, p=0.084) in the mean average sensitivity between the temporal hemifield (mean ± SE: 21.30 ± 0.88 dB) and nasal hemifield (mean ± SE: 21.88 ± 0.87 dB). There was no difference found in the interaction between the nasal/temporal hemifield and Dioptric blur ($F_{(9,81)}$= 1.809, p=0.079). Linear regression for the temporal hemifield was y=24.50-0.63x ($r^2$=0.982); and for the nasal hemifield was y=24.39-0.49x ($r^2$=0.978) (Figure 3-5).

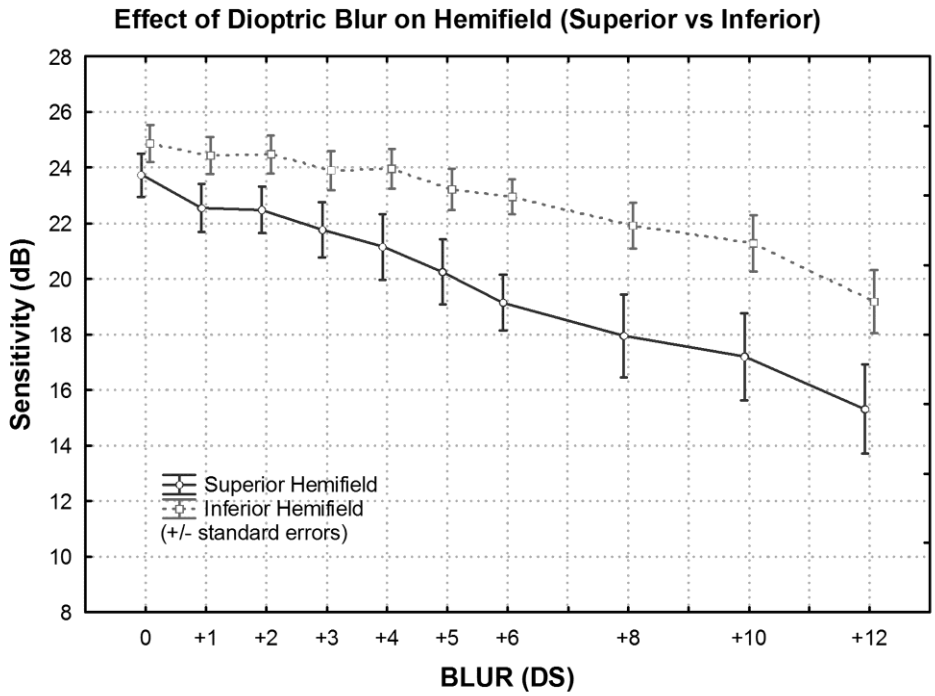


Figure 3-4 Illustration of the effect of blur by sup. /inf. hemifield. Sensitivity was significantly reduced in the superior hemifield ($p<0.001$).

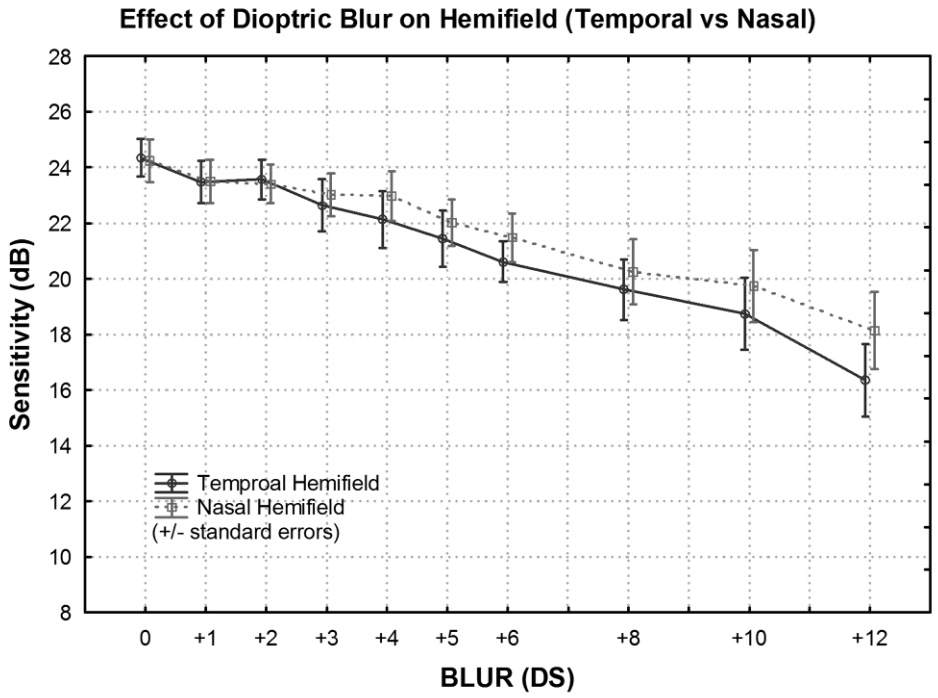


Figure 3-5 Illustration of the effect of blur by tmp. /nsl. hemifield. No differences were found between the nasal and temporal hemifields.

## 3.5 Discussion

Optical defocus is an important consideration when interpreting visual field outcomes; it has previously been shown that defocus reduces differential light sensitivity (DLS) as measured in conventional visual fields[4, 6, 7, 10, 29]. Our results were similar and showed that FDF sensitivity decreased with increased blur up to +12 DS. However, FDF demonstrated a greater tolerance to Dioptric blur with a slope of 0.56 dB/DS, compared to previously reported slopes of 1.26~1.45 dB/DS using a conventional Goldmann size III stimulus[4, 6, 7] (Figure 3-6). In addition, the effect of blur did not reach significance until an average of 6 DS was introduced, although eccentricity was a significant factor with the fovea showing no effect up to 10 DS, dropping to 4 DS at 21.2°.

Similar results were reported by Tyler[16] who tested the effect of optical blur on temporally modulated, flicker stimuli, and reported tolerance to blur up to +6.43 DS. FDT sensitivity also gave similar results being tolerant to blur of up to +6.00[23]. The FDF stimuli used in this study, with a temporal frequency of 15 Hz, gave results that were consistent with those of other temporally driven stimuli[16, 17, 23].

We found the tolerance to Dioptric blur was less at an eccentricity of 21.2° when compared to all the more centrally located stimuli (< 12.7°). Linear regression analysis showed a steeper slope at 21.2° (-0.79) eccentricity than at fixation (-0.49), 4.2° (-0.42) and 12.7° (-0.47) across the tested range of blur. Goldstick and Weinreb[6] described a decrease in sensitivity with increased eccentricity up to 30 degrees. They also stated that +1.00 DS influenced the mean sensitivity significantly within the 30° visual field. Similar results were described by Heuer et al. [7] using the same size III Goldmann stimulus.

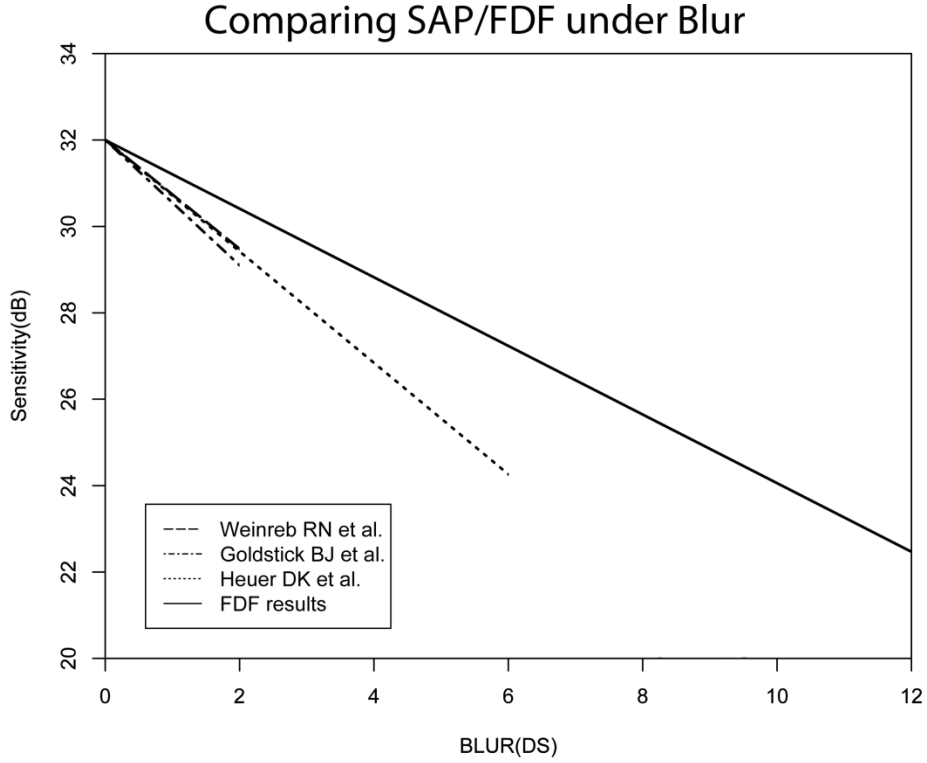


Figure 3-6 Comparison of the effect of blur on SAP/FDF. Comparison of the effects of dioptric blur on differential light sensitivity in our study and previous studies investigating the Goldmann size III stimulus.

Superior/inferior asymmetry and temporal/nasal symmetry were reported by Silva et al.[30] using FDT stimuli (0.25 cpd sinusoidal grating). Our study showed similar asymmetry with the superior hemifield being more affected by Dioptric blur than the inferior hemifield. Similarly, the intercept for the superior hemifield showed reduced sensitivity to FDF stimuli when compared to the inferior hemifield. These differences likely correspond to the lower ganglion cell density in the inferior retina[31, 32].

It is possible that the increased magnification induced by positive dioptric blur could confound the results. For a thin lens of power F, spectacle magnification is M= 1/1-zF,

where z is the distance between the lens and the entrance pupil of the eye[33]. The maximum spectacle magnification in our experiment for +12 DS lens with a back vertex distance of 12mm would be approximately 13%. We have previously shown that for a 5$^{o}$ stimulus size, as used in this study, such an effect would be minimal[27].

In conclusion, Flicker Defined Form showed increased resistance to blur when compared to conventional standard automated perimetry, and gave a similar performance to other temporally modulated stimuli.

# Chapter 4
# Detection of Functional Defect in Early Glaucoma using Standard Automated Perimetry and Flicker Defined Form Perimetry

## 4.1 Overview

**Purpose:** To compare the detection of functional loss in early glaucoma using standard automated perimetry and flicker defined form perimetry.

**Methods:** 156 participants with early to moderate glaucoma were recruited (average age: 62.6±11.0; 75 male, 78 OD). Humphrey Field Analyzer (HFA) SITA-Std 24-2 visual fields were used to classify participants using a modified Hodapp-Parrish-Anderson criteria, resulting in 130 eyes with early glaucoma and 26 with moderate glaucoma (MD: -2.12±2.04dB; PSD: 2.56±1.78dB). The Heidelberg Edge Perimeter (HEP) was used to perform both standard automated perimetry (HEP-SAP) and flicker defined form perimetry (HEP-FDF). Of note is that both forms of perimetry share the identical normative database. Participants were tested on 3 visits within a 3 month period, including HFA SITA-Std 24-2 (visit 1), HEP-SAP ASTA-Std 24-2 (visit 2&3) and HEP-FDF ASTA-Std 24-2 (all visits). Subjects with unreliable visual fields were excluded from the study.

**Results:** The HEP-FDF gave more defects (2514 Pattern Deviation (PD) < 5%, 1568 < 1%, 1357 less than 0.5%; MS:13.33±6.34 dB) than HEP-SAP (1817 PD < 5%, 833 < 1%, 647 < 0.5%; MS: 27.89 ±3.91 dB). Test-retest characteristics were similar for both HEP-FDF(CoR=0.82dB) and HEP-SAP(CoR=0.75dB). Test time was significantly longer for

HEP-FDF (463.12±150.97 sec) than HEP-SAP (353.19±75.84 sec)($p<0.001$), due to the larger number of field defects detected by HEP-FDF.

**Conclusion:** Visual field defects were detected earlier by HEP -FDF when compared to HEP SAP in early glaucoma. Both tests gave similar test-retest characteristics. There was a similar test-time for similar amounts of defect. The greater the defect the longer the test time.

## 4.2 Introduction

Standard automated perimetry has been widely accepted to detect visual function loss and monitor disease progression in glaucoma. The detection of visual field defects compliments the defects found in structural measurements in glaucoma diagnosis[1, 2]. It has been estimated that visual field abnormality can be detected after more than 30% retinal nerve fibre loss. However, in the Ocular Hypertension Treatment Study 85.9% of abnormal test points were unconfirmed when repeated [3]. The variability of abnormal visual field locations was found to be higher than normal locations[4-7]. When using standard automated perimetry locations with defect less than 20dBs have high test-retest variability[4, 5, 8], and repeated testing is recommended for early diagnosis and the monitoring of progression[9].

Flicker defined form (FDF) was developed in an attempt to better detect visual field loss in early glaucoma. The stimulus is generated using a full field of flickering random dots on an achromatic, mean luminance background. A 5 degree diameter stimulus is generated by changing the phase of the flickering dots within the stimulus area to be opposite that of the background dots. This creates an illusory, pop-up target. The subject was instructed to

respond to the “pop-up” illusion. In an observational study, this technique has shown potential for higher sensitivity and specificity in the detection of early glaucoma[10]. In early glaucoma, FDF visual field defect correlated better with estimates of retinal nerve fiber layer thickness than standard automated perimetry, especially in the superior temporal and inferior temporal quadrant[11]. A recent study concluded that FDF perimetry found more patients with abnormalities identified by the glaucoma hemifield test (GHT) and cluster point analysis (CPA) than conventional perimetry[12].

The purpose of our study is to compare the visual field results in patients with early glaucoma using FDF and standard automated perimetry (SAP) on the Heidelberg Edge Perimeter (HEP) and to investigate their test re-test characteristics. The normative database used identical participants and analyses for HEP-SAP and HEP-FDF tests, which for the first time allows for the comparison of different functional tests using the same “normal” database. Testing threshold strategies were also identical for both tests, and help reduce other test specific biases [8, 13].

## 4.3 Methods

Participants and test protocol

165 patients with early glaucoma were recruited to participate in the study. The study adhered to the Declaration of Helsinki, informed consent was obtained from all participants prior to testing. Participants were recruited from multiple test sites including University of Waterloo, Southern California School of Optometry, Illinois College of Optometry, University of Houston College of Optometry, NY Harbor Health Care System and the

Toronto Western Hospital. Participants were tested 3 times over a 6 week period to minimize the chances of visual field change due to disease progression. One eye was randomly assigned if both eyes were eligible for the study. Patient history, slit lamp examination, Goldmann applanation tonometry, and Heidelberg Retina Tomograph II examination were performed on visit 1 prior to visual field testing, to ensure that patients met the inclusion criteria. After the initial visit, the Humphrey Field Analyzer (HFA; SITA-Std SAP) results were used to classify the severity of glaucoma based on a modified Hodapp-Parrish-Anderson criteria (Table 4-1). The sequence of tests were randomized, and included: Humphrey Field Analyser, 24-2 SITA-standard on visit 1, Heidelberg Edge Perimeter standard automated perimetry, 24-2 ASTA-standard (HEP-SAP) on visits 2 and 3, Heidelberg Edge Perimetry Flicker Defined Form perimetry 24-2 ASTA-standard (HEP-FDF) on all visits.

| **Visual field indices** | **Early Glaucoma** | **Moderate Glaucoma** |
|---|---|---|
| Mean Deviation | ≥ -6 dB | ≥ -12 dB |
| P<0.05 | Fewer than 25% (14/54) of locations on the pattern deviation plot | Fewer than 50% of locations on the pattern deviation plot |
| P<0.01 | Fewer than 7/54 of locations on the pattern deviation plot | Fewer than 14/54 of locations on the pattern deviation plot |

Table 4-1 Modified Hodapp-Parrish-Anderson criteria.

The Heidelberg Edge Perimeter (Heidelberg Engineering GmbH) is a visual function testing device that uses a CRT screen. This allows the presentation of the standard Goldmann size III targets (HEP-SAP) and flicker defined form (FDF) targets. The device incorporates a real time eye tracker to monitor fixation and measures pupil size[14]. Standard automated perimetry (HEP-SAP)[14] presents a static white stimulus on an isoluminant background of 10 $cdm^{-2}$. The target size is 0.43 degrees (Goldmann size III) for 40dB to 16dB during the test, and increases in size from 15dB to 0dB to provide perceptual equivalence to the Humphrey Field Analyzer (Carl Zeiss Meditec, Dublin, USA).

Flicker defined form (HEP-FDF)[14] is generated using an achromatic background of $50cdm^{-2}$ covered with random dots flickering at 15 Hz (0.34 diameter, 3.5 dot/degree). The stimulus appears when the flicker phase of a 5 degree patch becomes opposite to the background dots.

An Adaptive Staircase Thresholding Algorithm (ASTA-std)[14] is used to estimate sensitivity for both HEP-SAP and HEP-FDF. Four seed points at 15*15 were tested using a 4-2-2 algorithm, neighboring locations then used a 2-2 strategy with the test terminating when within age-matched confidence limits.

## 4.4 Results

Nine participants were excluded from the study due to severe glaucoma and/or unreliable visual field results (FP>15%, FN>20%). The mean age of our sample was 62.6±11.0 years, ranging from 31 to 87 years. There were 81 females. 130 of the 156 eyes were classified as having early glaucoma, and 26 were classified as having moderate

glaucoma, using the modified Hodapp-Parrish-Anderson criteria. Average Mean Deviation (MD) of the HFA-SAP was -2.12 ± 2.04 dB, ranging from -7.90~ 1.66 dB. Average Pattern Standard Deviation (PSD) of the HFA-SAP was 2.56 ± 1.78 dB.

The frequency of defect depth categories were compared between visit 3 of the HEP-SAP and HEP-FDF. Frequency counts of the Total Deviation (TD) and Pattern Deviation (PD) normal, 5%>p>2%, 2%>p>1%, 1%>p>0.5% and p<0.5% defect depths were compared (Figure 4-1). There were significantly greater TD defect counts for HEP-FDF, PD were similar with HEP-SAP other than defect p<0.5%. This suggests that when a HEP-FDF stimuli are defective, they are more likely to present as deep defect.

Based on the probability classification, i.e. “normal”, “5%>p>2%”, “2%>p>1%”, “1%>p>0.5%” and “p<0.5%”, the frequency of TD retest sensitivity deviation was examined (the difference of test and retest) (Figure 4-2). There was a wider spread of retest sensitivity values as the defects deepened. HEP-SAP had less spread in all classifications compared to HEP-FDF, however, the HEP-FDF retest was more repeatable (i.e. average differences closer to the 0) when defect was detected.

Test-retest was compared using the results from visit 2 and visit 3. 5% and 95% confidence limits were plotted and fitted with a Lowess function (Figure 4-3a and 4-3b). The HEP-SAP variability increased at approximately 20 dB and lower sensitivities. HEP-FDF variability remained similar over the entire range of testing. The HEP-SAP Bland-Altman plot showed a mean of differences (MoD) of -0.17dB and Coefficient of Repeatability (CoR) of 5.33dB (Figure 4-3c); HEP-FDF Bland-Altman plot showed a MoD of -0.37dB and a CoR of 7.05 dB (Figure 4-3d).

HEP-FDF showed more spread than HEP-SAP but more precision (peak close to 0dB), with a slight increase in the spread as defect deepened.

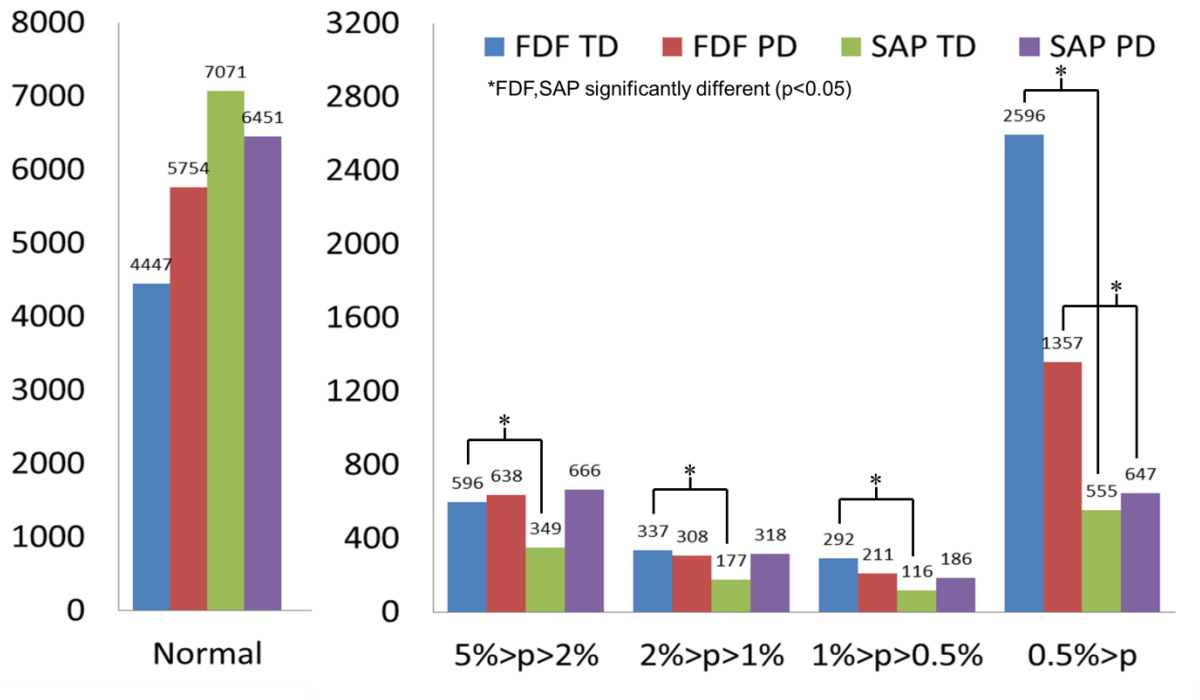


Figure 4-1 Counts of TD and PD using HEP-FDF and HEP-SAP. All test locations for 156 participants were classified for HEP-FDF and HEP-SAP. TD defect counts were significantly greater for HEP-FDF. PD were similar, other than at p<0.5%, though the normal databases were matched.

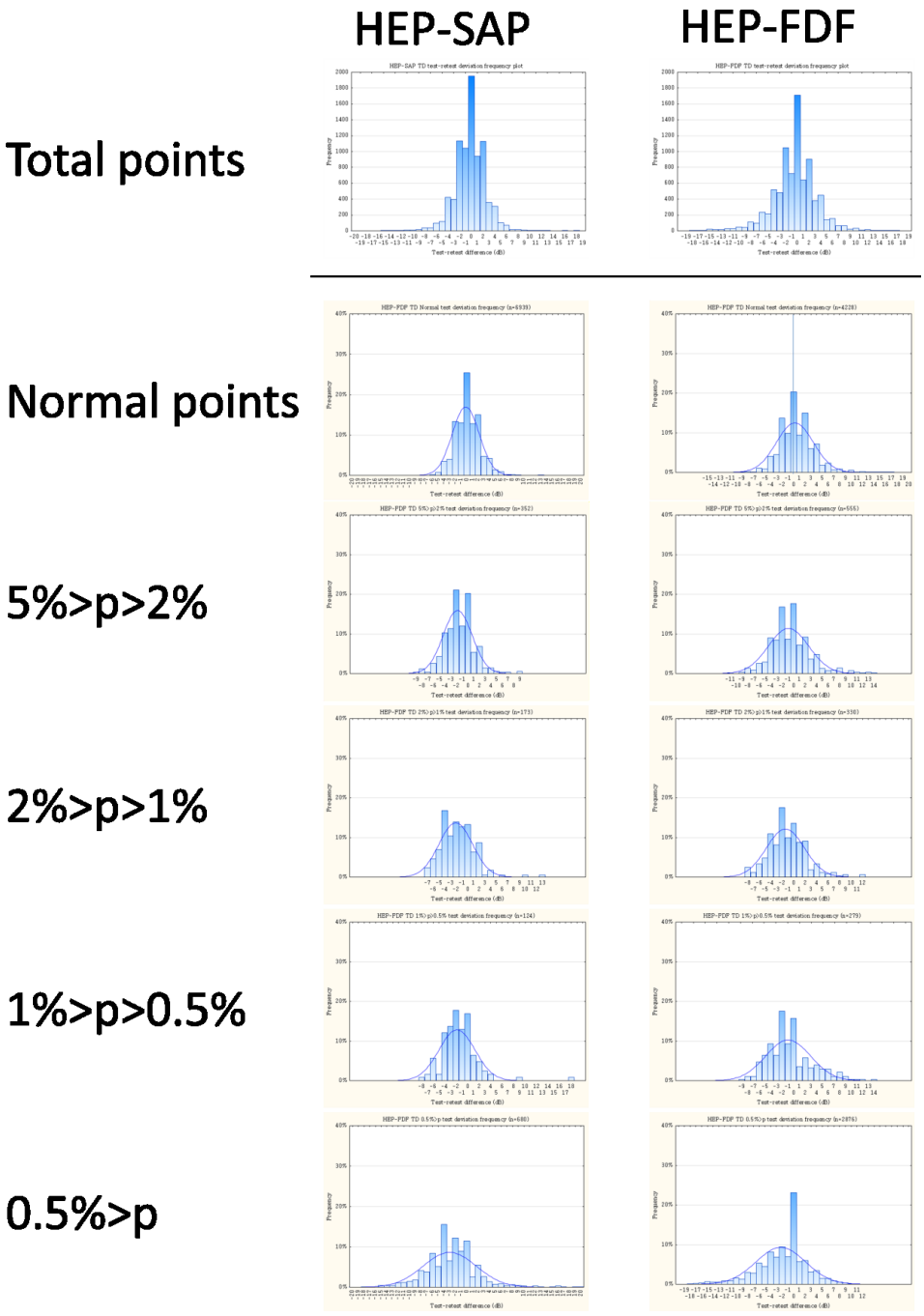


Figure 4-2 Plots showing frequency distribution of TD retest difference. HEP-SAP showed less spread when defects were close to “normal”, and gradually increase of spread with more defect.

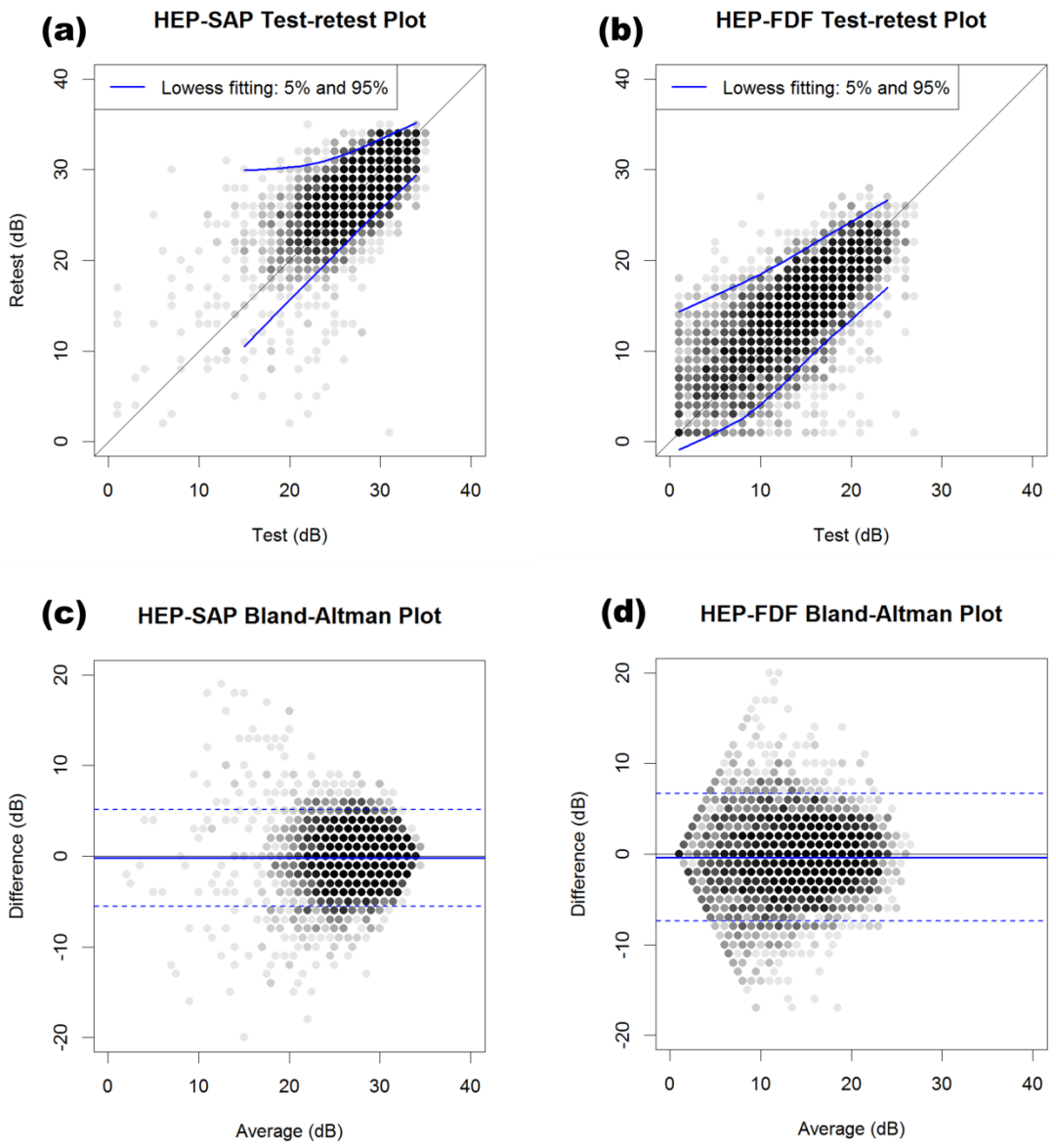


Figure 4-3 Test-retest plot of HEP-SAP and HEP-FDF sensitivity. a. The HEP-SAP test-retest difference decreased below 20 dB. b. HEP-FDF test-retest was similar across defect range. c. HEP-SAP Bland Altman plot showed a Mean of Differences of -0.17dB, CoR=5.33dB. d. HEP-FDF Bland Altman plot showed a Mean of Differences of -0.37dB, CoR= 7.05dB.

Repeatability of the probability classification was also calculated. When a location was classified as abnormal ("5%>p>2%", "2%>p>1%", "1%>p>0.5%" and "0.5%>p"), higher percentages of repeated abnormal classifications were found using HEP-FDF (Table 4-2). When a location was classified at a certain probability, higher percentages of the same classification was found when testing with HEP-FDF compared to HEP-SAP (Table 4-3).

| | FDF | SAP |
|---|---|---|
| TD | 56.6% | 32.9% |
| PD | 38.1% | 21.8% |

Table 4-2 Repeatability of probability classification (test abnormal and retest abnormal)

| | FDF | SAP |
|---|---|---|
| TD | 77.7% | 53% |
| PD | 62.1% | 46% |

Table 4-3 Repeatability of probability classification (test classification equals retest classification)

Figure 4-4 shows the relationship between HEP-SAP and HEP-FDF. Principal curve[15] analysis showed an almost linear relationship between SAP/FDF between SAP sensitivities greater than 22dB. However, FDF showed a much greater defect depth, with a slope of 2 over this range.

Test time was different between HEP-SAP and HEP-FDF ($p<0.001$). The average test time in our sample is $354.2 \pm 77.6$ and $458.4 \pm 150.3$ seconds for the two different tests respectively. The distribution is shown using a violin plot in Figure 4-5.

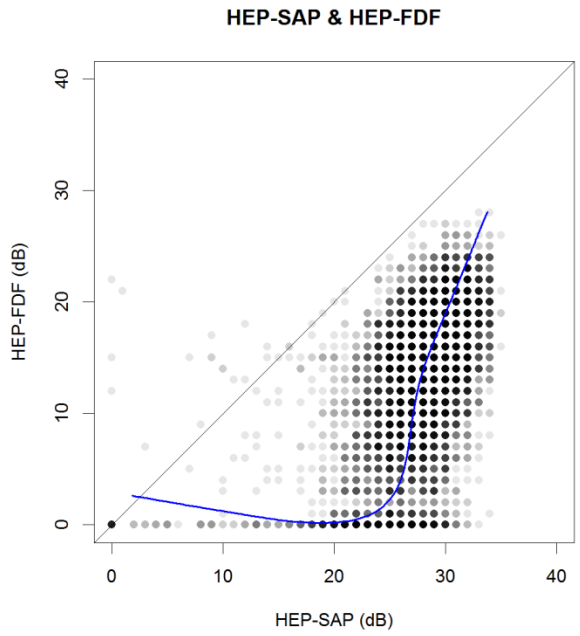


Figure 4-4 Principal curve fitting through scatterplot of HEP-SAP and HEP-FDF for visit 3. A linear slope of approximately 2 was found between HEP-SAP and HEP-FDF when HEP-SAP sensitivity was tested greater than 22dB.

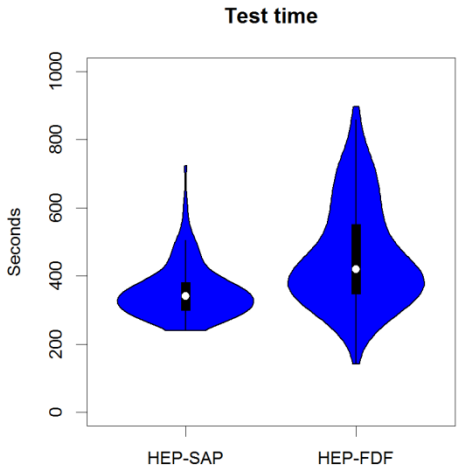


Figure 4-5 Violin plot of test times between HEP-SAP and HEP-FDF. Test-time was different between HEP-SAP and HEP-FDF ($p<0.001$). HEP-FDF took a longer time due to more defect depth and a greater number of presentations.

## 4.5 Discussion

Test-retest variability of HEP-SAP increased dramatically at locations where more defect was present (<20dB), this was similar to findings in other studies[4, 5, 8]. When HEP-SAP defect is deeper, the retest is more variable, whereas the HEP-FDF test-retest results showed similar variability across the perimeter's testing range, although variability is slightly greater in locations with the deepest abnormality (0.5%>p). There was a steep, linear relationship between SAP and FDF when HEP-SAP gave a sensitivity of 22 dB or greater, with a slope of approximate 2. When patients with early glaucoma were tested and defect was present, HEP-FDF has twice the decibel steps than HEP-SAP to detect initial glaucoma damage.

The fundamentals of the two stimuli are different, making comparison of HEP-SAP and HEP-FDF by decibel values problematic. Previous studies looking at the effective dynamic range of perimeters have analyzed the testing range and its variability[6]. If the same approach was used in our testing, the HEP-SAP showed 3 discriminable threshold sensitivity steps in our early group of glaucoma patients, while the HEP-FDF showed 4 discriminable threshold sensitivity steps. Whether this extra step is relevant in the management of glaucoma progression cannot be determined due to the nature of our cross-sectional study design. However, we can conclude that in early glaucoma testing, the HEP-FDF has an advantage over HEP-SAP by providing more range of measurement.

The normative database of HEP-SAP and HEP-FDF was derived from the same group of "normal" patients. In addition, the threshold estimation strategy is also identical for both techniques. This allows us to compare the two tests based on the same group of "age matched normals" to rule out the effect of different normative databases and test strategies when comparing different perimetry tests. In our group of patients, the classification in the total deviation and pattern deviation plots showed significant difference in the number of defects detected on our early glaucoma patients. The HEP-FDF classified more defects than HEP-SAP. This indicates that the HEP-FDF is detecting more abnormal locations in the early stage of glaucoma compared to HEP-SAP.

Our finding that the ability of FDF to detect early defect when compared to SAP agrees with a previous observational study[10]. An improved structure-function relationship for FDF than SAP in the inferior temporal and superior temporal regions of the optic nerve was also reported[11]. Abnormal HEP-FDF glaucoma hemifield classifications and defect clusters

were found when SAP results were within normal limits[12]. However, combining results of different functional tests may further improve disease detection[16].

Test time was longer for the HEP-FDF. This result was not surprising with both methods using the same threshold estimation strategy and the HEP-FDF finding more defect than the HEP-SAP. More defect results in more stimulus presentations resulting in a longer test time. The target size of the HEP-SAP and HEP-FDF differs, with HEP-FDF presenting a larger stimulus. This size difference could possibly be contributing to a better test-retest repeatability[17, 18].

In our study, we investigated visual field defects in patients with early to moderate glaucoma using SAP and FDF. Most subjects showed little abnormality using standard automated perimetry. The HEP-FDF detected more and deeper visual field defects. FDF allowed function loss to be detected earlier than SAP. There are advantages in the detection of early functional damage in glaucoma, however, FDF might not be suitable for the management of disease progression given the initial defect depth often found when using FDF.

# Chapter 5
# The Structure-Function Relationship between Scanning Laser Tomography, Flicker Defined Form Perimetry and Standard Automated Perimetry in Early Glaucoma

## 5.1 Overview

**Purpose:** To investigate the structure and function relationship between scanning laser tomography (SLT), flicker defined form (FDF) perimetry and standard automated perimetry (SAP).

**Method:** One eye of 119 participants (mean age 63.45±9.12 years, 40 to 83 years, female=61) with early to moderate glaucoma performed SAP, FDF and scanning laser tomography in 3 visits over a 6 week period. The Heidelberg Edge Perimeter (HEP) was used to present both the FDF and SAP stimuli. Data was analyzed using normative databases from the same participants. The relationship between global and sectoral optic nerve (ON) parameters (Heidelberg Retina Tomograph; HRT) and the corresponding mean sensitivity (MCD; $cdm^{-2}$) of FDF and SAP were analyzed.

**Results:** The mean MCDs for FDF and SAP were 16.10±9.30 and 17.38±6.42 $cdm^{-2}$. There was a significant correlation between the FDF and SAP MCD, and HRT rim area ($p<0.001$), with FDF giving better correlations. Robust locally weighted regression of the inferior-temporal sector comparing the fit of FDF/HRT and SAP/HRT revealed different structure-function relationships, with FDF/HRT showing a steep slope and clear synergy

below a rim area of 0.18 $mm^2$, and SAP/HRT being relatively flat across the entire range of measurement.

**Conclusions:** There was moderate to poor linear correlation comparing HEP/HRT results in participants with early glaucoma, with the best correlation found in the inferior temporal sector of the optic nerve. FDF correlated better with HRT than SAP, and detected glaucomatous visual field loss earlier than SAP. FDF showed a strong structure-function relationship below an ON rim area of approximately 1.3$mm^2$ (0.18 $mm^2$ for the I-T sector).

## 5.2 Introduction

Combining both structural and functional information in the diagnosis of early glaucoma has been shown to improve diagnostic performance when compared to considering individual tests in isolation[1-9]. A slight to moderate correlation has been reported between measures of structure and function,[10-16] and it has been proposed that there is a linear correlation between retinal ganglion cell density and visual sensitivity if both are measured using a similar scale, whether linear[6, 15, 17] or logarithmic[18, 19]. Several models that attempt to combine structure and function in glaucoma diagnosis have been published[7-9, 20, 21]. Longitudinal studies suggest that measurements made from structural techniques and functional techniques identified different subgroups of patients.[4, 5, 22] Most studies suggest that detection of structural damage using optical coherence tomography preceded the detection of functional damage with standard automated perimetry (SAP).[23] Better test re-test reliability and the use of variable target sizes could possibly account for the different correlations found in these studies[24, 25].

Currently, standard automated perimetry (SAP) is the reference standard for assessing the visual field and progression in glaucoma. Analysis of an individual's response to the traditional white-on-white stimulus provides information about possible types and stages of ocular disease according to the pattern and extent of the defect recorded during testing[26]. Various alternative methods to SAP have also been developed: FDT, Pulsar, MDT, SWAP, etc.

Flicker defined form[27] (FDF) is generated by flickering random dots on a background of known luminance. Dots within the stimulus area flicker in counter-phase to those outside the stimulus area, creating an illusory stimulus. The stimulus appears to "pop-up" from the background. The Heidelberg Edge Perimeter (HEP; Heidelberg Engineering, Heidelberg, Germany) uses a 5 degree diameter FDF stimulus for its 24-2 and 30-2 programs (3 degree diameter for 10-2), in addition to performing SAP[34]. Several studies have reported the advantages that a larger stimulus size offers, including better test repeatability and being less affected by defocus[24, 35]. The HEP-SAP uses the traditional Goldmann size III target (0.43$^{o}$ diameter) between 40dB and 16dB, at which point the monitor based system is unable to produce a sufficiently bright stimulus. To compensate the stimulus remains approximately equiluminant between 15dB and 0dB, but increases in size in order to generate stimuli of equivalence to SAP, size III. This has the added advantage of improving the test-retest characteristics in the <15dB range, resulting in narrower confidence intervals and tighter definitions of abnormality.

The purpose of our study was to investigate the correlation between structure and function using scanning laser tomography, flicker defined form perimetry and standard automated perimetry.

## 5.3 Methods

In this cross-sectional cohort study, participants were recruited from the Glaucoma Service of the Toronto Western Hospital, University Health Network, Toronto. The sample consisted of 119 participants ranging from 40-83 years (mean age 63.45 ± 9.12 years, female= 61), and diagnosed with early (105) to moderate (14) glaucoma. If both eyes were eligible for inclusion, one eye of each participant was randomly assigned (57 OD). This study adhered to the declaration of Helsinki, informed consent was obtained from all participants.

Recruitment criteria required early to moderate glaucoma using a modified Hodapp-Parrish-Anderson classification. Early glaucoma was defined using Humphrey visual fields (Carl Zeiss Meditec, Dublin, CA) whereby mean deviation (MD) was better than -6dB, less than 14 locations on the pattern deviation plot were depressed at the 0.05 level, and less than 7 locations were depressed at the 0.01 level. The classification of moderate glaucoma was assigned when mean deviation (MD) was better than -12dB, less than 27 locations on the pattern deviation plot were depressed at the 0.05 level, and less than 14 locations were depressed at the 0.01 level. Exclusion criteria included best corrected visual acuity (BCVA) worse than 20/30 (6/9) in either eye; refractive error greater than 5 diopters sphere or 2.5 diopters cylinder; any optic neuropathy other than glaucoma; any ocular/systemic disease that would affect the visual field; unreliable visual fields, showing a false positive rate of

15% or greater, a false negative rate of 20% or greater; and poor quality scanning laser tomography (SLT) images.

The study consisted of 3 visits over a 6 week period. Standard eye examinations including family history, visual acuity, slit lamp biomicroscopy, Goldmann tonometry, and fundus photography were performed during the first visit of the study to ensure subjects met the study criteria. Humphrey Field Analyzer (HFA) II (Carl Ziess Meditec, CA, USA) 24-2 SITA standard visual field tests were performed on both eyes during the first visit and the stage of glaucoma was defined according to the modified Hodapp-Parrish-Anderson classification.

Flicker defined form perimetry (HEP-FDF) 24-2 ASTA-Standard was performed on all 3 visits using the HEP. Standard automated perimetry using the HEP (HEP-SAP) 24-2 ASTA-Standard test was performed on visits two and three. Scanning laser tomography images of the optic nerve were acquired on the first two visits using the Heidelberg Retina Tomograph II (HRT II, Heidelberg Engineering, Heidelberg, Germany). Visual field tests were done in random order. HRT was done at the end of visit. The last visit was used for analyses to minimize the learning effect.

Statistical analysis: The HEP-SAP/HEP-FDF visual fields were organized by location into six sectors corresponding to the six HRT Moorfields' regression analysis sectors as proposed by Garway-Heath and colleagues[36]. Linear regression and Pearson's correlation coefficients were used to analyze the relationship between global and sectoral mean luminance ($cdm^2$) of HEP-SAP/ HEP-FDF and HRT rim area. In addition, the relationship was expressed using robust locally weighted regression (Lowess smoothing) (R package

version 1.5.2)[37]. Kappa analysis was used to score the concordance between global and sectoral classifications. Classifications for both the HRT and HEP sectors were defined as within normal limits (WNL) (<95$^{th}$ percentile of the normal database), borderline (BL) (95%-99% of the normal database), and outside normal limits (ONL) (>99% of the normal database).

## 5.4 Results

Group mean descriptive statistics of HEP-FDF mean luminance (MCD), HEP-SAP mean luminance, and HRT parameters are given in Table 5-1.

Linear regression of HEP-FDF and HRT results showed a mild to moderate (r=-0.27~-0.52) correlation between mean luminance and rim area, with the best correlation in the inferior-temporal sector (r=-0.52) and the worst correlation in the nasal sector (r=-0.27). The relationship between HEP-FDF mean luminance and global rim area is shown in Figure 5-1, while the relationship for the inferior temporal sector is shown in Figure 5-2. Results of correlation coefficient values between HEP-FDF mean luminance and HRT rim area are provided in Table 5-2. Figures 5-1 and 5-2 also show the relationship using robust locally weighted regression. There is a clear inflection point, showing the rim area below which a clear and steep correlation exists between the measures of structure and function, at approximately 1.3mm$^2$ for the global comparison and 0.18mm$^2$ in the inferior temporal sector.

There was a mild correlation between mean luminance as measured by HEP-SAP and rim area as assessed by HRT (r=-0.05~-0.45). The linear relationship between mean

luminance and global rim area is shown in Figure 5-3, and for the inferior temporal sector in Figure 5-4. The correlation coefficients between HEP-SAP mean luminance and HRT rim area are provided in Table 5-2. There is no obvious inflection point following robust locally weighted regression in figures 3 and 4, showing the flat slope of linear relationship between SAP and HRT rim area.

Kappa analysis was performed to investigate the concordance between classifications (Table 5-3). Fair concordance was found in 4 of the 6 sectors (superior-nasal, nasal, inferior-nasal, and inferior temporal), when comparing HEP-FDF Mean Deviation (MD) and HRT rim area. However, the superior-temporal and temporal sectors showed only slight concordance between classifications. Fair concordance was found in the temporal, inferior-temporal, inferior-nasal and nasal sector when comparing HEP-SAP MD and HRT rim area. There was only slight concordance in the other two sectors (Table 5-4).

Figures 5-5 (FDF) and 6 (HRT) superimpose the classification information for all the HRT and HEP data with the robust locally weighted regression for the inferior-temporal sector. The fit plotted between FDF and HRT data showed a steep slope from a rim area of approximately 0.18mm$^2$ and lower, whereas the SAP and HRT provided relatively flat distributions across the whole measurement range. It is clear that there is substantial agreement in the classification of abnormality between HEP-FDF and HRT, but there is also disagreement with both structure and function showing independent abnormality. However, there were fewer times when SAP was abnormal and only 4 participants showed an abnormal SAP and normal HRT, whereas there were a substantial number that showed an abnormal HRT rim area and normal SAP. The number of “abnormal” HEP-FDF results that both agree

and precede HRT detection (abnormal was defined when classified as ONL and BL), indicates that HEP-FDF was better than SAP at detecting early functional loss associated with glaucoma (Table 5-5 and Figure 5-5 & 5-6).

| | Global | Nasal | Inferior Nasal | Inferior Temporal | Macula | Superior Temporal | Superior Nasal |
|---|---|---|---|---|---|---|---|
| SAP MCD±SD ($cdm^{-2}$) | 17.38±6.42 | 17.27±5.60 | 19.53±6.53 | 16.29±5.42 | 13.83±2.12 | 16.04±4.81 | 17.32±5.32 |
| FDF MCD±SD ($cdm^{-2}$) | 16.10±9.30 | 14.63±10.28 | 22.29±13.19 | 17.93±12.61 | 11.97±8.16 | 14.29±10.56 | 12.80±8.15 |
| HRT rim area (mm2) | 1.30±0.38 | 0.37±0.12 | 0.20±0.07 | 0.16±0.07 | 0.20±0.09 | 0.17±0.06 | 0.19±0.06 |
| HRT C-D ratio | 0.37±0.19 | 0.23±0.21 | 0.26±0.20 | 0.43±0.23 | 0.57±0.21 | 0.39±0.21 | 0.28±0.21 |
| HRT rim volume (mm3) | 0.33±0.16 | 0.10±0.06 | 0.06±0.04 | 0.04±0.02 | 0.02±0.01 | 0.04±0.02 | 0.06±0.03 |
| HRT cup shape measure | -0.12±0.08 | -0.17±0.16 | -0.10±0.16 | -0.03±0.10 | -0.05±0.08 | -0.04±0.14 | -0.11±0.15 |
| HRT RNFL thickness (mm) | 0.23±0.08 | 0.25±0.12 | 0.31±0.14 | 0.22±0.12 | 0.08±0.03 | 0.28±0.11 | 0.32±0.12 |
| FSM | 0.02±2.10 | | | | | | |
| RB | 0.77±1.06 | | | | | | |

Table 5-1 Descriptive statistics on HEP-FDF, HEP-SAP and HRT parameters.

| | Global | S-T | T | I-T | S-N | N | I-N |
|---|---|---|---|---|---|---|---|
| FDF MCD vs HRT rim area | -0.46 | -0.36 | -0.33 | -0.52 | -0.31 | -0.27 | -0.29 |
| SAP MCD vs HRT rim area | -0.26 | -0.35 | -0.28 | -0.45 | -0.27 | -0.05 | -0.17 |

Table 5-2 Correlation coefficient value (r) between HEP $cdm^{-2}$ and HRT parameters

| | FDF & HRT | SAP & HRT |
|---|---|---|
| Nasal | 0.20 | 0.20 |
| Inf/nsl | 0.28 | 0.27 |
| Inf/temp | 0.23 | 0.30 |
| Temp | 0.02 | 0.35 |
| Sup/temp | 0.13 | 0.14 |
| Sup/nsl | 0.31 | 0.18 |

Table 5-3 Kappa score showing concordance between HEP-FDF/HEP-SAP MD and HRT rim area classification.

| **FDF** | **N** | **IN** | **IT** | **T** | **ST** | **SN** | **TOTAL** |
|---|---|---|---|---|---|---|---|
| **OUTSIDE** | 18 | 29 | 21 | 3 | 7 | 11 | 89 |
| **BORDERLINE** | 2 | 3 | 4 | 2 | 5 | 5 | 21 |
| **WITHIN** | 37 | 30 | 32 | 44 | 38 | 33 | 214 |
| **TOTAL** | 57 | 62 | 57 | 49 | 50 | 49 | 324 |
| **SAP** | **N** | **IN** | **IT** | **T** | **ST** | **SN** | **TOTAL** |
| **OUTSIDE** | 7 | 10 | 8 | 1 | 3 | 4 | 33 |
| **BORDERLINE** | 1 | 3 | 6 | 9 | 5 | 3 | 27 |
| **WITHIN** | 51 | 46 | 47 | 66 | 51 | 52 | 313 |
| **TOTAL** | 59 | 59 | 61 | 76 | 59 | 59 | 373 |

Table 5-4 Number of agreements between classifications measured by HRT and FDF in each sector.

| | I-T SAP | I-T FDF |
|---|---|---|
| Both Normal | 50% | 31.37% |
| Both Abnormal | 19.32% | 35.29% |
| Structure normal, function Abnormal | 4.55% | 20.59% |
| Structure abnormal, function normal | 26.14% | 12.75% |

Table 5-5 Frequency of agreements in the Inferior Temporal (I-T) sector comparing HRT rim area and FDF/SAP MCD.

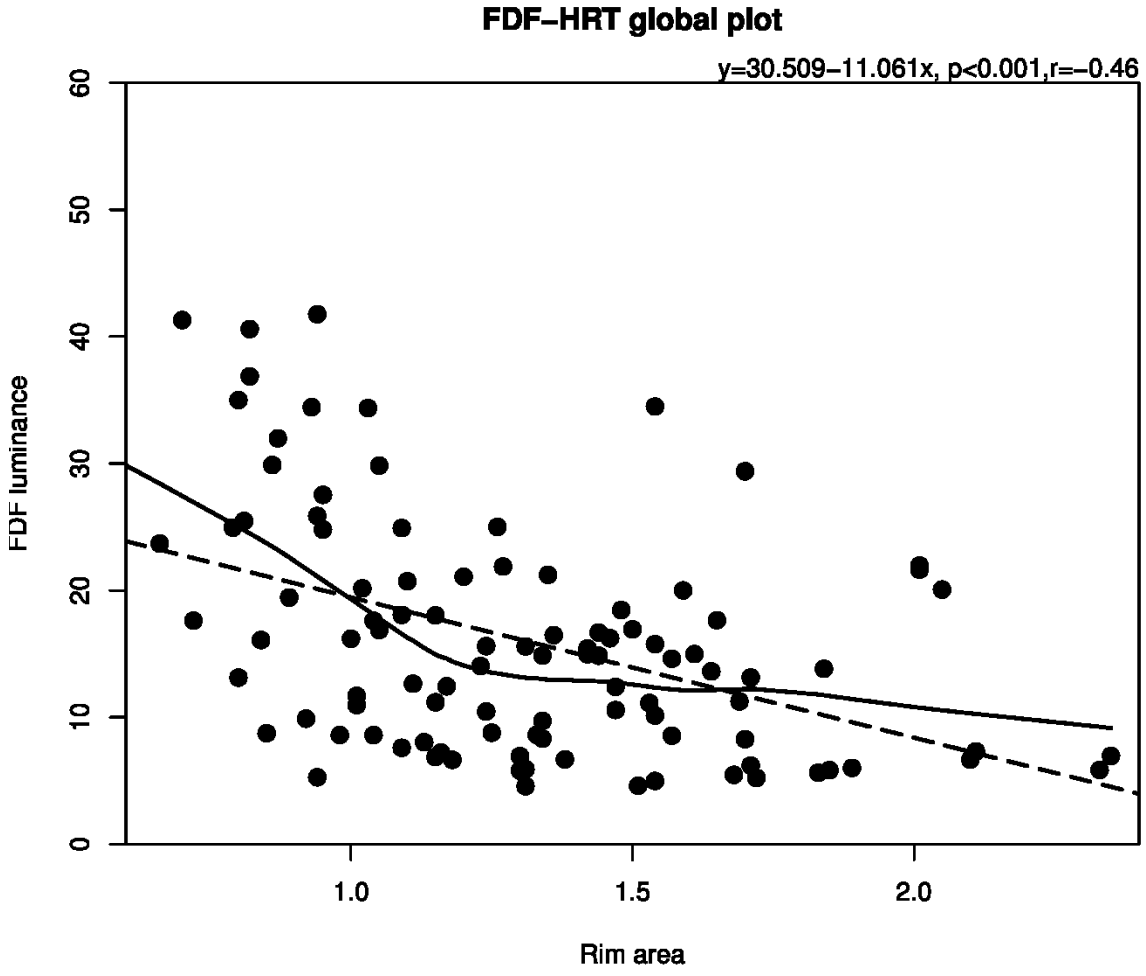


Figure 5-1 The relationship between global HEP-FDF mean luminance ($cdm^{-2}$) and HRT rim area ($mm^2$). The correlation coefficient (r) is 0.46. Robust locally weighted regression (solid line) shows a clear infection point at a rim area of approximately $1.3mm^2$, below which a clear and steep correlation exists between the measures of structure and function.

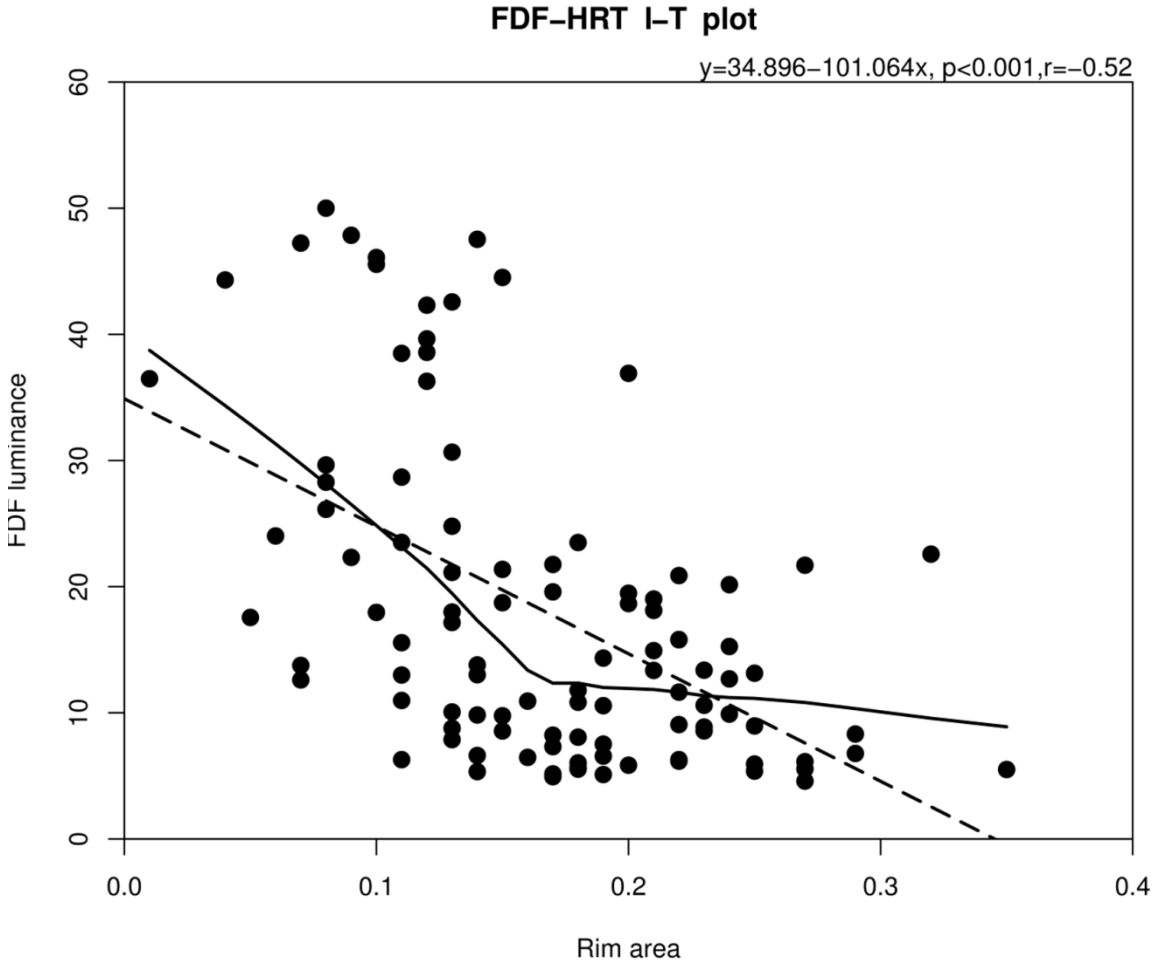


Figure 5-2 The relationship between HEP-FDF mean luminance ($cdm^{-2}$) and HRT rim area ($mm^2$) in the inferior-temporal sector. The correlation coefficient (r) is 0.52. Robust locally weighted regression (solid line) shows an infection point at a rim area of approximately $0.18mm^2$, below which a clear and steep correlation exists between the measures of structure and function.

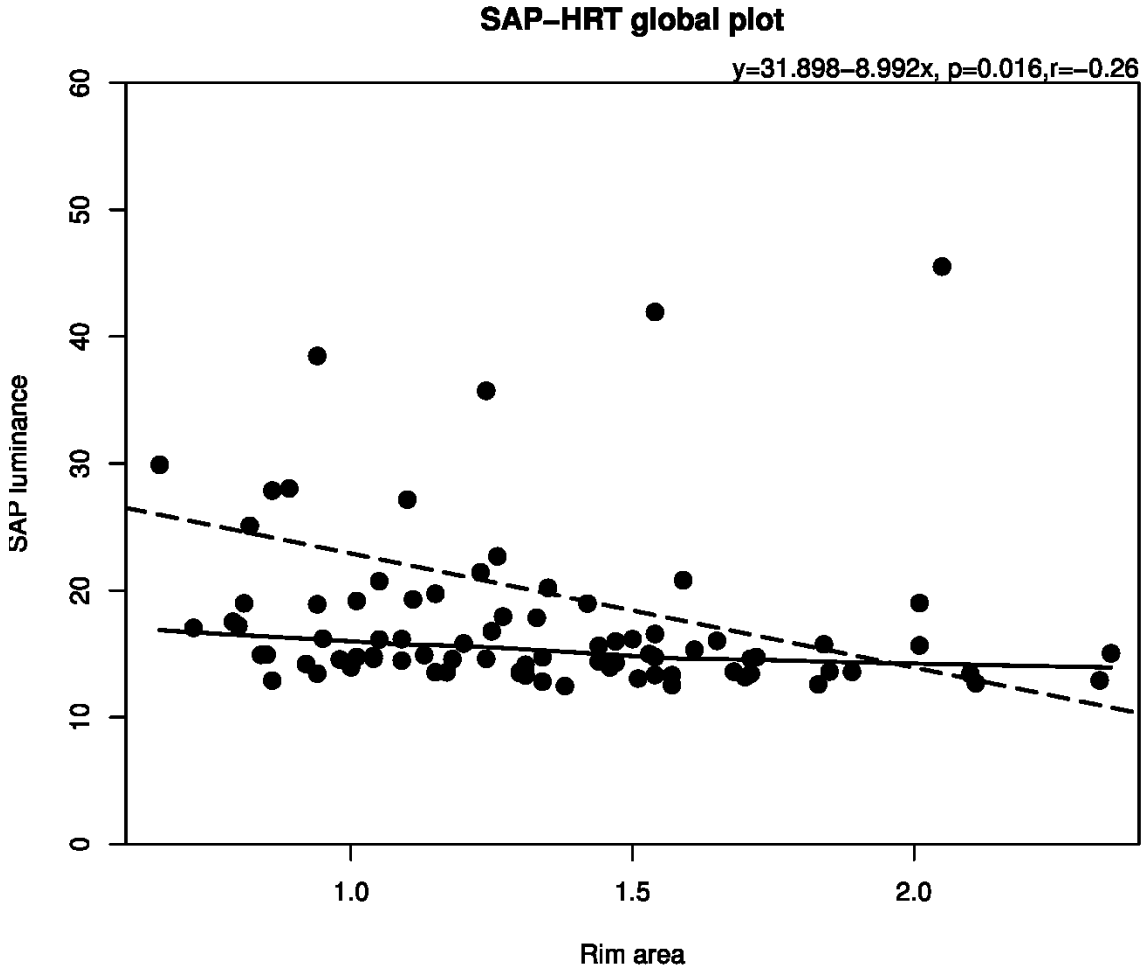


Figure 5-3 The relationship between global HEP-SAP mean luminance ($cdm^{-2}$) and HRT rim area ($mm^2$). Note the relatively flat distribution of SAP luminance indicating that there was little SAP visual field loss present in the sample. The correlation coefficient (r) is 0.26.

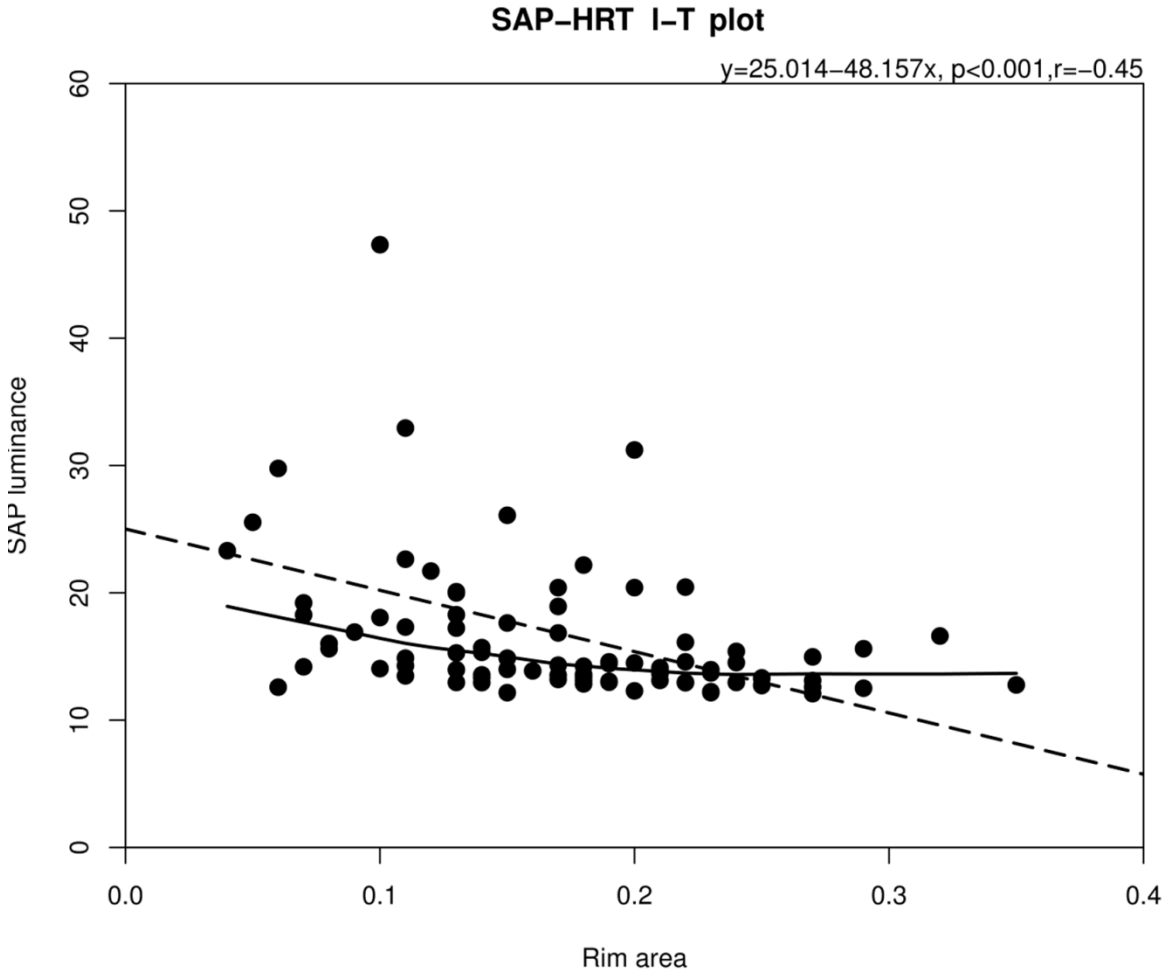


Figure 5-4 The relationship between HEP-SAP mean luminance ($cdm^{-2}$) and HRT rim area ($mm^2$) in the inferior-temporal sector. The correlation coefficient (r) is 0.45. Robust locally weighted regression (solid line) shows a slight infection point at a rim area of approximately $0.16mm^2$, below which a weak correlation exists between the measures of structure and function.

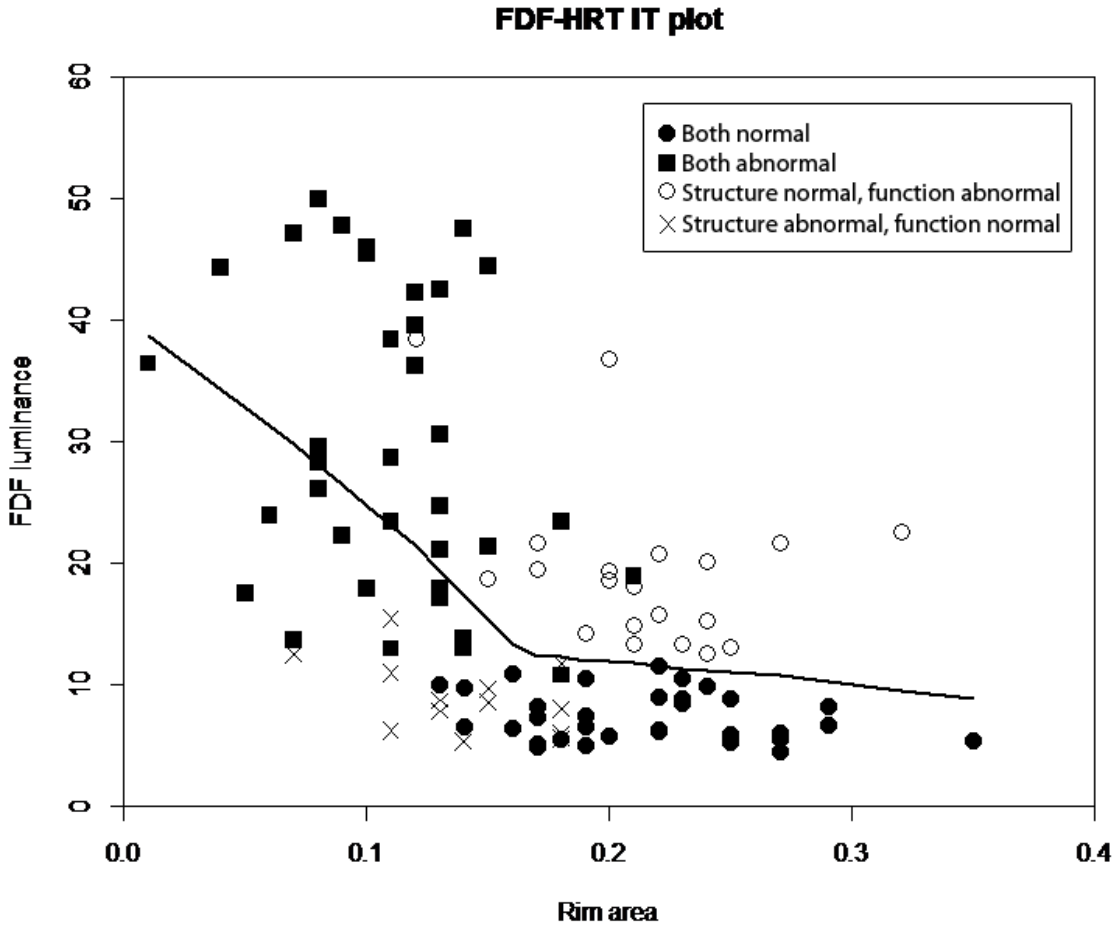


Figure 5-5 Robust locally weighted regression showing the relationship between HEP-FDF mean luminance ($cdm^{-2}$) and HRT rim area ($mm^2$) in inferior-temporal sector. The symbols illustrate the amount of abnormality for the measures of structure and function and their relative overlap. It can be seen that there is substantial agreement but also disagreement with both structure and function showing independent abnormality.

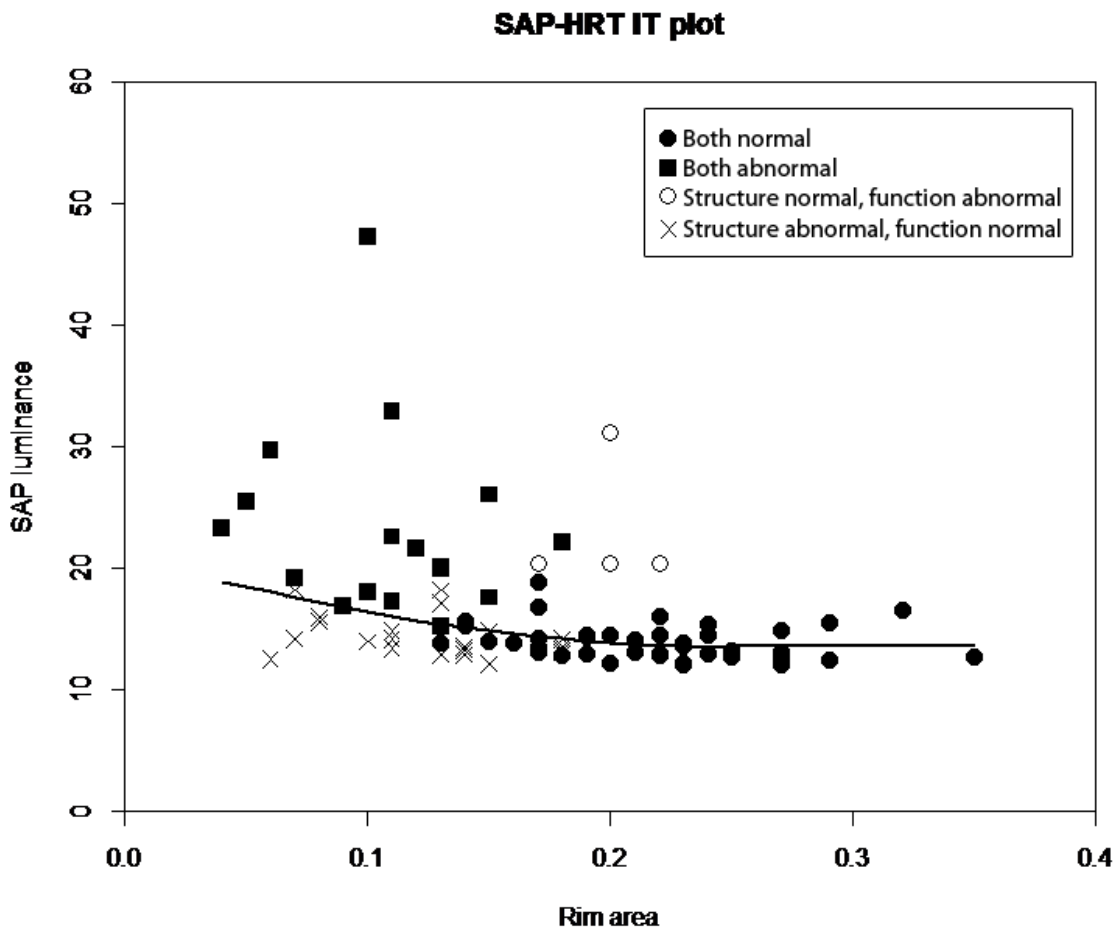


Figure 5-6 Robust locally weighted regression showing the relationship between HEP-SAP mean luminance ($cdm^{-2}$) and HRT rim area ($mm^2$) in inferior-temporal sector. The symbols illustrate the amount of abnormality for the measures of structure and function and their relative overlap. It can be seen that there are fewer times when SAP was abnormal and only 4 participants that showed abnormal SAP and normal HRT, whereas there are a substantial number that showed an abnormal HRT rim area and normal SAP.

## 5.5 Discussion

Previous studies have shown correlations between visual field defects and glaucomatous changes to the optic nerve or retinal nerve fiber layer[11-13, 16, 23]. However, because the sensitivity and specificity of the detection tools differ and the definition of "early glaucoma" varies, correlations reported are inconsistent. A longitudinal study investigating patients with early glaucomatous visual field defects found that patients who had field change also had disc change, but less than half that had disc change also showed field change[4]. That optic nerve defects were more detectable doesn't mean that the visual function was unaffected, simply that the loss of function could not be detected by SAP[38]. The SAFE study investigated a cohort of glaucoma suspects with elevated intraocular pressure (IOP) and normal SAP fields over a four-year period, and concluded that the glaucomatous optic disc was predictive of the subsequent development of glaucomatous visual field defects. However, there could be visual field defect when there was no optic disc damage, and also optic nerve damage when no visual field defect was present[3]. In a group of participants with early glaucoma taken from the Diagnostic Innovations in Glaucoma Study (DIGS), agreement was shown to be minimal between the diagnosis of glaucoma using visual field tests and HRT, with 48% of patients classified as normal by both tests[2]. A recent study reported a significantly better correlation between structure and function with FDF stimuli compared to frequency doubling technology (FDT) or SAP. Results were similar to our study, with the highest correlation found in the superior temporal sector. However, correlations were higher as the sample consisted of more established disease, with the

majority of participants having moderate to severe disease; the average MD SAP was -7.92±4.65dB compared to an average MD SAP of -0.63±1.91 dB in our study[16].

In the current study, results yielded poor to moderate correlations when comparing structure and function in participants with early glaucoma. This was expected given that the glaucomatous damage was at such an early stage. We agree with the previous studies suggesting that high resolution structural measurements are more sensitive than standard automated perimetry in the early stages of glaucomatous optic neuropathy. One possible explanation is the difference in variability between the different measures,[23] no great surprise given the subjective nature of visual field testing compared to the objective imaging techniques.

We used the FDF stimuli in an attempt to detect functional defects earlier than SAP. Uniquely the same normal database was used for both techniques, that is, the same participants were tested using both methods and the analytical treatment of the data was identical. We have shown that there were no significant differences when assessing classification concordance for SAP and FDF versus HRT. Both structural and functional approaches agreed on the categorization of normal, borderline and outside normal limits. However, when looking at the frequency of agreement in each classification, FDF agreed with HRT more when outside normal limits, whereas SAP was more conservative and had better agreement with the normal classifications. This reinforces the notion that FDF is more sensitive than SAP for the detection of early glaucoma.

Correlations between the structure and function of early glaucoma were mild to moderate in our study with the best correlation found in the inferior temporal sector (r=-0.52

for FDF and r=-0.45 for SAP). It should be noted that most of the sample used had normal SAP results. Previous studies performed on patients with optic nerve damage and early focal visual field loss demonstrated that damage occurs most frequently at the inferior temporal[10, 14, 15] and superior temporal[12] sectors, with HRT showing either diffuse or focal sector abnormality, or no damage at all[39]. The structure and function relationship has also been found to better correlate in the superior temporal and inferior temporal regions[11]. However, it was also considered that using different groups of patients and different analyses could account for different structure-function relationships. Our results are similar to previous studies, showing the best correlation in the inferior temporal sector.

When robust locally weighted regression was used to show the relationship between structure and function in early glaucoma, in the I-T sector, there was a change of slope at a rim area of approximately 0.18mm$^2$, suggesting that the FDF's ability to detect early glaucomatous visual field loss was superior to HEP-SAP which gave a relatively flat relationship across the whole measurement range. FDF gave more abnormal points and correlated better with the abnormal HRT results than SAP.

Structural abnormality and perimetric defects frequently coexist even at the very earliest stages of glaucomatous damage[40]. Shah et. al.[1] proposed that combining structural and functional tests could enhance the sensitivity of glaucoma detection. Racette and colleagues[7] suggested that combining short wavelength automated perimetry (SWAP) and HRT II resulted in improved diagnostic accuracy when compared to using SWAP or HRT II parameters alone. In a longitudinal study of ocular hypertensive (OHT) patients, it was suggested that it was important to use both HRT and SAP measurements to achieve a

relatively high frequency of disease progression detection[5]. Poor agreement between rim area and visual field progression was found, suggesting that monitoring both results are important in glaucoma progression management[5]. A recent study combining structure and function information using machine learning classifiers found significantly improved diagnostic performance in early glaucoma,[21] and an improved predictive performance[22]. Better estimation of glaucoma progression can also be achieved combining both structure and function measurements[8, 9].

The test-retest characteristics of each technique plays an important role in the correlation and potential combination of results. Within the HRT II parameters "rim area" and "mean cup depth" were the least variable, reference height and image quality were factors that most influenced rim area variability[41]. It has been suggested that in perimetry larger stimuli give more repeatable measurements of the sensitivity[42] and better test-retest reliability[24]. The better correlation of FDF with HRT rim area in our study might be explained by the distinct psychophysical characteristics of the FDF stimulus, but also the larger target size (5 degree diameter) compared to SAP.

In conclusion, the results of our study showed moderate to poor linear correlation between structure and function when comparing HEP and HRT in participants with early, largely pre-perimetric glaucoma, with the best correlation being found in the inferior temporal region of the optic nerve. Using analysis based upon the same normative database for HEP-FDF and HEP-SAP, there was better correlation with FDF. A steeper slope was found for the regression analysis for FDF. Agreement in the structure and function relationship was better for FDF than SAP in the "outside normal limits" classification. In this

study FDF was able to detect glaucomatous visual field loss earlier than SAP and demonstrated a clearer relationship with ONH rim area.

# Chapter 6

# Discussion

## 6.1 Flicker Defined Form: Visual field application

The two main objectives of clinical visual field testing in patients with glaucoma is the detection of early defect and the documentation of disease progression. In the detection of glaucoma, the use of a normative database provides the examiner with the statistical tools to classify visual function as “normal” or “abnormal” based within accepted limits of Type I (alpha) and Type 2 (beta) errors. The documentation of disease progression is related to the definition of detectable change, which is dependent on the test-retest characteristics of the test. When test-retest gives a narrow confidence interval it is easier for the clinician to differentiate measurement noise and be confident of true change. The ideal visual field testing in glaucoma should have a large dynamic range, minimal test-retest variability and high correlation to the RGC function.

Previous studies showed that flicker defined form was a magnocellular pathway dominant stimuli[1,2], and is a complex visual task that might have potential advantages in the early detection of glaucoma[3]. A prototype of the Heidelberg Edge Perimetry was designed to display flicker defined form generated stimuli. A normative database was first established to describe the relationship between flicker defined from sensitivity and age (Chapter 2). A second order polynomial fit was found to best describe the relationship between age and sensitivity, with a relatively flat slope from 20 to 60 year and a steeper slope from the age of 60 years. Characteristics of the FDF visual field database described symmetry within the

field similar to that of the traditional visual field: the inferior hemifield gave higher sensitivity than the superior field, and the central field gave higher sensitivity than the peripheral field. We found a 0.747 dB difference between the first tested and second tested eye in our study, which was reported to be similar to previous results found in FDT testing[4,5]. Fatigue and contrast adaptation was thought to be less likely to contribute to this finding.

Standard automated perimetry has been widely used as the most common method to assess central visual field sensitivity, and its ability of detect and follow disease progression has been well documented. There are a few fundamental differences when comparing the FDF to the traditional differential light stimuli. First, the stimuli are created by flickering dots at a temporal frequency of 15Hz. Though the stimuli are temporally driven, their perception is also influenced by area[2]. Second, the stimulus size used in our study was a 5 degree diameter patch. The larger target size and temporal characteristics can partially explain its tolerance to dioptric blur. It is also noted that there is a similar test-retest ability throughout the dynamic range of the test.

Application of the FDF as a visual field stimulus has potential for the early glaucoma detection and in disease progression. Our study defined the "normal" database from a sample of 20-80 year old subjects. More "abnormal" locations were detected when using the FDF perimeter compared to SAP in our group of participants with early glaucoma. The repeatability of FDF on early glaucoma patients was similar across the testing range with a slightly higher variability at the lower sensitivity values. More discriminable threshold sensitivity steps were found in our test group of early glaucoma patients, this allows better follow-up of progression. However, the range of defects in our group of early SAP defects

gave a spread of defects throughout the measurement range when using FDF (Figure 4-3). With disease progression, we suspect that the FDF test will show a floor effect in more advanced glaucoma with sensitivity less than 22dB tested on SAP. There are advantages in early detection using FDF as a visual field stimulus, however, it may not be suitable for the management of progression management for moderate to severe disease.

## 6.2 Structure and Function relationship using FDF

In this thesis, we compared the structure and function relationship between flicker defined form and standard automated perimetry with the Heidelberg retina tomography. It is important to note that the normative database collected for the FDF and SAP was based on the same sets of patients, thus, when comparing the structure and function relationship between them and the HRT, the potential bias that can be caused by differences in the characteristics of the normal databases will be minimal.

Both structural measurements and functional tests play an important role in glaucoma diagnosis and follow-up. Throughout the course of the disease each instrument, whether measuring structure or function, has its optimal dynamic range. Currently, no measurement shows linear change throughout the course of the disease. Our data showed that FDF revealed defects in early glaucoma testing when the SAP was normal. These defects corresponded to the early rim area loss detected by the HRT. In addition, when SAP showed early defect, FDF showed deeper and more extensive defect.

Implicit within the understanding of our measurements is that we are not measuring the loss of individual retinal ganglion cells. The relationship between each test and retinal ganglion cell function is determined by many factors including the dynamic range of the instrument. Recent studies have attempted to estimate retinal ganglion cell survival using structural and functional measurements[6,7].

Besides the number of cells and its functional or structural measurements, the spatial relationship of defects are also affected by tested area. The HRT measures the optic nerve head, whereas the visual field is sampling the retina from the macula and beyond. The sampling density per ganglion cell varies, *i.e.* the central retina is undersampled when compared to the periphery, this is due to the higher density of ganglion cells in the central retina. Using the Garway-Heath mapping of HRT sectors and visual field locations[8], we found the earliest glaucoma defects presented in the inferior temporal sector, which is where the highest correlation coefficient is found between structure and function. However, we need to recognize that mapping of the optic nerve head and the visual field might differ between individuals. Customized mapping has recently been proposed when comparing the structure and function relationships[9]. This might affect how the structure and function relationship is measured in individuals.

Temporal relationships of structure and function measurements also influence the outcome of its relationship. Optic nerve damage is most often reported to occur prior to standard visual field damage. In our cross-sectional study using FDF stimuli (Chapter 5), a change of slope between structure and function relationship in the inferior temporal sector and corresponding visual field locations indicated that FDF function testing is able to detect

early glaucomatous loss when rim area is below 0.18mm$^2$. Agreement of classification also provided evidence that when HRT rim area decreased and FDF field loss agreed. However, there was also disagreement between tests with examples of each showing independent abnormality. Combining structure and function measurements in early glaucoma diagnosis and progression is clearly beneficial.

With all the different tests available, there is clearly an advantage to measuring as many different aspects of the disease as possible. The technology that is available today determines how well the "current" tools detect damage and measure disease progression. We should treat structure and function as independent measures when looking at glaucoma. By combining the various independent measurements, we can be more confident of our ability to detect disease and detect change.

There are strengths and limitations to the research presented in this thesis. There were problems comparing SAP and FDF data. This is not only due to the difference in the stimuli themselves, but also the scaling of stimuli sensitivity. The decibel scales are fundamentally different. We attempted to compare the different scales by using measures of total deviation and pattern deviation, critically calculated using the same normative database. This allowed us to compare the results independent of the effect of age and the relative sensitivity scale. The dynamic range of flicker defined form in the course of glaucoma progression follow-up is unknown, and the temporal relationship between FDF and other tests is yet to be addressed. It would be interesting to investigate if FDF visual field loss is a predictive measure of future SAP loss. Patterns of early defect using FDF should be further researched; does FDF show similar but earlier defect or are the clusters of loss different to the earliest

defect found by SAP. Current technology is providing new tools to measure the structure and function of the eye. The relationship between flicker defined form and optical coherence tomography should be researched. In addition, future longitudinal studies should be performed to investigate the temporal aspects of structural and functional damage and their relationships.

In summary, our study established the normative database for the Heidelberg Edge Perimetry (Chapter 2). We have established the relationship between FDF sensitivity and age, and defined the statistical "normal". Normal limits were defined as an effect of age in each tested. Our study provided a foundation for further flicker defined form perimetry related research. The results of this thesis provided a normative database for the FDF stimuli, which can permit development of analytical tools for the HEP. Flicker defined form stimuli as a visual field target is relatively resistant to optical blur (Chapter 3), and has the advantage of providing meaningful data without requiring optimal refractive correction. In our cross-sectional study of early glaucomatous patients (Chapter 4), more visual field defects were detected by FDF. The test-retest results for FDF showed more uniform test-retest throughout the range of sensitivity values (Chapter 4). When structure-function relationships were investigated between FDF and HRT, moderate to poor linear correlation was found in our group of early glaucoma patients (Chapter 5). However, FDF correlated better with HRT than SAP in patients with early glaucoma. The best correlation was found in the inferior temporal sector of the optic nerve. We suggest that structure and function measurements both add independent value in early detection and the monitoring of progression.

# References

## Chapter 1


1. Fronimopoulos J, Lascaratos J. The terms glaucoma and cataract in the ancient Greek and Byzantine writers. Documenta Ophthalmologica. 1991;77(4):369-375.

2. Tsatsos M, Broadway D. Controversies in the history of glaucoma: is it all a load of old Greek? British Journal of Ophthalmology. 2007;91(11):1561-1562.

3. Roodhooft JMJ. Leading causes of blindness worldwide. Bulletin of Belgian Societies of Ophtalmology. 2002;(283):19-25.

4. Kingman S. Glaucoma is second leading cause of blindness globally. Bulletin of World Health Organization. 2004;82(11):887-888.

5. Pascolini D, Mariotti SP. Global estimates of visual impairment: 2010. British Journal of Ophthalmology. 2012;96(5):614-618.

6. Cruess AF, Gordon KD, Bellan L, Mitchell S, Pezzullo ML. The cost of vision loss in Canada. 2. Results. Canadian Journal of Ophthalmology. 2011;46(4):315-318.

7. Quigley HA, Broman AT. The number of people with glaucoma worldwide in 2010 and 2020. British Journal of Ophthalmology. 2006;90(3):262-267.

8. Tham Y-C, Li X, Wong TY, Quigley HA, Aung T, Cheng C-Y. Global prevalence of glaucoma and projections of glaucoma burden through 2040: a systematic review and meta-analysis. Ophthalmology. 2014;121(11):2081-2090.

9. Parrish RK. Visual Function and Quality of Life Among Patients With Glaucoma. Archives of Ophthalmology. 1997;115(11):1447.

10. Janz NK, Wren PA, Lichter PR, et al. The Collaborative Initial Glaucoma Treatment Study: interim quality of life findings after initial medical or surgical treatment of glaucoma. Ophthalmology. 2001;108(11):1954-1965.

11. Nelson P, Aspinall P, Papasouliotis O, Worton B, O'Brien C. Quality of life in glaucoma and its relationship with visual function. Journal of Glaucoma. 2003;12(2):139-150.

12. McKean-Cowdin R, Wang Y, Wu J, Azen SP, Varma R. Impact of visual field loss on health-related quality of life in glaucoma: the Los Angeles Latino Eye Study. Ophthalmology. 2008;115(6):941-948.e1.

13. Spaeth G, Walt J, Keener J. Evaluation of quality of life for patients with glaucoma. American Journal of Ophthalmology. 2006;141(1 Suppl):S3-S14.

14. Hayreh SS. The optic nerve head circulation in health and disease. Ophthalmic Literature. 1996;49(2):111.

15. Hayreh SS. Blood supply of the optic nerve head. Ophthalmic Literature. 1997;50(1):17.

16. Kupfer C, Chumbley L, Downer JDC. Quantitative Histology of Optic Nerve Optic Tract and Lateral Geniculate Nucleus of Man. Journal of Anatomy. 1967;101:393

17. Balazsi a G, Rootman J, Drance SM, Schulzer M, Douglas GR. The effect of age on the nerve fiber population of the human optic nerve. American Journal of Ophthalmology. 1984;97(6):760-766.

18. Repka MX, Quigley HA. The effect of age on normal human optic nerve fiber number and diameter. Ophthalmology. 1989;96(1):26-32.

19. Jonas JB, Muller-Bergh JA, Schlotzer-Schrehardt UM, Naumann GO. Histomorphometry of the human optic nerve. Investigative Ophthalmology & Visual Science. 1990;31(4):736-744.

20. Quigley HA. Early detection of glaucomatous damage: II. Changes in the appearance of the optic disk. Survey of Ophthalmology. 1985;30(2): 117-126.

21. Provis JM, van Driel D, Billson FA, Russell P. Human fetal optic nerve: Overproduction and elimination of retinal axons during development. Journal of Comparative Neurology. 1985;238(1):92-100.

22. Kee CW, Koo HJ, Ji YH, Kim SW. Effect of optic disc size or age on evaluation of optic disc variables. British Journal of Ophthalmology. 1997;81(12):1046-1049.

23. Dolman CL, McCormick Q, Drance SM. Aging of the optic nerve. Archives of Ophthalmology. 1980;98(11):2053-2058.

24. Lieberman MF, Maumenee AE, Green WR. Histologic studies of the vasculature of the anterior optic nerve. American Journal of Ophthalmology. 1976;82(3):405-423.

25. Anderson DR. Ultrastructure of human and monkey lamina cribrosa and optic nerve head. Archives of Ophthalmology. 1969;82(4):800-814.

26. Quigley HA, Addicks EM. Regional Differences in the Structure of the Lamina Cribrosa and their Relation to Glaucomatous Optic-Nerve Damage. 1981.

27. Radius RL. Regional Specificity in Anatomy at the Lamina Cribrosa. Archives of Ophthalmology. 1981;99(3):478-480.

28. Radius RL. Anatomy of the optic nerve head and glaucomatous optic neuropathy. Survey of Ophthalmology. 1987;32(1):35-44.

29. Hernandez MR, Luo XX, Igoe F, Neufeld AH. Extracellular matrix of the human lamina cribrosa. American Journal of Ophthalmology. 1987;104(6):567-576.

30. Minckler DS. Histology of optic nerve damage in ocular hypertension and early glaucoma. Survey of Ophthalmology. 1989;33 Suppl:401-411.

31. Radius RL, Anderson DR. Rapid axonal transport in primate optic nerve. Distribution of pressure-induced interruption. Archives of Ophthalmology. 1981;99(4):650-654.

32. Quigley HA. Ganglion cell death in glaucoma: pathology recapitulates ontogeny. Australian and New Zealand Journal of Ophthalmology. 1995;23(2):85-91.

33. Quigley HA, Nickells RW, Kerrigan LA, Pease ME, Thibault DJ, Zack DJ. Retinal ganglion cell death in experimental glaucoma and after axotomy occurs by apoptosis. Investigative Ophthalmology & Visual Science. 1995;36(5):774-786.

34. Quigley HA, Sanchez RM, Dunkelberger GR, L'Hernault NL, Baginski TA. Chronic glaucoma selectively damages large optic nerve fibers. Investigative Ophthalmology & Visual Science. 1987;28(6):913-920.

35. Iwata K, Kurosawa A, Sawaguchi S. Wedge-shaped retinal nerve fiber layer defects in experimental glaucoma preliminary report. Graefe's Archive for Clinical and Experimental Ophthalmology. 1985;223(4):184-189.

36. Quigley HA. Reappraisal of the mechanisms of glaucomatous optic nerve damage. Eye (Lond). 1987;1 (Part 2):318-322.

37. Hernandez MR, Pena JD. The optic nerve head in glaucomatous optic neuropathy. Archives of Ophthalmology. 1997;115(3):389-395.

38. Hernandez MR, Andrzejewska WM, Neufeld AH. Changes in the extracellular matrix of the human optic nerve head in primary open-angle glaucoma. American Journal of Ophthalmology. 1990;109(2):180-188.

39. Quigley HA. Neuronal death in glaucoma. Progress in Retinal and Eye Research. 1999;18(1):39-57.

40. Quigley HA, Dunkelberger GR, Green WR. Chronic human glaucoma causing selectively greater loss of large optic nerve fibers. Ophthalmology. 1988;95(3):357-363.

41. Glovinsky Y, Quigley HA, Dunkelberger GR. Retinal ganglion cell loss is size dependent in experimental glaucoma. Investigative Ophthalmology & Visual Science. 1991;32(3):484-491.

42. Yan DB, Coloma FM, Metheetrairut A, Trope GE, Heathcote JG, Ethier CR. Deformation of the lamina cribrosa by elevated intraocular pressure. British Journal of Ophthalmology. 1994;78(8):643-648.

43. Quigley HA, Hohman RM, Addicks EM, Massof RW, Green WR. Morphologic changes in the lamina cribrosa correlated with neural loss in open-angle glaucoma. American Journal of Ophthalmology. 1983;95(5):673-691.

44. Airaksinen PJ, Drance SM, Douglas GR, Mawson DK, Nieminen H. Diffuse and localized nerve fiber loss in glaucoma. American Journal of Ophthalmology. 1984;98(5):566-571.

45. Miller KM, Quigley HA. The clinical appearance of the lamina cribrosa as a function of the extent of glaucomatous optic nerve damage. Ophthalmology. 1988;95(1):135-138.

46. Dandona L, Hendrickson, Quigley H. Selective effects of experimental glaucoma on axonal transport by retinal ganglion cells to the dorsal lateral geniculate nucleus. Investigative Ophthalmology & Visual Science. 1991;32(5):1593-1599.

47. Mitchell P, Smith W, Chey T, Healey PR. Open-angle glaucoma and diabetes: the Blue Mountains eye study, Australia. Ophthalmology. 1997;104(4):712-718.

48. Mitchell P, Hourihan F, Sandbach J, Wang JJ. The relationship between glaucoma and myopia: the Blue Mountains Eye Study. Ophthalmology. 1999;106(10):2010-2015.

49. Mitchell P, Wang JJ, Hourihan F. The relationship between glaucoma and pseudoexfoliation: the Blue Mountains Eye Study. Archives of Ophthalmology (Chicago, Ill 1960). 1999;117(10):1319-1324.

50. Mitchell P, Lee AJ, Rochtchina E, Wang JJ. Open-angle glaucoma and systemic hypertension: the blue mountains eye study. Journal of Glaucoma. 2004;13(4):319-326.

51. Healey PR, Mitchell P. Optic disk size in open-angle glaucoma: the Blue Mountains Eye Study. American Journal of Ophthalmology. 1999;128(4):515-517.

52. Mitchell P, Cumming RG, Mackey DA. Inhaled corticosteroids, family history, and risk of glaucoma. Ophthalmology. 1999;106(12):2301-2306.

53. Canadian Glaucoma Study: 1. Study design, baseline characteristics, and preliminary analyses. Canadian Journal of Ophthalmology. 2006;41(5):566-575.

54. Chauhan BC, Mikelberg FS, Balaszi AG, LeBlanc RP, Lesk MR, Trope GE. Canadian Glaucoma Study: 2. risk factors for the progression of open-angle glaucoma. Archives of Ophthalmology (Chicago, Ill 1960). 2008;126(8):1030-1036.

55. Chauhan BC, Mikelberg FS, Artes PH, et al. Canadian Glaucoma Study: 3. Impact of risk factors and intraocular pressure reduction on the rates of visual field change. Archives of Ophthalmology (Chicago, Ill 1960). 2010;128(10):1249-1255.

56. Johnson C a., Sample P a., Cioffi G a., Liebmann JR, Weinreb RN. Structure and function evaluation (SAFE): I. criteria for glaucomatous visual field loss using standard automated perimetry (SAP) and short wavelength automated perimetry (SWAP). American Journal of Ophthalmology. 2002;134:177-185.

57. Johnson CA, Sample PA, Zangwill LM, et al. Structure and function evaluation (SAFE): II. Comparison of optic disk and visual field characteristics. American Journal of Ophthalmology. 2003;135(2):148-154.

58. Heijl A, Leske MC, Bengtsson B, Hyman L, Bengtsson B, Hussein M. Reduction of intraocular pressure and glaucoma progression: results from the Early Manifest Glaucoma Trial. Archives of Ophthalmology (Chicago, Ill 1960). 2002;120(10):1268-1279.

59. Kass MA, Heuer DK, Higginbotham EJ, et al. The Ocular Hypertension Treatment Study: a randomized trial determines that topical ocular hypotensive medication delays or prevents the onset of primary open-angle glaucoma. Archives of Ophthalmology (Chicago, Ill 1960). 2002;120(6):701-713; discussion 829-830.

60. Comparison of glaucomatous progression between untreated patients with normal-tension glaucoma and patients with therapeutically reduced intraocular pressures. Collaborative Normal-Tension Glaucoma Study Group. American Journal of Ophthalmology. 1998;126(4):487-497.

61. Ederer F, Gaasterland DE, Sullivan EK. The Advanced Glaucoma Intervention Study (AGIS): 1. Study design and methods and baseline characteristics of study patients. Controlled Clinical Trials. 1994;15(4):299-325.

62. Advanced Glaucoma Intervention Study. 2. Visual field test scoring and reliability. Ophthalmology. 1994;101(8):1445-1455.

63. The Advanced Glaucoma Intervention Study (AGIS): 3. Baseline characteristics of black and white patients. Ophthalmology. 1998;105(7):1137-1145.

64. The Advanced Glaucoma Intervention Study (AGIS): 4. Comparison of treatment outcomes within race. Seven-year results. Ophthalmology. 1998;105(7):1146-1164.

65. Musch DC, Lichter PR, Guire KE, Standardi CL. The Collaborative Initial Glaucoma Treatment Study: study design, methods, and baseline characteristics of enrolled patients. Ophthalmology. 1999;106(4):653-662.

66. Anderson DR, Patella VM. Automated Static Perimetry. Mosby; 1999.

67. Hodapp E, Parrish RK, Anderson DR. Clinical Decisions in Glaucoma. Mosby; 1993.

68. Kerrigan-Baumrind LA, Quigley HA, Pease ME, Kerrigan DF, Mitchell RS. Number of ganglion cells in glaucoma eyes compared with threshold visual field tests in the same persons. Investigative Ophthalmology & Visual Science. 2000;41(3):741-748.

69. Turpin A, McKendrick AM. What reduction in standard automated perimetry variability would improve the detection of visual field progression? Investigative Ophthalmology & Visual Science. 2011;52(6):3237-3245.

70. Bengtsson B, Heijl A. A visual field index for calculation of glaucoma rate of progression. American Journal of Ophthalmology. 2008;145(2):343-353.

71. Kudrna GR, Stanley MA, Remington LA. Pupillary dilation and its effects on automated perimetry results. Journal of the American Optometric Association. 1995;66(11):675-680.

72. Weinreb RN, Perlman JP. The effect of refractive correction on automated perimetric thresholds. American Journal of Ophthalmology. 1986;101(6):706-709.

73. Goldstick BJ, Weinreb RN. The Effect of Refractive Error on Automated Global Analysis Program G-1. American Journal of Ophthalmology. 1987;104(3):229-232.

74. Heuer DK, Anderson DR, Feuer WJ, Gressel MG. The influence of refraction accuracy on automated perimetric threshold measurements. Ophthalmology. 1987;94(12):1550-1553.

75. Owsley C. Aging and vision. Vision Research. 2011;51(13):1610-1622.

76. Owsley C. Visual processing speed. Vision Research. 2013;90:52-56.

77. Burk RO, Vihanninjoki K, Bartke T, et al. Development of the standard reference plane for the Heidelberg retina tomograph. Graefe's Archive for Clinical and Experimental Ophthalmology. 2000;238(5):375-384.

78. Vihanninjoki K, Burk ROW, Teesalu P, Tuulonen A, Airaksinen PJ. Optic disc biomorphometry with the Heidelberg Retina Tomograph at different reference levels. Acta Ophthalmologica Scandinavica. 2002;80(1):47-53.

79. Bathija R, Zangwill L, Berry CC, Sample PA, Weinreb RN. Detection of early glaucomatous structural damage with confocal scanning laser tomography. Journal of Glaucoma. 1998;7(2):121-127.

80. Nakamura H, Maeda T, Suzuki Y, Inoue Y. Scanning laser tomography to evaluate optic discs of normal eyes. Japanese Journal of Ophthalmology. 43(5):410-414.

81. Brigatti L, Caprioli J. Correlation of visual field with scanning confocal laser optic disc measurements in glaucoma. Archives of Ophthalmology (Chicago, Ill 1960). 1995;113(9):1191-1194.

82. Mikelberg FS, Parfitt CM, Swindale N V, Graham SL, Drance SM, Gosine R. Ability of the heidelberg retina tomograph to detect early glaucomatous visual field loss. Journal of Glaucoma. 1995;4(4):242-247.

83. Weinreb RN, Lusky M, Bartsch DU, Morsman D. Effect of repetitive imaging on topographic measurements of the optic nerve head. Archives of Ophthalmology (Chicago, Ill 1960). 1993;111(5):636-638.

84. Mikelberg FS, Wijsman K, Schulzer M. Reproducibility of topographic parameters obtained with the heidelberg retina tomograph. Journal of Glaucoma. 1993;2(2):101-103.

85. Lusky M, Bosem ME, Weinreb RN. Reproducibility of optic nerve head topography measurements in eyes with undilated pupils. Journal of Glaucoma. 1993;2(2):104-109.

86. Janknecht P, Funk J. The Heidelberg Retina Tomograph: reproducibility and measuring errors in different pupillary widths using a model eye. Klinische Monatsblatter fur Augenheilkunde. 1994;205(2):98-102.

87. Zangwill LM, Berry CC, Weinreb RN. Optic disc topographic measurements after pupil dilation. Ophthalmology. 1999;106(9):1751-1755.

88. Tomita G, Honbe K, Kitazawa Y. Reproducibility of measurements by laser scanning tomography in eyes before and after pilocarpine treatment. Graefe's Archive for Clinical and Experimental Ophthalmology. 1994;232(7):406-408.

89. Zangwill L, Irak I, Berry CC, Garden V, de Souza Lima M, Weinreb RN. Effect of cataract and pupil size on image quality with confocal scanning laser ophthalmoscopy. Archives of Ophthalmology (Chicago, Ill 1960). 1997;115(8):983-990.

90. Strouthidis NG, White ET, Owen VMF, Ho T a, Hammond CJ, Garway-Heath DF. Factors affecting the test-retest variability of Heidelberg retina tomograph and Heidelberg retina tomograph II measurements. British Journal of Ophthalmology. 2005;89:1427-1432.

91. Brigatti L, Weitzman M, Caprioli J. Regional test-retest variability of confocal scanning laser tomography. American Journal of Ophthalmology. 1995;120(4):433-440.

92. Ong LS, Mitchell P, Healey PR, Cumming RG. Asymmetry in optic disc parameters: the Blue Mountains Eye Study. Investigative Ophthalmology & Visual Science. 1999;40(5):849-857.

93. Hawker MJ, Ainsworth G, Vernon SA, Dua HS. Observer agreement using the Heidelberg retina tomograph: the Bridlington Eye Assessment Project. Journal of Glaucoma. 17(4):280-286.

94. Caprioli J, Miller JM. Correlation of structure and function in glaucoma. Quantitative measurements of disc and field. Ophthalmology. 1988;95(6):723-727.

95. Racette L, Medeiros FA, Bowd C, Zangwill LM, Weinreb RN, Sample PA. The impact of the perimetric measurement scale, sample composition, and statistical method on the structure-function relationship in glaucoma. Journal of Glaucoma. 2007;16(8):676-684.

96. Marín-Franch I, Malik R, Crabb DP, Swanson WH. Choice of statistical method influences apparent association between structure and function in glaucoma. Investigative Ophthalmology & Visual Science. 2013;54(6):4189-4196.

97. Harwerth RS, Carter-Dawson L, Shen F, Smith EL, Crawford ML. Ganglion cell losses underlying visual field defects from experimental glaucoma. Investigative Ophthalmology & Visual Science. 1999;40(10):2242-2250.

98. Airaksinen PJ, Drance SM, Douglas GR, Schulzer M, Wijsman K. Visual field and retinal nerve fiber layer comparisons in glaucoma. Archives of Ophthalmology (Chicago, Ill 1960). 1985;103(2):205-207.

99. Malik R, Swanson WH, Garway-Heath DF. 'Structure-function relationship in glaucoma: past thinking and current concepts. Clinical & Experimental Ophthalmology. 2012;40(4):369-80.

100. Harwerth RS, Carter-Dawson L, Smith EL, Barnes G, Holt WF, Crawford ML. Neural losses correlated with visual losses in clinical perimetry. Investigative Ophthalmology & Visual Science. 2004;45(9):3152-60.

101. Curcio C, Allen K. Topography of ganglion cells in human retina. Journal of Comparative Neurology. 1990;300(1):5-25.

102. Quigley HA, Katz J, Derick RJ, Gilbert D, Sommer A. An evaluation of optic disc and nerve fiber layer examinations in monitoring progression of early glaucoma damage. Ophthalmology. 1992;99(1):19-28.

103. Sommer A, Katz J, Quigley HA, et al. Clinically detectable nerve fiber atrophy precedes the onset of glaucomatous field loss. Archives of Ophthalmology (Chicago, Ill 1960). 1991;109(1):77-83.

104. Chauhan BC, McCormick T a, Nicolela MT, LeBlanc RP. Optic disc and visual field changes in a prospective longitudinal study of patients with glaucoma: comparison of scanning laser tomography with conventional perimetry and optic disc photography. Archives of Ophthalmology. 2001;119:1492-1499.

105. Kamal DS, Garway-Heath DF, Hitchings R a, Fitzke FW. Use of sequential Heidelberg retina tomograph images to identify changes at the optic disc in ocular hypertensive patients at risk of developing glaucoma. British Journal of Ophthalmology. 2000;84:993-998.

106. Medeiros FA, Zangwill LM, Anderson DR, et al. Estimating the rate of retinal ganglion cell loss in glaucoma. American Journal of Ophthalmology. 2012;154(5):814-824.e1.

107. Racette L, Chiou CY, Hao J, et al. Combining functional and structural tests improves the diagnostic accuracy of relevance vector machine classifiers. Journal of Glaucoma. 2010;19(3):167.

**Chapter 2**

1. Livingstone MS, Hubel DH. Psychophysical evidence for separate channels for the perception of form, color, movement, and depth. The Journal of Neuroscience. 1987;7(11):3416-3468.

2. Rogers-Ramachandran DC, Ramachandran VS. Psychophysical evidence for boundary and surface systems in human vision. Vision Research. 1998;38(1):71-77.

3. Trope GE, Hatchi W, Harrison E. The phantom contour illusion letter test: a new psychophysical test for glaucoma? Perimetry Update 1994/95, Kugler. 1995:405-409.

4. Quaid PT, Flanagan JG. Defining the limits of flicker defined form: effect of stimulus size, eccentricity and number of random dots. Vision Research. 2005;45(8):1075-1084.

5. Brenton RS, Phelps CD. The normal visual field on the Humphrey field analyzer. Ophthalmologica. 1986;193(1-2):56-74.

6. Adams CW, Bullimore M a, Wall M, Fingeret M, Johnson C a. Normal aging effects for frequency doubling technology perimetry. Optometry & Vision Science. 1999;76(8):582-587.

7. Anderson AJ, Johnson C a., Fingeret M, et al. Characteristics of the normative database for the Humphrey Matrix perimeter. Investigative Ophthalmology & Visual Science. 2005;46:1540-1548.

8. Gardiner SK, Johnson C a, Spry PGD. Normal age-related sensitivity loss for a variety of visual functions throughout the visual field. Optometry & Vision Science. 2006;83(7):438-443.

9. Jaffe GJ, Alvarado JA, Juster RP. Age-related changes of the normal visual field. Archives of Ophthalmology. 1986;104(7):1021.

10. Spry PGD. Senescent changes of the normal visual field: an age-old problem. Optometry & Vision Science. 2001;78(6):436.

11. Goren D, Flanagan JG. Is flicker-defined form (FDF) dependent on the contour? Journal of Vision. 2008;8(4):1-11.

12. Hitchings RA. Selective ganglion cell death in glaucoma. British Journal of Ophthalmology. 2000;84(7):678-679.

13. Spry PGD, Johnson CA, Mansberger SL, Cioffi GA. Psychophysical investigation of ganglion cell loss in early glaucoma. Journal of Glaucoma. 2005;14(1):11-19.

14. Spry PG, Johnson CA. Senescent changes of the normal visual field: an age-old problem. Optometry & Vision Science. 2001;78(6):436-441.

15. Anderson AJ, Johnson C a. Effect of dichoptic adaptation on frequency-doubling perimetry. Optometry & Vision Science. 2002;79(2):88-92.

16. Johnson CA, Adams CW, Lewis RA. Fatigue effects in automated perimetry. Applied Optics. 1988;27(6):1030-1037.

17. Hudson C, Wild JM, O'Neill EC. Fatigue effects during a single session of automated static threshold perimetry. Investigative Ophthalmology & Visual Science. 1994;35(1):268-280.

18. Fuhr PS, Hershner TA, Daum KM. Ganzfeld blankout occurs in bowl perimetry and is eliminated by translucent occlusion. Archives of Ophthalmology (Chicago, Ill 1960). 1990;108(7):983-988.

19. Schiefer U, Pascual JP, Edmunds B, et al. Comparison of the new perimetric GATE strategy with conventional full-threshold and SITA standard strategies. Investigative Ophthalmology & Visual Science. 2009;50:488-494.

20. Bengtsson B, Heijl A, Olsson J. Evaluation of a new threshold visual field strategy, SITA, in normal subjects. Swedish Interactive Thresholding Algorithm. Acta Ophthalmologica Scandinavica. 1998;76(2):165-169.

**Chapter 3**

1. Ogle KN. Blurring of the retinal image and contrast thresholds in the fovea. Journal of the Optical Society of America. 1960;50(4):307-15.

2. Ogle KN. Peripheral contrast thresholds and blurring of the retinal image for a point light source. Journal of the Optical Society of America. 1961;51(11):1265-8.

3. Campbell FW, Green DG. Optical and retinal factors affecting visual resolution. The Journal of Physiology. 1965;181(3):576-93.

4. Weinreb RN, Perlman JP. The effect of refractive correction on automated perimetric thresholds. American Journal of Ophthalmology. 1986;101(6):706-9.

5. Atchison DA. Effect of defocus on visual field measurement. Ophthalmic & Physiological Optics. 1987;7(3):259-65.

6. Goldstick BJ, Weinreb RN. The effect of refractive error on automated global analysis program G-1. American Journal of Ophthalmology. 1987;104(3):229-32.

7. Heuer DK, Anderson DR, Feuer WJ, Gressel MG. The influence of refraction accuracy on automated perimetric threshold measurements. Ophthalmology. 1987;94(12):1550-3.

8. House PH, Drance SM, Schulzer M, Wijsman K. The effect of refractive blur on the visual field using the ring perimeter. Acta Ophthalmologica. 1990;68(1):87-90.

9. Henson DB, Morris EJ. Effect of uncorrected refractive errors upon central visual field testing. Ophthalmic & Physiological Optics. 1993;13(4):339-43.

10. Mutlukan E. The effect of refractive blur on the detection sensitivity to light offsets in the central visual field. Acta Ophthalmologica. 1994;72(2):189-94.

11. Pesudovs K, Brennan NA. Decreased uncorrected vision after a period of distance fixation with spectacle wear. Optometry & Vision Science. 1993;70(7):528-31.

12. Mon-Williams M, Tresilian JR, Strang NC, Kochhar P, Wann JP. Improving vision: Neural compensation for optical defocus. Proceedings of the Royal Society of London B: Biological Sciences. 1998;265(1390):71-7.

13. Anderson RS, McDowell DR, Ennis FA. Effect of localized defocus on detection thresholds for different sized targets in the fovea and periphery. Acta Ophthalmologica. 2001;79(1):60-3.

14. Sloan LL, Brown DJ. Area and luminance of test object as variables in projection perimetry. Vision Research. 1962;2(12):527-41.

15. Heuer DK, Anderson DR, Feuer WJ, Gressel MG. The influence of refraction accuracy on automated perimetric threshold measurements. Ophthalmology. 1987;94(12):1550-3.

16. Tyler C.W. Analysis of normal flicker sensitivity and its variability in the visuogram test. Investigative Ophthalmology & Visual Science. 1991;32(9):2552-60.

17. Lachenmayr B.J., Gleissner M. Flicker perimetry resists retinal image degradation. Investigative Ophthalmology & Visual Science. 1992;33(13):3539-42.

18. Johnson CA, Samuels SJ. Screening for glaucomatous visual field loss with frequency-doubling perimetry. Investigative Ophthalmology & Visual Science. 1997;38(2):413-25.

19. Maddess T, Goldberg I, Dobinson J, Wine S, Welsh AH, James AC. Testing for glaucoma with the spatial frequency doubling illusion. Vision Research. 1999;39(25):4258-73.

20. Maddess T, Severt WL. Testing for glaucoma with the frequency doubling illusion in the whole, macular and eccentric visual fields. Australian and New Zealand Journal of Ophthalmology. 1999;27(3-4):194-6.

21. Quaid P, Simpson T, Flanagan J. Frequency doubling illusion: Detection vs. form resolution. Optometry and Vision Science. 2005;82(1):36-42.

22. Artes PH, Nicolela MT, McCormick TA, LeBlanc RP, Chauhan BC. Effects of blur and repeated testing on sensitivity estimates with frequency doubling perimetry. Investigative Ophthalmology & Visual Science. 2003;44(2):646-52.

23. Anderson AJ, Johnson CA. Frequency-doubling technology perimetry and optical defocus. Investigative Ophthalmology & Visual Science. 2003;44(9):4147-52.

24. Flanagan JG, William-Lyn D, Trope GE, Hatch W, Harrison E. The phantom contour illusion letter test: A new psychophysical test for glaucoma? Perimetry Update 1994/95. Kugler. 1995:405-409.

25. Goren D, Quaid PT, Flanagan JG. Perceived spatial frequency of a temporally defined illusion: Flicker defined form (FDF). Investigative Ophthalmology & Visual Science. 2005;46.

26. Goren D, Flanagan JG. Is flicker-defined form (FDF) dependent on the contour? Journal of Vision. 2008;8(4):1-11.

27. Quaid PT, Flanagan JG. Defining the limits of flicker defined form: Effect of stimulus size, eccentricity and number of random dots. Vision Research. 2005;45(8):1075-84.

28. Heidelberg Engineering GmbH. Heidelberg edge perimeter operating instructions software version 2.1. E-002 ed. Heidelberg Engineering GmbH, ed. Heidelberg. Germany: Heidelberg Engineering GmbH; 2010.

29. Herse PR. Factors influencing normal perimetric thresholds obtained using the humphrey field analyzer. Investigative Ophthalmology & Visual Science 1992;33(3):611-7.

30. Silva MF, Maia-Lopes S, Mateus C, Guerreiro M, Sampaio J, Faria P, Castelo-Branco M. Retinal and cortical patterns of spatial anisotropy in contrast sensitivity tasks. Vision Research. 2008;48(1):127-35.

31. Curcio CA, Allen KA. Topography of ganglion cells in human retina. Journal of Comparative Neurology. 1990;300(1):5-25.

32. Shapley R, Kaplan E, Soodak R. Spatial summation and contrast sensitivity of X and Y cells in the lateral geniculate nucleus of the macaque. Nature. 1981;292(5823):543-5.

33. Harris WF. Magnification, blur, and ray state at the retina for the general eye with and without a general optical instrument in front of it. 1. distant objects. Optometry & Vision Science. 2001;78(12):888-900.

**Chapter 4**

1. Ng D, Zangwill LM, Racette L, Bowd C, Pascual JP, Bourne RRA, Boden C, Weinreb RN, Sample PA. Agreement and repeatability for standard automated perimetry and confocal scanning laser ophthalmoscopy in the diagnostic innovations in glaucoma study. American Journal of Ophthalmology. 2006;142(3):381-6.

2. Racette L, Chiou CY, Hao J, Bowd C, Goldbaum MH, Zangwill LM, Lee TW, Weinreb RN, Sample PA. Combining functional and structural tests improves the diagnostic accuracy of relevance vector machine classifiers. Journal of Glaucoma. 2010;19(3):167.

3. Keltner JL, Johnson CA, Quigg JM, Cello KE, Kass MA, Gordon MO. Confirmation of visual field abnormalities in the ocular hypertension treatment study. Archives of Ophthalmology. 2000;118(9):1187.

4. Chauhan BC, Johnson CA. Test-retest variability of frequency-doubling perimetry and conventional perimetry in glaucoma patients and normal subjects. Investigative Ophthalmology & Visual Science. 1999;40(3):648-56.

5. Artes PH, Hutchison DM, Nicolela MT, LeBlanc RP, Chauhan BC. Threshold and variability properties of matrix frequency-doubling technology and standard automated perimetry in glaucoma. Investigative Ophthalmology & Visual Science. 2005;46(7):2451-7.

6. Wall M, Woodward KR, Doyle CK, Zamba G. The effective dynamic ranges of standard automated perimetry sizes III and V and motion and matrix perimetry. Archives of Ophthalmology. 2010;128(5):570-6.

7. Wall M, Doyle CK, Zamba K, Artes P, Johnson CA. The repeatability of mean defect with size III and size V standard automated perimetry. Investigative Ophthalmology & Visual Science.2013;54(2):1345-51.

8. Artes PH, Iwase A, Ohno Y, Kitazawa Y, Chauhan BC. Properties of perimetric threshold estimates from full threshold, SITA standard, and SITA fast strategies. Investigative Ophthalmology & Visual Science. 2002;43(8):2654-9.

9. Sample PA, Bosworth CF, Blumenthal EZ, Girkin C, Weinreb RN. Visual function-specific perimetry for indirect comparison of different ganglion cell populations in glaucoma. Investigative Ophthalmology & Visual Science. 2000; 41(7): 1783-1790

10. Hasler S, Stürmer J. First experience with the heidelberg edge perimeter® on patients with ocular hypertension and preperimetric glaucoma. Klinische Monatsblätter für Augenheilkunde. 2012;229(04):319-22.

11. Lamparter J, Russell RA, Schulze A, Schuff A, Pfeiffer N, Hoffmann EM. Structure-function relationship between FDF, FDT, SAP, and scanning laser ophthalmoscopy in glaucoma patients. Investigative Ophthalmology & Visual Science. 2012;53(12):7553-9.

12. Reznicek L, Lamparter J, Vogel M, Kampik A, Hirneiss C. Flicker defined form perimetry in glaucoma suspects with normal achromatic visual fields. Current Eye Research. 2014:1-7.

13. Bengtsson B, Heijl A. Diagnostic sensitivity of fast blue-yellow and standard automated perimetry in early glaucoma: A comparison between different test programs. Ophthalmology 2006;113(7):1092-7.

14. Heidelberg Engineering GmbH. Heidelberg edge perimeter operating instructions software version 2.1. E-002 ed. Heidelberg Engineering GmbH, ed. Heidelberg. Germany: Heidelberg Engineering GmbH; 2010.

15. Hastie T, Stuetzle W. Principal curves. Journal of the American Statistical Association 1989;84(406):502-16.

16. Sample PA, Bosworth CF, Blumenthal EZ, Girkin C, Weinreb RN. Visual function–specific perimetry for indirect comparison of different ganglion cell populations in glaucoma. Investigative Ophthalmology & Visual Science. 2000;41(7):1783-90.

17. Wall M, Brito CF, Woodward KR, Doyle CK, Kardon RH, Johnson CA. Total deviation probability plots for stimulus size v perimetry: A comparison with size III stimuli. Archives of Ophthalmology. 2008;126(4):473-9.

18. Maddess T. The influence of sampling errors on test-retest variability in perimetry. Investigative Ophthalmology & Visual Science. 2011;52(2):1014-22.

**Chapter 5**

1. Shah NN, Bowd C, Medeiros FA, Weinreb RN, Sample PA, Hoffmann EM, Zangwill LM. Combining structural and functional testing for detection of glaucoma. Ophthalmology. 2006;113(9):1593-602.

2. Ng D, Zangwill LM, Racette L, Bowd C, Pascual JP, Bourne RRA, Boden C, Weinreb RN, Sample PA. Agreement and repeatability for standard automated perimetry and confocal scanning laser ophthalmoscopy in the diagnostic innovations in glaucoma study. American Journal of Ophthalmology. 2006;142(3):381-6.

3. Johnson CA, Sample PA, Zangwill LM, Vasile CG, Cioffi GA, Liebmann JR, Weinreb RN. Structure and function evaluation (SAFE): II. comparison of optic disk and visual field characteristics. American Journal of Ophthalmology. 2003;135(2):148-54.

4. Chauhan BC, McCormick TA, Nicolela MT, LeBlanc RP. Optic disc and visual field changes in a prospective longitudinal study of patients with glaucoma: Comparison of scanning laser tomography with conventional perimetry and optic disc photography. Archives of Ophthalmology. 2001;119(10):1492.

5. Strouthidis NG, Scott A, Peter NM, Garway-Heath DF. Optic disc and visual field progression in ocular hypertensive subjects: Detection rates, specificity, and agreement. Investigative Ophthalmology & Visual Science. 2006;47(7):2904-10.

6. Harwerth RS, Quigley HA. Visual field defects and retinal ganglion cell losses in patients with glaucoma. Archives of Ophthalmology. 2006;124(6):853.

7. Racette L, Chiou CY, Hao J, Bowd C, Goldbaum MH, Zangwill LM, Lee TW, Weinreb RN, Sample PA. Combining functional and structural tests improves the diagnostic accuracy of relevance vector machine classifiers. Journal of Glaucoma. 2010;19(3):167.

8. Medeiros FA, Leite MT, Zangwill LM, Weinreb RN. Combining structural and functional measurements to improve detection of glaucoma progression using bayesian hierarchical models. Investigative Ophthalmology & Visual Science. 2011;52(8):5794-803.

9. Medeiros FA, Zangwill LM, Anderson DR, Liebmann JM, Girkin CA, Harwerth RS, Fredette MJ, Weinreb RN. Estimating the rate of retinal ganglion cell loss in glaucoma. American Journal of Ophthalmology. 2012;154(5):814-824.e1.

10. Ferreras A, Pablo LE, Garway-Heath DF, Fogagnolo P, García-Feijoo J. Mapping standard automated perimetry to the peripapillary retinal nerve fiber layer in glaucoma. Investigative Ophthalmology & Visual Science. 2008;49(7):3018-25.

11. Racette L, Medeiros FA, Bowd C, Zangwill LM, Weinreb RN, Sample PA. The impact of the perimetric measurement scale, sample composition, and statistical method on the structure-function relationship in glaucoma. Journal of Glaucoma. 2007;16(8):676-84.

12. Bowd C, Zangwill LM, Medeiros FA, Tavares IM, Hoffmann EM, Bourne RR, Sample PA, Weinreb RN. Structure–function relationships using confocal scanning laser ophthalmoscopy, optical coherence tomography, and scanning laser polarimetry. Investigative Ophthalmology & Visual Science. 2006;47(7):2889-95.

13. Hoffmann EM, Medeiros FA, Sample PA, Boden C, Bowd C, Bourne RR, Zangwill LM, Weinreb RN. Relationship between patterns of visual field loss and retinal nerve fiber layer thickness measurements. American Journal of Ophthalmology. 2006;141(3):463-71.

14. El Beltagi TA, Bowd C, Boden C, Amini P, Sample PA, Zangwill LM, Weinreb RN. Retinal nerve fiber layer thickness measured with optical coherence tomography is related to visual function in glaucomatous eyes. Ophthalmology. 2003;110(11):2185-91.

15. Nilforushan N, Nassiri N, Moghimi S, Law SK, Giaconi JA, Coleman A, Caprioli J, Nouri-Mahdavi K. Structure-function relationships between spectral-domain OCT and standard achromatic perimetry. Investigative Ophthalmology & Visual Science. 2012;53(6),2740-8.

16. Lamparter J, Russell RA, Schulze A, Schuff AC, Pfeiffer N, Hoffmann EM. Structure-function relationship between FDF, FDT, SAP, and scanning laser ophthalmoscopy in glaucoma patients. Investigative Ophthalmology & Visual Science. 2012;53(12):7553-9.

17. Schlottmann PG, De Cilla S, Greenfield DS, Caprioli J, Garway-Heath DF. Relationship between visual field sensitivity and retinal nerve fiber layer thickness as measured by scanning laser polarimetry. Investigative Ophthalmology & Visual Science. 2004;45(6):1823-9.

18. Swanson WH, Felius J, Pan F. Perimetric defects and ganglion cell damage: Interpreting linear relations using a two-stage neural model. Investigative Ophthalmology & Visual Science. 2004;45(2):466-72.

19. Harwerth RS, Carter-Dawson L, Smith EL, Crawford MLJ. Scaling the structure−function relationship for clinical perimetry. Acta Ophthalmologica Scandinavica 2005;83(4):448-55.

20. Hood DC, Anderson SC, Wall M, Kardon RH. Structure versus function in glaucoma: An application of a linear model. Investigative Ophthalmology & Visual Science. 2007;48(8):3662-8.

21. Bizios D, Heijl A, Bengtsson B. Integration and fusion of standard automated perimetry and optical coherence tomography data for improved automated glaucoma diagnostics. BMC Ophthalmology. 2011;11(1):20.

22. Bowd C, Lee I, Goldbaum MH, Balasubramanian M, Medeiros FA, Zangwill LM, Girkin CA, Liebmann JM, Weinreb RN. Predicting glaucomatous progression in glaucoma suspect eyes using relevance vector machine classifiers for combined structural and functional measurements. Investigative Ophthalmology & Visual Science. 2012;53(4),2382-9.

23. Harwerth RS, Vilupuru AS, Rangaswamy NV, Smith EL. The relationship between nerve fiber layer and perimetry measurements. Investigative Ophthalmology & Visual Science. 2007;48(2):763-73.

24. Wall M, Woodward KR, Doyle CK, Artes PH. Repeatability of automated perimetry: A comparison between standard automated perimetry with stimulus size III and V, matrix, and motion perimetry. Investigative Ophthalmology & Visual Science. 2009;50(2):974-9.

25. Owen VMF, Strouthidis NG, Garway-Heath DF, Crabb DP. Measurement variability in Heidelberg retina tomograph imaging of neuroretinal rim area. Investigative Ophthalmology & Visual Science. 2006;47(12):5322-30.

26. Anderson DR, Patella V. Automated static perimetry. Mosby Year Book St Louis; 1992.

27. Flanagan JG, William-Lyn D, Trope GE, Hatch W, Harrison E. The phantom contour illusion letter test: A new psychophysical test for glaucoma? Perimetry Update 1994/95. Kugler. 1995:405-409.

28. Livingstone MS, Hubel DH. Psychophysical evidence for separate channels for the perception of form, color, movement, and depth. Journal of Neuroscience. 1987;7(11):3416-68.

29. Rogers-Ramachandran DC, Ramachandran VS. Psychophysical evidence for boundary and surface systems in human vision. Vision Research. 1998;38(1):71-7.

30. Goren D, Flanagan JG. Is flicker-defined form (FDF) dependent on the contour? Journal of Vision. 2008;8(4):1-11.

31. Jackson GR, Owsley C. Visual dysfunction, neurodegenerative diseases, and aging. Neurologic Clinics. 2003;21(3):709-28.

32. Lundh BL, Gottvall E. Peripheral contrast sensitivity for dynamic sinusoidal gratings in early glaucoma. Acta Ophthalmologica Scandinavica. 1995;73(3):202-6.

33. Harwerth RS, Smith III EL. Investigations with degenerate gratings. Perimetry Update 1996/97. Kugler. 1997:3-12.

34. Heidelberg Engineering GmbH. Heidelberg edge perimeter operating instructions software version 2.1. E-002 ed. Heidelberg Engineering GmbH, ed. Heidelberg. Germany: Heidelberg Engineering GmbH; 2010.

35. Anderson RS, McDowell RD, Ennis FA. Effect of localized defocus on detection thresholds for different sized targets in the fovea and periphery. Acta Ophthalmologica Scandinavica. 2001;79(1):60-3.

36. Garway-Heath DF, Viswanathan A, Westcott M, Kamal D, Fitzke F, Hitchings RA. Relationship between perimetric light sensitivity and optic disk neuroretinal rim area. Perimetry Update 1998/99. Kugler. 1999:381-9.

37. Cleveland WS. Robust locally weighted regression and smoothing scatterplots. Journal of the American statistical association. 1979:829-36.

38. Sample PA. Glaucoma is present prior to its detection with standard automated perimetry: Is it time to change our concepts? Graefe's Archive for Clinical and Experimental Ophthalmology. 2003;241(3):168-9.

39. Emdadi A, Zangwill L, Sample PA, Kono Y, Anton A, Weinreb RN. Patterns of optic disk damage in patients with early focal visual field loss. American Journal of Ophthalmology. 1998;126(6):763-71.

40. Ugurlu S, Hoffman D, Garway-Heath DF, Caprioli J. Relationship between structural abnormalities and short-wavelength perimetric defects in eyes at risk of glaucoma. American Journal of Ophthalmology. 2000;129(5):592-8.

41. Strouthidis N, White E, Owen V, Ho T, Hammond C, Garway-Heath D. Factors affecting the test-retest variability of Heidelberg retina tomograph and Heidelberg retina tomograph II measurements. British Journal of Ophthalmology. 2005;89(11):1427-32.

42. Pearson PM, Schmidt LA, Ly-Schroeder E, Swanson WH. Ganglion cell loss and age-related visual loss: A cortical pooling analysis. Optometry and Vision Science. 2006;83(7):444.

**Chapter 6**

1. Goren D, Quaid PT, Flanagan JG. Perceived spatial frequency of a temporally defined illusion: Flicker defined form (FDF). Investigative Ophthalmology & Visual Science. 2005;46.

2. Goren D, Flanagan JG. Is flicker-defined form (FDF) dependent on the contour? Journal of Vision. 2008;8(4):1-11.

3. Johnson CA. Psychophysical measurement of glaucomatous damage. Survey of Ophthalmology. 2001;45 Suppl 3:S313-S318; discussion S322-S324.

4. Adams CW, Bullimore M a, Wall M, Fingeret M, Johnson C. Normal aging effects for frequency doubling technology perimetry. Optometry & Vision Science. 1999;76(8):582-587.

5. Anderson AJ, Johnson C a., Fingeret M, et al. Characteristics of the normative database for the Humphrey Matrix perimeter. Investigative Ophthalmology & Visual Science. 2005;46(4):1540-1548.

6. Tatham AJ, Weinreb RN, Zangwill LM, Liebmann JM, Girkin CA, Medeiros FA. Estimated retinal ganglion cell counts in glaucomatous eyes with localized retinal nerve fiber layer defects. American Journal of Ophthalmology. 2013;156(3):578-587.e1.

7. Raza AS, Hood DC. Evaluation of the Structure-Function Relationship in Glaucoma Using a Novel Method for Estimating the Number of Retinal Ganglion Cells in the Human Retina. Investigative Ophthalmology & Visual Science. 2015;56(9):5548-5556.

8. Garway-Heath DF, Viswanathan A, Westcott M, Kamal D, Fitzke F, Hitchings RA. Relationship between perimetric light sensitivity and optic disk neuroretinal rim area. Perimetry Update 1998/99. Kugler. 1999:381-389.

9. Ballae Ganeshrao S, Turpin A, Denniss J, McKendrick AM. Enhancing Structure-Function Correlations in Glaucoma with Customized Spatial Mapping. Ophthalmology. 2015;122(8):1695-1705.